Bruno Miguel Domingues da Cunha

Licenciado em Ciências da Engenharia Electrotécnica e de Computadores

High Performance Faster-than-Nyquist Signaling

Dissertação apresentada para obtenção do Grau de Mestre em Engenharia Electrotécnica e de Computadores, pela Universidade Nova de Lisboa, Faculdade de Ciências e Tecnologia.

Orientadores: Rui Dinis, Professor Associado com Agregação, FCT-UNL
Luís Bernardo, Professor Auxiliar com Agregação, FCT-UNL

Júri:

Presidente: Prof. Doutor Paulo Montezuma

Arguente: Prof. Doutor Francisco Cercas

Vogal: Prof. Doutor Rui Dinis

Setembro, 2014

High Performance Faster-than-Nyquist Signaling

Strive not to be a success, but rather to be of value.

Albert Einstein

To all my friends and family.

Acknowledgments

I owe my deepest thanks and acknowledgements to so many people that, in different ways, helped me over the course of writing my dissertation, motivated and guided me into the right path or just made me look the right way with perseverance and a smile on my face. For all of you that made this possible my most sincere and heartfelt thank you.

First and foremost I offer my sincerest gratitude to both my advisors, Prof. Dr. Rui Dinis and Prof. Dr. Luis Bernardo, for welcoming me so warmly as their student. Thank you for all the help in the development and the writing of this thesis. Their constant and unconditional guidance, patience and knowledge are some of the most valuable assets that I will carry with me for the future.

I would like to acknowledge Prof. Rui Dinis for introducing me to the exciting world of wireless communication. It is an honor to have met such a brilliant and yet so approachable and down to earth person. I will always recall him every time I hear the word "teacher".

I will always remember the precious help and all the support given by Prof. Luis Bernardo who, in the most difficult moments, has motivated and guided me on this academic journey. His expertise in communication networks, combined with a selfless attitude, made him such a valuable asset on this work. His genuine support will be always valued.

To someone who is more than a colleague and whose availability was crucial

throughout this dissertation, Francisco Ganhão, who is one of the most helpful and supportive people I have come across in my life. A rare and kind human being that will always have my sincere gratitude and friendship. A special word to Rosário Caldeira, whose unconditional help enriched even more this document.

It is said that college times are the best years of our lives and I totally agree. To all of those who made my university experience unique and striking, who helped me in difficult times and shared the good ones a big thank you. To everyone in the Electrical Engineering Department's Telecommunications office for their help in the most stressful moments. A special word for the whole AEFCT football team, for all the happy moments shared. You are like family to me!

To all my loyal and most dear friends who helped all the way through college, their support and advice since the very first moments have made all the difference. The way that all of them touched my life is so unique and diverse that I could not have done without any of them. Their support since the beginning of my thesis was my most powerful weapon. Thank you André Ricardo, Luís Ramos, Flávio Silva, João Marques, André Ramos, Tomás Henriques, Bernardo Fontes, António Magalhães, Fernando Franco, Pedro Moiteiro, Diogo Freire, Tiago Estêvão, Pedro Granada, João Santos, Carolina Damas and more recently Guilherme Rosa, José Coelho, Pedro Brites, José Soares, Nuno Barreira and André Arrimar.

Last, but definitely not least, a big and special thank you to the most important part of my life: my family. I am deeply indebted to my parents, Francisco and Irene, for their never-ending support and believing in me. Thank you also to my sister Ana for everything she has taught me over the years. To my beloved grandparents Rosa and Adão, the strongest couple alive, and Cândida and Manuel, two truly inspiring people. Finally, to my beloved Margarida, for being always present and for blindly believing in my capacity even when I doubted myself.

This work is also yours. Thank you all.

Resumo

Num sistema de telecomunicações móveis, os canais de propagação multi-percurso dispersivos no tempo afectam consideravelmente a ligação ascendente da comunicação de dados do terminal móvel (MT). É normalmente proposta a técnica SC-FDE (Single Carrier with Frequency Domain Equalization) para lidar com canais altamente dispersivos no tempo para este tipo de comunicação. No entanto, os sistemas actuais baseiam-se no teorema de Nyquist e assumem que um sistema de comunicações móveis necessita de uma banda de frequências no mínimo de $2W$ por MT. Por outro lado, a técnica Faster-than-Nyquist (FTN) assume que é possível utilizar uma banda de até 0.802 da banda de Nyquist original com perdas mínimas - apesar disto, a literatura corrente apenas conseguiu propor receptores demasiado complexos para uma caracterização simples do canal de comunicação sem fios. Além disso, a ligação ascendente entre o MT e a BS do SC-FDE pode ser afectada de forma intensa devido a desvanecimentos profundos ou pobres condições de canal; para lidar com este problema, utiliza-se a técnica Diversity Combining (DC) Hybrid ARQ (H-ARQ) que combina múltiplas cópias do pacote enviado pelo MT a fim de criar um pacote confiável no receptor.

Nesta dissertação consideramos o uso de sinalização FTN para a ligação ascendente num sistema de comunicações móveis com igualização SC-FDE e um receptor baseado em IB-DFE (Iterative Block with Decision Feedback Equalization), aliado a um esquema de acesso ao meio agendado com H-ARQ (Hybrid Automatic Repeat reQuest), especialmente desenvolvido tendo em conta as características do sinal

FTN. Esta abordagem alcança melhores resultados que a sinalização de Nyquist ao aproveitar a largura de banda adicional oferecida pelo pulso root-raised cosine pulse para diversidade.

Juntamente com um modelo analítico do PER (Packet Error Rate), os resultados das simulações efectuadas demonstram que o receptor apresenta um melhor desempenho quando comparado com um sistema normal, com melhorias ao nível do débito do sistema e energia gasta por pacote (EPUP).

Palavras Chave: Matched Filter Bound, SC-FDE, IB-DFE, FTN, Recepção Multi-Pacote, Interferência Inter-Simbólica (ISI), DC, H-ARQ.

Abstract

In a wireless broadband context, multi-path dispersive channels can severely affect data communication of Mobile Terminals (MTs) uplink. Single Carrier with Frequency-Domain Equalization (SC-FDE) has been proposed to deal with highly dispersive channels for the uplink of broadband wireless systems. However, current systems rely on older assumptions of the Nyquist theorem and assume that a system needs a minimum bandwidth $2W$ per MT. Faster-Than-Nyquist (FTN) assumes that it is possible to employ a bandwidth as low as 0.802 of the original Nyquist bandwidth with minimum loss - despite this, the current literature has only proposed complex receivers for a simple characterization of the wireless channel. Furthermore, the uplink of SC-FDE can be severely affected by a deep-fade and or poor channel conditions; to cope with such difficulties Diversity Combining (DC) Hybrid ARQ (H-ARQ) is a viable technique, since it combines the several packet copies sent by a MT to create reliable packet symbols at the receiver.

In this thesis we consider the use of FTN signaling for the uplink of broadband wireless systems employing SC-FDE based on the Iterative Block with Decision Feedback Equalization (IB-DFE) receiver with a simple scheduled access Hybrid Automatic Repeat reQuest (H-ARQ) specially designed taking into account the characteristics of FTN signals. This approach achieves a better performance than Nyquist signaling by taking advantage of the additional bandwidth employed of a root-raised cosine pulse for additional diversity.

Alongside a Packet Error Rate (PER) analytical model, simulation results show that

this receiver presents a better performance when compared with a regular system, with higher system throughputs and a lower Energy per Useful Packet (EPUP).

Keywords: Matched Filter Bound, SC-FDE, IB-DFE, FTN, Multipacket Reception, Inter-Symbol Interference (ISI), Diversity Combining, H-ARQ.

Acronyms

3GPP	*3^{rd} Generation Partnership Project*
ARQ	*Automatic Repeat reQuest*
AWGN	*Additive White Gaussian Noise*
BER	*Bit Error Rate*
BPSK	*Binary Phase Shift Keying*
BS	*Base Station*
CC	*Code Combining*
CDMA	*Code Division Multiple Access*
CIR	*Channel Impulsive Response*
CP	*Cyclic Prefix*
DAMA	*Demand Assigned Multiple Access*
DC	*Diversity Combining*
DFE	*Decision Feedback Equalization*
DFT	*Discrete Fourier Transform*
DS-CDMA	*Direct-Sequence CDMA*
EPUP	*Energy Per Useful Packet*
FDE	*Frequency Domain Equalization*
FDMA	*Frequency Division Multiple Access*
FEC	*Forward Error Correction*
FFT	*Fast Fourier Transform*
FTN-SA	*Faster-Than-Nyquist Scheduled Access*
FTN	*Faster-Than-Nyquist*

H-ARQ	*Hybrid Automatic Repeat reQuest*
HSDPA	*High-Speed Downlink Packet Access*
HSUPA	*High-Speed Uplink Packet Access*
IB-DFE	*Iterative Block Decision Feedback Equalization*
IDFT	*Inverse Discrete Fourier Transform*
IEEE	*Institute of Electrical and Electronics Engineering*
IFFT	*Inverse Fast Fourier Transform*
ISI	*InterSymbol Interference*
LTE	*Long Term Evolution*
M-QAM	*Multi-level Quadrature Amplitude Modulation*
MAC	*Medium Access Control*
MFB	*Matched Filter Bound*
MMSE	*Minimum Mean Square Error*
MSE	*Minimum Square Error*
MT	*Mobile Terminal*
OFDM	*Orthogonal Frequency Division Multiplexing*
PAPR	*Peak-to-Average Power Ratio*
PER	*Packet Error Rate*
PMEPR	*Peak-to-Mean Envelope Power Ratio*
PSD	*Power Spectral Density*
PSK	*Phase Shift Keying*
QAM	*Quadrature Amplitude Modulation*
QoS	*Quality of Service*
QPSK	*Quadrature Phase Shift Keying*
SA	*Scheduled Access*
SC-FDE	*Single Carrier with Frequency Domain Equalization*
SC	*Single Carrier*
SINR	*Signal-to-Interference-plus-Noise Ratio*

SNR	*Signal-to-Noise Ratio*
TDMA	*Time Division Multiple Access*
UMTS	*Universal Mobile Telecommunication System*
WLAN	*Wireless Local Area Network*

Contents

List of Figures

List of Tables

List of Symbols

A_c	Carrier Amplitude
a_n	n^{th} symbol in a burst
B_e	Number of bits per symbol
$B_k^{(i)}$	Feedback coefficients of the IB-DFE
$\mathbb{E}[N](\beta)$	Expected service time for a TDMA with FTN factor β
$\mathbb{E}\left[N^{(1)}\right]$	Service time of the long FTN block
$\mathbb{E}\left[N^{(2)}\right]$	Service time of the short FTN block
$\mathbb{E}[\tau]$	Mean service time for SA-FTN
d	Distance in meters
E_b	Average bit energy
E_p	Packet transmission energy
f_c	Carrier frequency
F_k	Feed-forward component in a linear receiver
$F_k^{(l,i)}$	Feed-forward coefficients of the IB-DFE
G_{FTN}	Throughput gain of FTN signaling

G_1	Gain factor at a distance of $d = 1$ m
H_k	Channel frequency response
i	ith iteration of the receiver
j	Slot time of the FTN block
J	Number of members in a group of MTs
l	l-th packet transmission
L	Maximum number of transmissions
K	Redundancy used for bandwidth diversity
M	Number of bits in a data packet
M_l	Link margin gain
N	Number of symbols in a data block
N_0	Power spectral density of the noise
N_{cp}	Cyclic prefix length
N_{iter}	Number of iterations of the IB-DFE
N_k	Channel noise for the k-th frequency
$P(f)$	Signal frequency response
$P^{\dagger}(f)$	Signal replicas of a data block
$p(t)$	Signal time response
Q_x	Probability of having $x - 1$ failed transmissions

R_s	Signal bit rate
$S_{sat}(\beta)$	Saturated throughput for a FTN factor β
T_1	Large slot time for SA-FTN with H-ARQ
T_2	Short slot time for SA-FTN with H-ARQ
T_s	Signal period
W	Signal Bandwidth
$x_I(t)$	In-phase signal component
$x_Q(t)$	Quadrature signal component
Y_k	Frequency domain data samples
α	Raised cosine pulse roll-off factor
β	Faster-than-Nyquist reduction factor
β_T	Ratio of the transmission power over the amplifier's power
$\gamma^{(i)}$	Residual ISI component
$\epsilon_p^{(l)}$	Packet error rate for a l-th transmission
κ	Characteristic power-path loss
ξ	Inverted SNR
$\rho^{(i)}$	Correlation coefficient
σ_N^2	Total variance of the channel noise
$\Phi(\beta)$	Energy per useful packet for a FTN factor β

$\Phi(x)$	Gaussian error function
ϕ_c	Carrier phase
ν_P	Peak-to-Average Power Ratio

Chapter 1

Introduction

1.1 Motivation

The design of future broadband wireless systems presents considerable challenges since those systems are expected to have high power and spectral efficiencies over communication channels that, due to multipath signal propagation between the transmitter and the receiver, are subjected to strong time-dispersive effects [1], [2]. However, it is known that high power and spectral efficiencies are confliting goals since the increase in one is achieved at the decrease of the other.

It is well known that the minimum bandwidth for a bandlimited transmission without Inter-Symbol Interference (ISI), also known as Nyquist bandwidth, is half the symbol rate. This is possible to achieve by employing sinc pulses that satisfy the Nyquist criterion. Since symbol-spaced pulses are orthogonal, a relatively simple receiver based on a matched filter can present optimum performance, identical to the one achieved when an isolated pulse is transmitted. To overcome the implementation difficulties inherent to the use of a sinc pulse (i.e. filter with ideal rectangular shape), most communication systems employ the so-called raised-cosine pulses (actually square-root raised-cosine pulses are employed in this dissertation; after a matched filter raised-cosine pulses are obtained), wich are simple to implement, although

occupy a slightly higher bandwidth (tipically with a roll-off factor above 0.25) wich reduces the system's spectral efficiency. This extra bandwidth is generally regarded as an unavoidable price to pay when designing communication systems in general and wireless communication systems in particular, wich are known to have significant power and bandwidth constraints.

A much less known fact is that it is possible to achieve optimum asymptotic performance with a bandwidth below the minimum Nyquist band. In fact, by employing the so-called Faster-than-Nyquist (FTN) signaling the transmission band can be reduced to around 80% without compromising the minimum Euclidean distance between differente binary sequences, in spite of the inherent ISI levels [3]. This remarkable result was almost completely ignored for over 30 years mainly because the optimum receiver with FTN signaling was too complex. However, due to spectrum scarcity and advances in signal processing there is a renewed interest in FTN (see [4] and references within). Faster-than-Nyquist signaling is particularly interesting for broadband wireless systems. However, the scenario is even more complex if we consider that the ISI inherent to FTN signaling is combined with the ISI associated to multipath time-dispersive effects, which leads to much higher ISI levels that cannot be handled by conventional FTN receivers (even the simplified receivers from [5], [6] are too complex). Block transmission techniques combined with Frequency-Domain Equalization (FDE) such as Orthogonal Frequency Division Multiplexing (OFDM) [2] and Single-Carrier with FDE (SC-FDE) [7] are widely recognized as the best candidates for the downlink and uplink, respectively [8], [9]. Although a linear FDE is suitable for OFDM, it is far from optimum for SC-FDE. In that case, the most promising FDE is the so-called nonlinear IB-DFE (Iterative Block Decision-Feedback Equalizer) [10].

Furthermore, in a time-dispersive channel, reception errors can be bothersome either due to poor channel conditions or a low Signal-to-Noise Ratio (SNR). To cope with channel errors, a BS can ask for additional copies of the same packet. Nevertheless,

those copies might present errors as well, since channel conditions might not vary for subsequent retransmissions leading to a throughput degradation. Fortunately, the use of Hybrid Automatic Repeat reQuest (H-ARQ) [11] can be useful in such conditions, specially when employing Diversity Combining (DC) H-ARQ [1], since it uses the individual copies from each symbol, received at the BS, to create a packet with better reliability with appropriate equalization techniques.

To take the full advantages of FTN signaling, a scheduled access H-ARQ architecture can be considered with two different data block sizes. After a failed transmission of a FTN slot with β size, the remaining symbol replicas can be retransmitted in a slot with size $1 - \beta$, allowing the receiver to combine them and achieve a Nyquist signaling equivalent performance. Such approach can achieve a bandwidth efficiency gain of up to $1/\beta$.

It is important to note that the models developed in this thesis are general in terms of the technology in use, since one of the main objectives of this thesis is to achieve energy and bandwidth efficiency for wireless communications in general.

1.2 Outline

This document is structured in a total of six chapters as enumerated in the paragraphs below.

After this brief introduction, chapter 2 presents some principles on the transmission techniques in use through this dissertation, such as modulation techniques, Nyquist and Faster-than-Nyquist signaling and equalization schemes, Medium Access Control (MAC) protocols and error correction schemes, such as Hybrid Automatic Repeat reQuest (H-ARQ) and diversity techiques.

In chapter 3 it is considered the use of Faster-than-Nyquist (FTN) signaling for the uplink of wireless broadband systems employing SC-FDE schemes. An IB-DFE receiver is presented, specially designed to cope with the overall ISI inherent to both FTN signaling and multi-path time dispersive channels. Results on the Bit Error Rate (BER) are discussed for different values of the FTN factor β, as well as for increasing iterations and bandwidth diversity methods.

Chapter 4 presents an efficient H-ARQ technique using TDMA that takes into account the characteristics of the FTN with SC-FDE scheme and the IB-DFE receiver considered in chapter 3. The employment of Diversity Combining (DC) is considered, since it uses the individual copies from each symbol received to create a packet with better reliability. Also, given the shorter bandwidth of the FTN pulse, the bandwidth efficiency of the system is depicted through an analytical model for the PER and MAC performance.

In chapter 5 a different MAC approach is proposed, considering a scheduled access FTN with H-ARQ architecture which uses two different data block sizes depending on the FTN factor β. This allows, given a high success rate of the initial FTN transmission achieved by the IB-DFE receiver, a bandwidth efficiency and throughput gains of up to $1/\beta$. An analytical model for the throughput and energy per useful packet (EPUP), as well as a simulation script are presented in order to validate the obtained results.

Finnaly, chapter 6 presents the document's conclusions.

1.3 Major Contributions

In result of the work developed in this thesis, the major contributions are enumerated below.[1]

A FTN signaling model for a SC-FDE context at the uplink, where the BS takes advantage of the full diversity from the root-raised cosine pulse using the IB-DFE technique for equalization is proposed in chapter 3. It presents similar results to an orthogonal pulse for a higher roll-off and a smaller bandwidth. The model and its results were submitted for the *2014 IEEE 80th Vehicular Technology Conference* (VTC2014-Fall).

A FTN PER model using the receiver proposed in chapter 3 and a DC H-ARQ architecture to enhance packet reception are presented. Analytical model and simulation results, depicted in chapter 4, were published in [12].

A Hybrid ARQ scheme combined with IB-DFE detection, both specially designed for FTN signaling, is proposed in chapter 5. A simple analytical model for this technique and its respective simulation results were submitted for the *2015 IEEE 81st Vehicular Technology Conference* (VTC2015-Spring).

[1]This work was supported by the FCT/MEC projects ADIN PTDC/EEI-TEL/2990/2012; COPWIN PTDC/EEI-TEL/1417/2012; MANY2COMWIN EXPL/EEI-TEL/0969/2013; CTS PEst-OE/EEI/UI0066/2011; IT PEst-OE/EEI/LA0008/2013 (HETCOP).

Chapter 2

Transmission Techniques

The main purpose of nowadays communication systems, in particular wireless systems, is to achieve low cost mobile terminals, hand to hand with higher data rates and high power and spectral efficiencies. To obtain it, non-linear power amplifiers are often used. In order to design constant envelope signals, able to cope with the high non-linear distortion of this type of amplification, we need to employ modulation schemes where information is transmitted in the signal phase, such as Phase Shift Keying (PSK). Therefore, this chapter will discuss PSK techniques, such as Binary-PSK (BPSK) and Quaternary-PSK (QPSK). To diminish the complexity of mobile terminals, the transmitter has to be as simple as possible, transferring all possible processes to the base station. This leads to the use of Single-Carrier (SC-FDE) schemes in the uplink, due to their efficiency against fading and ISI channels as well as implementation simplicity. In an higher level, the most efficient method of Medium Access and Error Control will be discussed, in order to organize admittance to the base station, as well as to detect and correct possible errors in transmitted data. Therefore, MAC techniques and error control schemes will be characterized, such as Hybrid-ARQ and diversity techniques, which plays an important role in the development of this dissertation.

The chapter is organized as follows: section 2.1 explains the basic principles behind

phase modulation methods, such as BPSK and QPSK schemes; section 2.2 shows a brief characterization of the support pulses used through this thesis; section 2.3 pays special attention to Faster-than-Nyquist signaling; section 2.4 gives an overall description of Single Carrier with Frequency Domain Equalization (SC-FDE); section 2.5 describes a non-linear frequency equalization method called Iterative Block Decision Feedback Equalization (IB-FDE), a deeply important tool regarding this dissertation; section 2.6 presents a brief description of medium access control schemes and, finally, section 2.7 focus on error correction schemes, specially the Hybrid-ARQ technique.

2.1 Phase Modulation Methods

In baseband data transmission, the entire sequence of input data is represented as a discrete wave modulated by pulse amplitude (PAM) that can be transmitted in a low pass channel. However, in wireless communications, due to constraints of the physical channel in use, the data stream is modulated onto a carrier, typically sinusoidal, limited in frequency by a predetermined band-pass channel as a microwave channel, a radio channel or a satellite channel. In any case, the modulation process involves switching (keying) the amplitude, frequency or phase of a sinusoidal carrier in accordance with the incoming data. In this section it is considered only phase modulation, more specifically Phase Shift Keying (PSK), a technique commonly used in most mobile communication applications.

2.1.1 Generality

Given a binary source that transmits the symbols 0 and 1, the modulation process evolves the phase keying of a sinusoidal carrier, maintaining the amplitude and

frequency of this signal constant, while switching the phase according to the original data stream.

Consider the sinusoidal carrier

$$x(t) = A_c\, cos(2\pi f_c t + \phi_c) \tag{2.1}$$

where A_c is the carrier amplitude, f_c the frequency and ϕ_c the carrier phase.

We may describe it in terms of its in-phase and quadrature component as

$$\begin{aligned} x(t) &= A_c\, cos(\phi_c)\; cos(2\pi f_c t) - A_c\, sen(\phi_c)\, sen(2\pi f_c t) \\ &= Re\left\{A_c\; e^{j\phi_c(t)}\; e^{j2\pi f_c t}\right\} \\ &= x_I(t)\, cos(2\pi f_c t) - x_Q(t)\, sen(2\pi f_c t)\,. \end{aligned} \tag{2.2}$$

The components $x_I(t)$ and $x_Q(t)$ are low-pass signals. They are uniquely defined in terms of the band-pass signal $x(t)$ and the carrier frequency f_c, provided that the half-bandwidth of $x(t)$ is less than the carrier frequency f_c.

2.1.2 Binary Phase Shift Keying

The binary PSK contains phase shifts of $\pm\ \pi$ radians. This signal can be expressed as

$$x(t) = A_c\, cos(2\pi f_c t + \phi_c) \tag{2.3}$$

where the phase component ϕ_c assumes the values

$$\phi_c(t) = \begin{cases} 0 & \text{, for symbol 1} \\ \pi & \text{, for symbol 0} \end{cases} \tag{2.4}$$

The in-phase and quadrature component of this signal are

$$x_I(t) = \pm A_c \qquad \text{and} \qquad x_Q(t) = 0 \tag{2.5}$$

and a BPSK signal constellation is shown in Fig. 2.1.

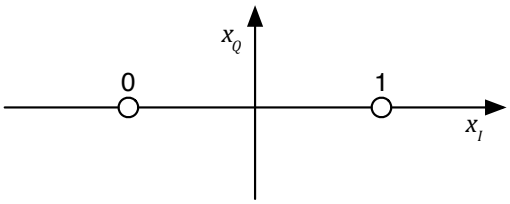

Figure 2.1: BPSK signal constellation.

The waveform of a BPSK signal is shown in Fig. 2.2.

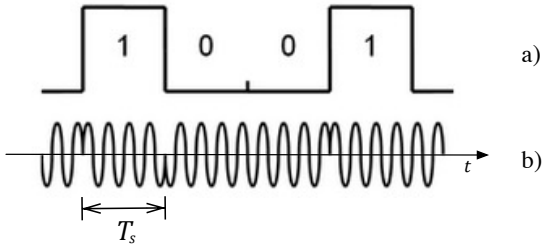

Figure 2.2: BPSK signal binary message (a) and transmitted waveform (b).

2.1.3 Quaternary Phase Shift Keying

The quaternary PSK can be expressed as a combination of two BPSK signals in quadrature. The carrier signal $x(t)$ used,

$$x(t) = A_c \, cos(2\pi f_c t + \phi_c) \tag{2.6}$$

has four possible values for the phase component ϕ_c, according to which symbol to

represent

$$\phi_c(t) = \begin{cases} \frac{\pi}{4} & \text{, for symbol 11} \\ \frac{3\pi}{4} & \text{, for symbol 01} \\ \frac{-3\pi}{4} & \text{, for symbol 00} \\ \frac{-\pi}{4} & \text{, for symbol 10} \end{cases} \tag{2.7}$$

Therefore, the in-phase and quadrature component of this signal are

input dibit	ϕ_c	$x_I(t)$	$x_Q(t)$
00	$\frac{-3\pi}{4}$	$-A\frac{\sqrt{2}}{2}$	$-A\frac{\sqrt{2}}{2}$
01	$\frac{3\pi}{4}$	$-A\frac{\sqrt{2}}{2}$	$A\frac{\sqrt{2}}{2}$
10	$\frac{-\pi}{4}$	$A\frac{\sqrt{2}}{2}$	$-A\frac{\sqrt{2}}{2}$
11	$\frac{\pi}{4}$	$A\frac{\sqrt{2}}{2}$	$A\frac{\sqrt{2}}{2}$

Table 2.1: Phase values for different symbols in QPSK.

A QPSK signal constellation is shown in Figure 2.3.

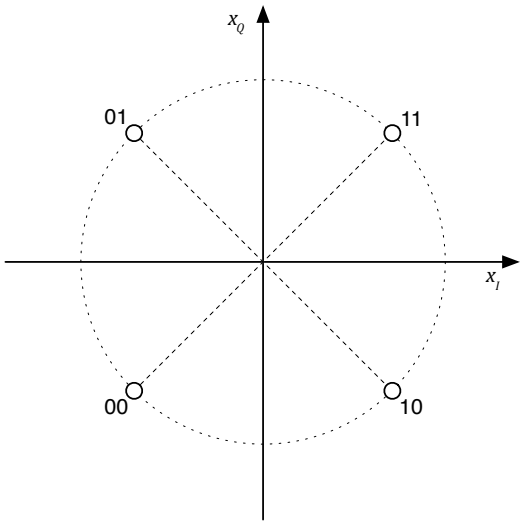

Figure 2.3: QPSK signal constellation.

2.2 Support Pulses

One of the biggest challenges in wireless communication lies in controlling the inter symbol interference (ISI) resulting from a dispersive communication channel. The choice of a proper pulse shape that not only eliminates this aspect but also optimizes the spectrum of the transmitted signal is, therefore, crucial. Let us consider

$$s(t) = \sum_k a_k \, r(t - kT_s) \tag{2.8}$$

where $r(t)$ is the support pulse, as the modulated signal to transmit, and T_s is the signal period. This signal is modified as a result of transmission (a convolution operation) through the channel of impulse response $h(t)$

$$x(t) = s(t) \star h(t) = \int_{-\infty}^{+\infty} s(\tau) \; h(t - \tau) \; d\tau \tag{2.9}$$

and then passed through a receive filter, resulting on $y(t)$ in the form of a modified PAM signal

$$y(t) = \sum_n a_k \, p(t - kT_s) \tag{2.10}$$

being $p(t)$ the received pulse[1] to be defined, result of the convolution

$$p(t) = r(t) \star h(t) \tag{2.11}$$

To guarantee zero ISI, the following conditions should be respected, known as the

[1] $r(t)$ is the pulse shape before matched filtering and $p(t)$ is the pulse shape after matched filtering.

"Nyquist criterion for distortionless baseband transmission". [13]

$$p(t) = p(kT_s) = \begin{cases} p(0) & , \quad k = 0 \\ 0 & , \quad k \neq 0 \end{cases}$$

$$\sum_n P(f - \frac{n}{T_s}) = C^{te} \tag{2.12}$$

Under this property, the only symbol different from zero at the decision time $t = kT_s$ will be a_k, therefore eliminating the inter symbol interference.

2.2.1 Ideal Nyquist Channel

The simplest form of satisfying (2.12) is to shape the frequency function $P(f)$ in form of a rectangular pulse, $rect(f)$, characterized by

$$P(f) = \begin{cases} \frac{1}{2W} & , \quad -W < f < W \\ 0 & , \quad |f| > W \end{cases} \tag{2.13}$$

with the overall bandwidth W defined by

$$W = \frac{R_s}{2} = \frac{1}{2T_s} \tag{2.14}$$

where W defines the bandwidth and R_s the bit rate of the pulse. From the Fourier-Transform, it is finally found that a signal waveform that respects the Nyquist criterion for zero ISI is defined by

$$\begin{aligned} p(t) &= \frac{sen\,(2\pi W t)}{2\pi W t} \\ &= sinc\,(2Wt) \end{aligned} \tag{2.15}$$

known as the *sinc* function. The bit rate value $R_b = 2W$ is called the "Nyquist rate"and the bandwidth W the "Nyquist bandwidth". According to this, the signal produced by (2.13) in frequency domain and (2.15) in time domain, and illustrated in figure 2.4 is known as the "ideal Nyquist pulse".

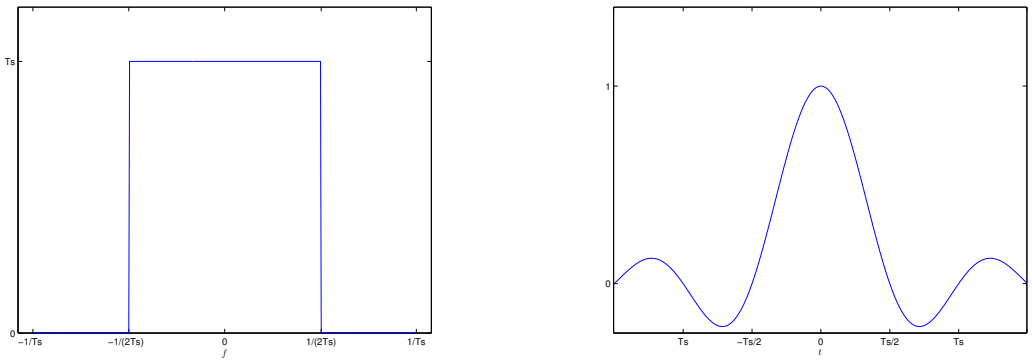

(a) (b)

Figure 2.4: Ideal Nyquist waveforms. Frequency spectrum (a) and time domain pulse (b).

2.2.2 Raised Cosine Pulses

In order to overcome the practical difficulties with ideal Nyquist channel design and to ensure the physical implementation of a zero ISI channel pulse, a different solution of the ideal Nyquist channel is required: one where a modified $P(f)$ decreases slowly towards zero. This type of pulse is characterized by a roll-off factor α, being $\alpha = 0$ equals to the ideal Nyquist channel described in the previous section. Its

mathematical equation in the frequency domain is

$$P_{RC}(f) = \begin{cases} T_s & , \quad f \leq \dfrac{1-\alpha}{2T_s} \\ \dfrac{T_s}{2}\left\{1 + cos\left[\dfrac{\pi T_s}{\alpha}\left(|f| - \dfrac{1-\alpha}{2T_s}\right)\right]\right\} & , \quad \dfrac{1-\alpha}{2T_s} < f < \dfrac{1+\alpha}{2T_s} \\ 0 & , \quad f \geq \dfrac{1+\alpha}{2T_s} \end{cases} \tag{2.16}$$

and in time domain is

$$p(t) = \left(sinc\left(\frac{t}{T_s}\right)\right)\left(\frac{cos\left(\frac{\pi\alpha t}{T_s}\right)}{1 - \frac{4\alpha^2 t^2}{T_s^2}}\right) . \tag{2.17}$$

Figure 2.5 illustrates these pulses, according to different *roll-off* factors.

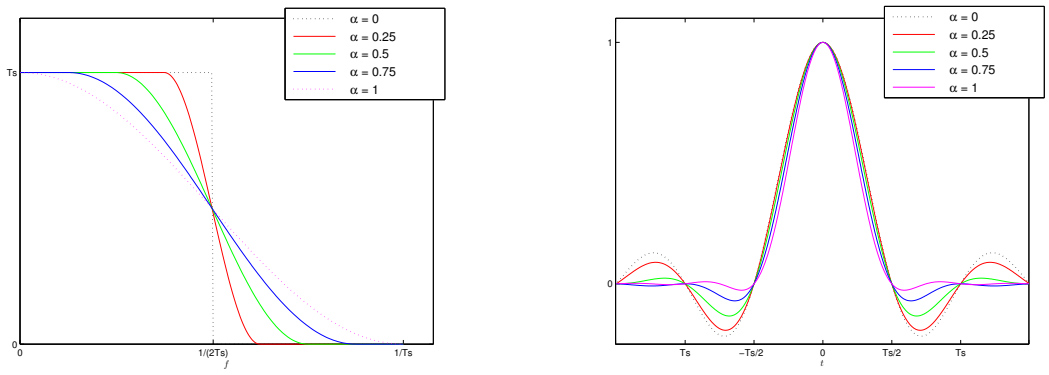

(a) (b)

Figure 2.5: Raised Cosine pulses in frequency domain (a) and time domain (b).

2.2.3 Root-Raised Cosine Pulses

The Root-Raised Cosine pulses, also known as Square-Root Raised Cosine, are Nyquist pulses of finite bandwidth that derives from the Raised Cosine filter of

section 2.2.2. Its mathematical expression could be written as

$$P_{RRC}(f) = \sqrt{|P_{RC}(f)|} \tag{2.18}$$

Therefore, the Raised Cosine pulse shape can be expressed as the multiplication of two Root-Raised Cosine pulses:

$$P_{RC}(f) = P_{RRC}(f) \cdot P_{RRC}(f) \tag{2.19}$$

As it is possible to observe in Figure 2.6, which illustrates these pulses according to different *roll-off* factors, and unlike the Raised Cosine filter, the Root-Raised Cosine impulse response is not zero at the intervals of $\pm T_s$. Only in the case of $\alpha = 0$ the Root-Raised Cosine has zeros at $\pm T_s$.

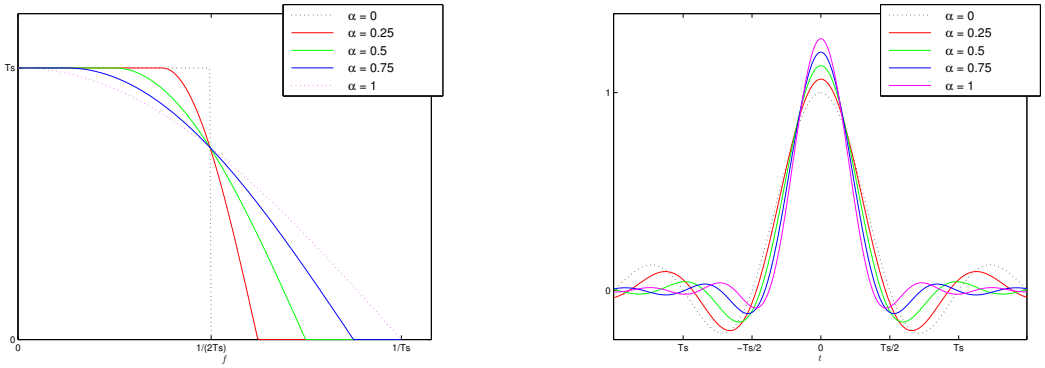

(a) (b)

Figure 2.6: Root-Raised Cosine pulses in the frequency domain (a) and time domain (b).

2.3 Faster-than-Nyquist Signaling

As seen before, a band-limited transmission without inter symbol interference (ISI) is possible to achieve by employing pulses that satisfy the Nyquist criterion, with the most popular being the so-called Raised Cosine pulses (and Root-Raised Cosine pulses as well), with a minimum bandwidth of half the symbol rate, also known as Nyquist bandwidth. The maximum spectral efficiency is associated to the minimum bandwidth, that increases with the roll-off factor α, usually required to be above 0.25, due to implementation difficulties. This extra bandwidth is generally regarded as unavoidable when designing wireless communication systems, however, it is still possible to achieve optimum asymptotic performance with a bandwidth below the minimum Nyquist bandwidth, through applying Faster-than-Nyquist signaling. In fact, for binary signaling we can reduce the symbol separation by a factor β up to 0.802 without asymptotic performance degradation, which is usually known as "Mazo's limit"[3]. This FTN factor, where $\beta \leq 1$, corresponds to the Nyquist bandwidth occupation W of the Faster-than-Nyquist pulse

$$\beta W = (1 - \Delta_f)\, W \ . \tag{2.20}$$

Figure 2.7 displays a Nyquist and FTN pulse with a roll-off factor of $\alpha = 0.5$ for a bandwidth $W = \frac{1}{T_s}$, in the frequency domain, where the pulse for FTN occupies only $\beta W = 0.802\ W$ and $\beta W = 0.7\ W$ of the Nyquist bandwidth. As observed, the FTN pulse, despite being smaller in bandwidth than the Nyquist pulse, it is capable of modulating a signal in the entire W bandwidth due to the extra bandwidth provided by the root-raised cosine. So, it is possible to observe that FTN signaling only requires $2\beta W$ of bandwidth if the roll-off factor α extends a total bandwidth of $2W$.

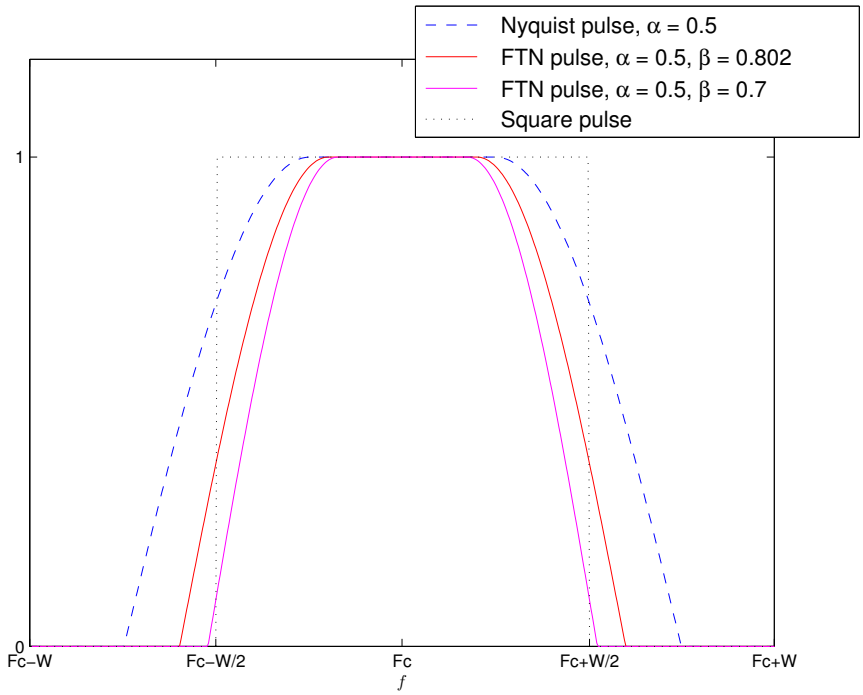

Figure 2.7: Root-raised cosine in the frequency domain for a roll-off $\alpha = 0.5$ for Nyquist and FTN signaling.

2.4 Single Carrier with Frequency Domain Equalization

To meet the high data rate requirements of nowadays mobile communications while dealing with time-dispersive channels, equalization techniques are required at the receiver side in order to compensate channel distortion and guarantee admissible performance. It is known that the Viterbi [14] equalizer is the optimum receiver to deal with this type of channel, although its complexity grows with the length of the Channel Impulsive Response (CIR). As result of its low complexity requirements, as well as reduced envelope fluctuations, Single Carrier modulation is an effective technique to cope with this problematic, being adopted for the uplink of 3GPP LTE and allowing cheaper user terminals with more efficient high-power amplifiers.

In SC-FDE schemes, data is transmitted in blocks of N useful symbols, resulting

from a direct mapping of the original data into a selected signal constellation. For a linear modulation, the complex envelope of an N-symbol burst can be written as

$$s(t) = \sum_{n=0}^{N-1} a_n \, r(t - nT_s) \tag{2.21}$$

where a_n is a complex coefficient that corresponds to the n^{th} symbol, mapped in the selected signal constellation (e.g., PSK (Phase Shift Keying) or QAM (Quadrature Amplitude Modulation) constellation), $r(t)$ represents the support pulse and T_s refers to the symbol duration. By applying the Fourier Transform (FT) to (2.21) we obtain

$$S(f) = \mathcal{F}\{s(t)\} = \sum_{k=0}^{N-1} A_k \, R(f) \, e^{-j2\pi f k T_s} \tag{2.22}$$

where $R(f)$ denotes the FT of the support pulse $r(t)$ and A_k the Discrete Fourier Transform (DFT) of a_n. Therefore, the transmission bandwidth associated with each data symbol is equal to the band occupied by $R(f)$. For a transmission without ISI at the receiver's matched filter bound, the $r(t)$ pulse must verify the following orthogonality condition

$$\int_{-\infty}^{+\infty} r(t - nT_s) \; r^*(t - n'T_s) \; dt = 0 \,, \quad n \neq n'. \tag{2.23}$$

If conventional SC modulations are employed requiring data transmission rates of Mbits/s over severely time-dispersive channels high signal distortion levels can arise, which will increase the complexity of the receiver equalization required to overcome this problem, as the transmission bandwidth becomes much greater than the channel's coherence bandwidth.

In order to prevent block contamination by ISI from the previous block, SC-FDE schemes use a cyclic prefix (CP) placed in the beginning of every transmitted block. This prefix, shown in Figure 2.8, is a repetition of the last N_{cp} data symbols in the

block and it is also useful to make the received block appear to be cyclic with period NT_s. To ensure that the inter-block interference (IBI), from the previous block, is absent, the length of the CP should be longer than the channel impulse response.

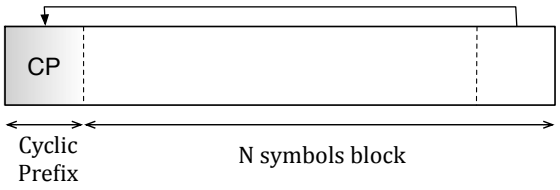

Figure 2.8: Data burst with Cyclic Prefix.

The complex envelope of the transmitted signal, a N symbols burst with a CP appended, is now

$$s(t) = \sum_{n=-N_{cp}}^{N-1} a_n \, r(t - nT_s) \ , \tag{2.24}$$

where $r(t)$ is the support pulse and T_s represents the symbol period. The transmission structure of a SC-FDE scheme is described in Figure 2.9, where a cyclic prefix is attached to the N symbols burst

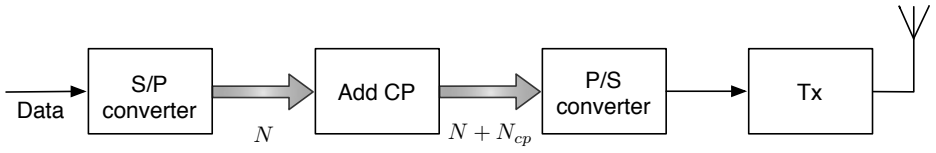

Figure 2.9: Basic SC-FDE transmitter.

and then modulated in the selected constellation and multiplied by the transmitted impulse $r(t)$, as observed in Figure 2.10 which represents the Tx block of the transmitter node.

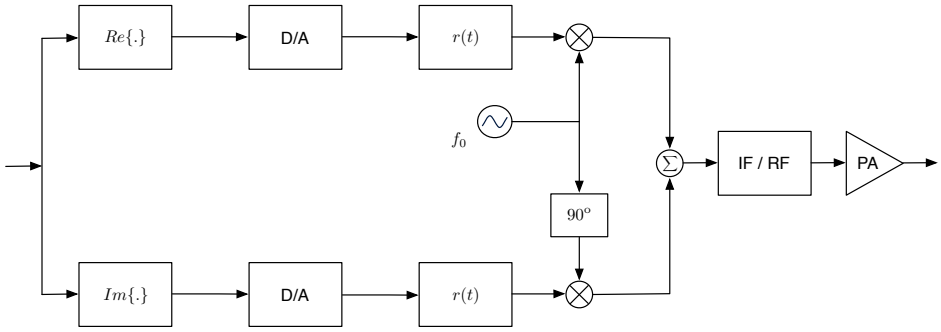

Figure 2.10: Tx block in a SC-FDE transmitter.

2.4.1 Linear Frequency Equalization

The use of block-wise transmission using FDE at the receiver's side is based on the DFT [8] [9], which can be efficiently implemented through the Fast Fourier Transform (FFT) algorithm. This approach reduces significantly the receiver's complexity and, when combined with modulations with low envelope fluctuations, can achieve reduced Peak-to-Mean Envelope Power Ratio (PMEPR) leading to low power amplification requirements.

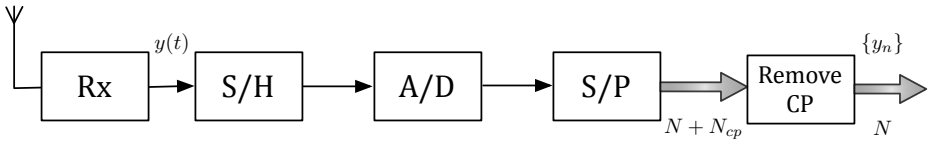

Figure 2.11: Basic SC-FDE receiver.

At the reception structure, represented in the diagram of Fig. 2.11 and 2.12, the received signal is demodulated, being down-converted and filtered, sampled and A/D converted The resulting signal is then converted to parallel and the CP samples are removed resulting on the N initial data symbols, leading in the time-domain the samples $\{y_n; n = 0, ..., N-1\}$.

The process of equalization begins with shifting the data block to frequency domain using a N-point FFT function, resulting the corresponding frequency-

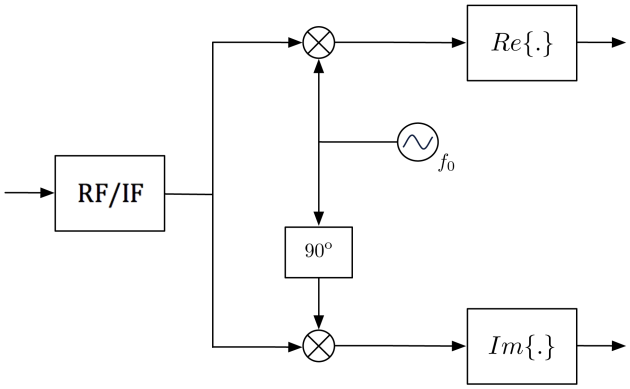

Figure 2.12: Rx block in a SC-FDE receiver.

domain samples $\{Y_k; k = 0, ..., N-1\}$, with Y_k given by

$$Y_k = H_k A_k + N_k \tag{2.25}$$

where H_k and N_k represents the channel frequency response and noise term in frequency-domain for the k^{th} frequency, respectively.

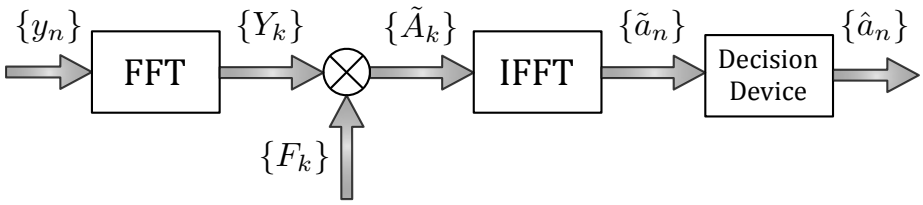

Figure 2.13: SC-FDE equalization structure.

After equalization and for a linear FDE, the estimated frequency-domain samples $\tilde{A}_k$ are given by

$$\tilde{A}_k = F_k Y_k \tag{2.26}$$

where $\{F_k; k = 0, ..., N-1\}$ represents a different coefficient value to each k^{th} frequency. This coefficient can be obtained under a Zero Forcing (ZF) criterion, which can be problematic when the channel presents several deep faded frequencies,

denoted by

$$F_k = \frac{1}{H_k} = \frac{H_k^*}{|H_k|^2} \ , \tag{2.27}$$

or by employing a Minimum Mean Square Error (MMSE) criterion, avoiding the previous stated problem and minimizing the combined effect of ISI and channel noise, which leads to the set of optimized coefficients

$$F_k = \frac{H_k^*}{\xi + |H_k|^2} \tag{2.28}$$

with ξ as the inverted signal-to-noise ratio (SNR). The equalized samples $\{\tilde{A}_k; k = 0, ..., N-1\}$ are then converted back to the time-domain by a IFFT block leading to the time-domain equalized samples $\{\tilde{a}_n; n = 0, ..., N-1\}$, which will be used to make decisions on the transmitted symbols.

2.5 Iterative Block with Decision Feedback Equalization

The previously described SC-FDE receiver is a linear FDE. Nevertheless, non-linear equalization such as decision feedback equalizers (DFE) can outperform linear equalizers, presenting itself as a popular choice when seeking for a good tradeoff between performance and complexity. However, as the time length of the channel response increases, conventional time-domain DFE becomes too complex and more sensitive to error propagation, specially when the feedback filters have a large number of taps. So, ideally the feedforward and feedback equalization should be kept completely in the frequency domain. An efficient way of doing this, for SC schemes, is by replacing the linear FDE by an IB-DFE. This IB-DFE scheme was proposed

in [17] and extended to diversity scenarios in [16]. These schemes implement both feedforward and feedback equalization in the frequency domain in an iterative way.

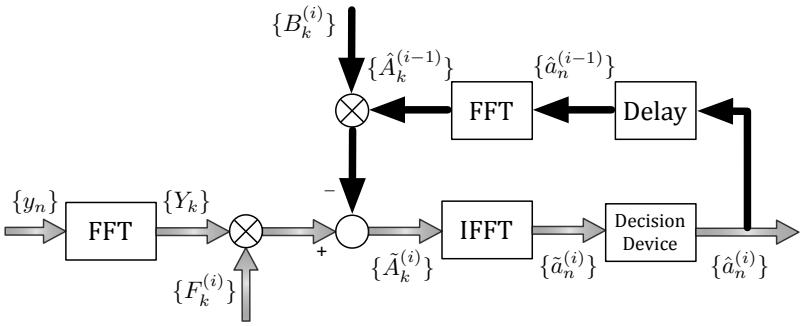

(a)

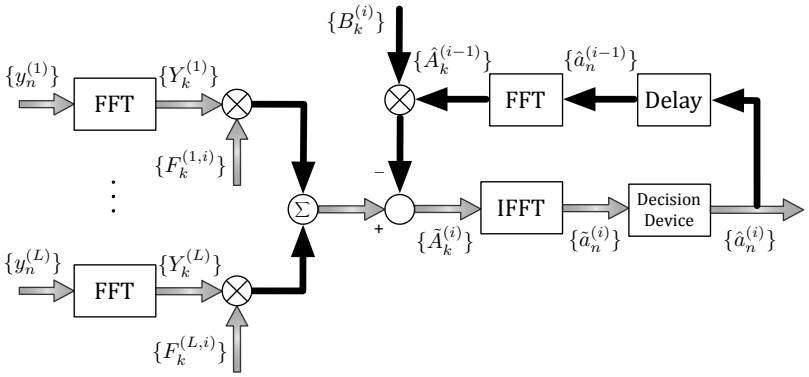

(b)

Figure 2.14: IB-DFE receiver block diagram without (a) and with an L-branch space diversity (b).

From Figure 2.14, it can be seen that for the first iteration, as there is no information regarding a_n, the IB-DFE reduces to a linear FDE. For the next iterations, the decisions from the previous operation are fed into the system, reducing significantly the error propagation problem. Therefore, after several iterations, we have an almost full cancellation of the residual ISI through the feedback coefficients, while the

feedforward coefficients perform an approximate matched filtering. Thus, it becomes clear that IB-DFE techniques offer a much better performance than non-iterative methods.

2.5.1 Definition

Let us consider an L-order space diversity IB-DFE for SC-FDE scheme. For a given i^{th} iteration, the $\tilde{A}_k^{(i)}$ frequency output samples are defined as

$$\tilde{A}_k^{(i)} = \sum_{l=1}^{L} F_k^{(l,i)} Y_k^l - B_k^{(i)} \hat{A}_k^{(i-1)} \ , \tag{2.29}$$

where $\{F_k^{(l,i)} \ ; \ k = 0, 1, ..., N-1; \ l = 1, ..., L\}$ and $\{B_k^{(i)} \ ; \ k = 0, 1, ..., N-1\}$ represents the feedforward and feedback equalizer coefficients, respectively, $\{Y_k^l \ ; \ k = 0, 1, ..., N-1\}$ is the DFT of the time-domain received block and $\{\hat{A}_k^{(i)} \ ; \ k = 0, 1, ..., N-1\}$ is the DFT of the hard-decision block of the $(i-1)^{th}$ iteration associated to the transmitted data block.

2.5.2 Receiver Parameters

The feedforward and feedback IB-DFE coefficients $F_k^{(i)}$ and $B_k^{(i)}$, respectively, are chosen in order to maximize the "Signal-to-Interference plus Noise Ratio"(SINR). Considering an IB-DFE with "hard-decisions", the optimum feedforward coefficients are given by

$$F_k^{(l,i)} = \frac{\kappa^{(i)} H_k^{(l)*}}{\xi + \left[1 - \left(\rho^{(i-1)}\right)^2\right] \sum_{l'=1}^{L} |H_k^{(l')}|^2} \ , \ l = 1, 2, ..., L \tag{2.30}$$

and the feedback coefficients are

$$B_k^{(i)} = \rho^{(i-1)} \left(\sum_{l'=1}^{L} F_k^{(l',i)} H_k^{(l')} - 1 \right) \tag{2.31}$$

where $\kappa^{(i)}$ is selected to ensure that $\gamma^{(i)} = 1$, ξ as the inverted signal-to-noise ratio (SNR) and the correlation coefficient $\rho^{(i)}$, a measure of the reliability of the decisions used in the feedback loop, is defined as

$$\rho^{(i)} = \frac{E\left[\hat{a}_n^{(i)} a_n^*\right]}{E\left[|a_n|^2\right]} = \frac{E\left[\hat{A}_k^{(i)} A_k^*\right]}{E\left[|A_k|^2\right]} \ . \tag{2.32}$$

The residual ISI component, $\gamma^{(i)}$, in the frequency domain, associated to the difference between the average channel frequency response after the feedforward filter, is defined as

$$\gamma^{(i)} = \frac{1}{N} \sum_{k=0}^{N-1} \sum_{l'=1}^{L} F_k^{(l',i)} H_k^{(l')} \ , \tag{2.33}$$

which would have a constant value for null ISI. Clearly, $\gamma^{(i)}$ can be regarded as the average overall channel frequency response at the i^{th} iteration, after combining the outputs of the L output filters.

It is important to remark that, for the first iteration ($i = 0$), the information about a_n is unavailable, which means that $\rho = 0$ and $B_k^{(0)} = 0$. Under these conditions, the values of $F_k^{(0)}$ are easily obtained by

$$F_k^{(l,0)} = \frac{\kappa^{(0)} H_k^{(l)*}}{\xi + \sum_{l'=1}^{L} |H_k^{(l')}|^2} \ , \ l = 1, 2, ..., L \tag{2.34}$$

corresponding to the optimum frequency-domain equalizer coefficients under the MMSE criterion. Therefore, the IB-DFE is reduced to a linear FDE on the first iteration. It is also worth mentioning that without diversity, the IB-DFE parameters

are derived from the equations above assuming $L = 1$.

2.5.3 IB-DFE with Soft Decisions

To improve the IB-DFE performance, increasing immunity against error propagation, it is possible to use "soft-decisions" by replacing the "blockwise averages" by "symbol averages", which can be done in the following way.
For a normalized QPSK constellation under a Gray mapping rule , i.e. $a_n^I = Re\{a_n\} = \pm 1$ and $a_n^Q = Im\{a_n\} = \pm 1$, following [17] and [18] we may write

$$\bar{a}_n^{I(i)} = tanh\left(\frac{L_n^{I(i)}}{2}\right) \tag{2.35}$$

and

$$\bar{a}_n^{Q(i)} = tanh\left(\frac{L_n^{Q(i)}}{2}\right) \ , \tag{2.36}$$

where L_n^I and L_n^Q are the LLRs (Log Likelihood Ratios) of a_n^I and a_n^Q, the in-phase and quadrature bit estimation, respectively, given by

$$L_n^I = \frac{2\,Re\{\tilde{a}_n^{(i)}\}}{\sigma_N^2} \tag{2.37}$$

and

$$L_n^Q = \frac{2\,Im\{\tilde{a}_n^{(i)}\}}{\sigma_N^2} \ , \tag{2.38}$$

with the total variance of the channel and interference noise, σ_N^2, given by

$$\sigma_N^2 \ = \ \frac{1}{2}E[|a_n - \tilde{a}_n^{(i)}|^2] \ \approx \ \frac{1}{2N}\sum_{n=0}^{N-1}|\hat{a}_n^{(i)} - \tilde{a}_n^{(i)}|^2. \tag{2.39}$$

In this case, the feedforward coefficients, $F_k^{(i)}$, are given by (2.30) and, since $\bar{A}_k^{(i)}$ is equivalent to $\rho^{(i)}\hat{A}_k^{(i)}$, the feedforward coefficients, $B_k^{(i)}$, are given by

$$B_k^{(i)} = F_k^{(i)} H_k - 1\,. \tag{2.40}$$

Finally, the estimated data symbols are obtained by

$$\tilde{A}_k^{(i)} = \sum_{l=1}^{L} F_k^{(l,i)}\, Y_k^l - B_k^{(i)}\, \bar{A}_k^{(i-1)}\,. \tag{2.41}$$

2.5.4 Conclusions

Clearly, the IB-DFE techniques offer much better performances than non-iterative methods [19]. With a conventional IB-DFE receiver the log-likehood values are computed on a symbol-by-symbol basis (i.e. it is not necessary to perform the channel decoding in the feedback loop). Consequently, conventional IB-DFE schemes can be considered as low complexity turbo equalizers [20] [21] since the feedback loop employs the equalizer outputs rather than the channel decoder outputs.

In Figure 2.15 it is shown the average BER performance for a fading channel. It is considered a SC modulation with a QPSK constellation, that uses a IB-DFE receiver with 1, 2, 3 and 4 iterations, as well as, for sake of comparison, the corresponding performances of the MFB and AWGN channel.

As it can be observed from the results, the E_b/N_0 required for BER = 10^{-4}, in the first iteration, is around 15 dB (corresponding to a linear FDE), reducing to 11 dB after two iterations and, after four iterations, the IB-DFE receiver stabilizes at less than 10 dB. This results make clear that the use of iterative receivers allows a significative performance improvement. Moreover, the asymptotic BER performance becomes close to the MFB after few iterations.

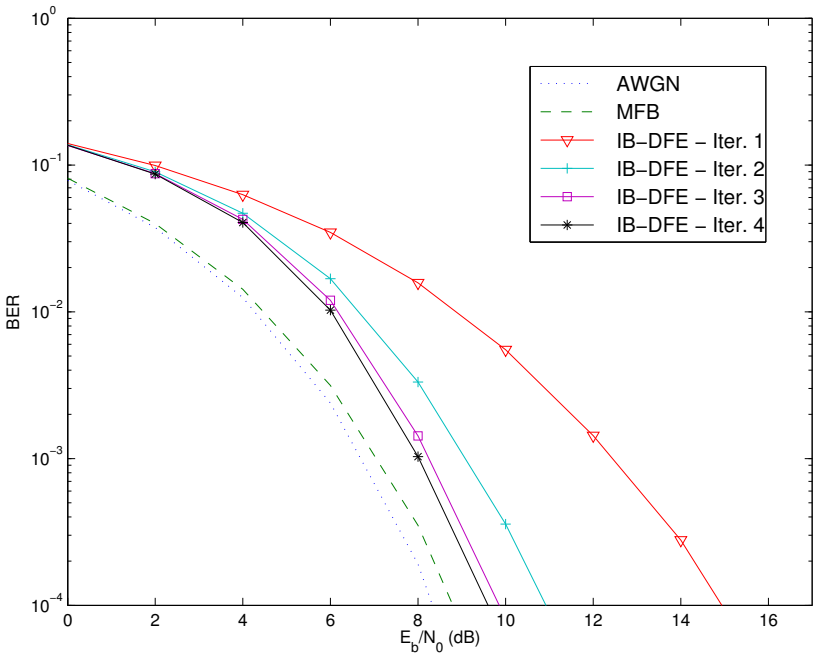

Figure 2.15: BER in a AWGN channel assuming different iterations of the IB-DFE receiver.

2.6 Medium Access Control

In telecommunications, Medium Access Control (MAC) schemes are important in a wireless environment to coordinate Mobile Terminals (MTs) eligible for packet transmission. This means that MAC protocols have the purpose to control the access of communicating stations to the wireless medium, sharing the network bandwidth [22]. Meanwhile, multiple MTs might contend the wireless channel and interfere with each other [23]. Therefore, the design of the access scheme is of extreme importance, since it should enhance the throughput of the system and diminish the interference between the different MTs. An analogy to this problem can be a room filled with people, all of them trying to talk with each other. If all of them talk at the same time, the message would not arrive correctly at the receptor due to the high level of noise.

In this chapter, methods of controlling the multiple access of MTs to the wireless

medium are presented. The first one to be presented is the Time Division Multiple Access (TDMA) that allocates to each user a pre-defined time slot. Then, the Frequency Division Multiple Access (FDMA) which determines a different bandwidth to each MT and, at last, the Demand Assigned Multiple Access (DAMA) method is presented, as a way of increasing efficiency through an advanced capacity of slot reservation.

More recently, in order to support higher data rates and to be able to cope with severe multi-path propagation, two additional solutions were adopted in the WiMax/3GPP-LTE systems: Orthogonal Frequency Division Multiplexing (OFDM) and Single-Carrier Frequency Domain Equalization (SC-FDE), being the last one of the basis to this dissertation, as already mentioned before.

2.6.1 Time Division Multiple Access

TDMA consists in the pre-allocation of a different time-slot for each user terminal. The communication of MTs is made in carriers with the same frequency and bandwidth, with the limitation of only being possible to one device at the same time. For this to be feasible, it is mandatory the previous scheduling of MTs in time-slots, so that the terminal can exactly know the time interval when it is allowed to communicate. A prefix is introduced to each burst in order to synchronize the time-slots and correspondent messages. This information is extremely relevant because of the problem of the terminal spacial mobility and subsequent "Round-Trip Time"variation.

A visual explanation of a TDMA scheme is shown in Figure 2.16, where it is possible to observe that for individual MTs a specific time interval is offered when the user is able to send and receive information.

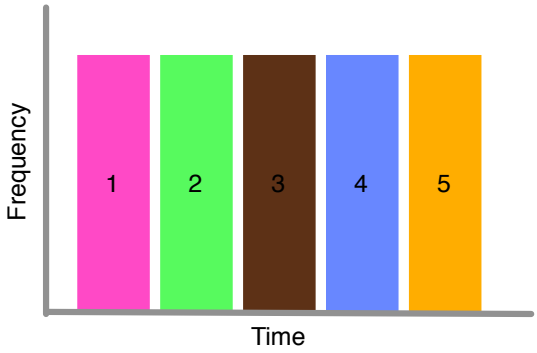

Figure 2.16: TDMA

2.6.2 Frequency Division Multiple Access

The FDMA channel access method is based on the Frequency Division Multiplexing (FDM) scheme, which associates different frequency bandwidth to each MT, that own full exclusivity of that band for its data stream. [22]

This technique was used in several communication systems before but, due to its limitations for a large bandwidth in ISI channels and receiver complexity, FDMA was improved by two additional approaches - OFDM and SC-FDE - used in Long Term Evolution (LTE) systems. An illustration of a FDMA scheme is shown in Fig. 2.17, where the assignment of individual frequencies for different users with no time restrictions can be observed.

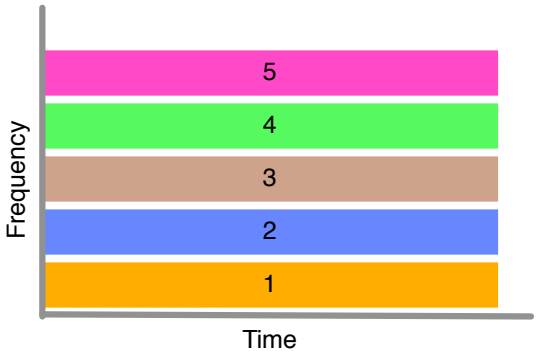

Figure 2.17: FDMA

2.6.3 Demand Assigned Multiple Access

DAMA is a class of multiple-access methods, intended to increase efficiency even more by an advance capacity reservation procedure. DAMA protocols allocate bandwidth to MTs according to their QoS constraints [24], based in FDMA or TDMA architectures, being suitable to situations where the traffic pattern is random and with large variations. Because of its ability to allocate capacity on demand, this protocol avoids an inefficient use of transponder capacity. MAC protocols that apply DAMA can use bandwidth efficiently and increase the throughput, due to the ability to allocate capacity on demand, following the station capacity requests. This reservation on demand can be explicit or implicit [25]. Regarding implicit reservation, stations compete for reservation slots by using Slotted Aloha. Slotted Aloha is a way to allocate users, by taking into account consensus among users on slot boundaries definition. By using slotted-Aloha protocol, the channel is slotted into segments with a duration exactly equal to single packet transmission time. Slotted-Aloha eliminates the partial overlapping, because terminals are synchronized to start the transmission of packets at the beginning of a slot. In Explicit Reservation, all frames have a control subframe with a sequence of bits, which serve to announce or reserve upcoming transmissions. This type of reservation scheme reserves future channel time, in order to send messages to a specific station.

2.7 Error Correction Schemes

When data is transmitted through a communication channel, it is subject to errors caused by a variety of reasons, such as multi-path fading and shadowing, among others [26]. With the purpose of eliminating this problem, or at least minimize it in order to ensure reliable communication some error correction techniques may

be employed. In this section, Forward Error Correction (FEC), Automatic Repeat Request (ARQ) and Diversity Techniques are discussed. As an important part of this dissertation, Hybrid-ARQ will be then discussed in detail.

2.7.1 Forward Error Correction

FEC schemes, also referred as error-correction codes, is a detection technique and posterior correction of ocasional errors in a data packet. The strategy used in FEC consists in the inclusion of additional redundant information in the data blocks to transmit, allowing the receiver to analyze and detect possible errors in order to confirm the correct reception of the package, or, if not, to correct the deficient data.

The FEC concept arrived during the 1940s, through the studies of R. W. Hamming, which proposed the famous Hamming codes at Bell laboratories, in order to prevent read errors in punch cards for rely-based electro-mechanical computers. In the following decades, new codes were born and, consequently, algorithms were created to handle these codes. During the evolution of FEC codes three generations can be identified. The first generation of FEC codes used linear block codes - it is based on hard decision coding, which consists in a single quantization level in a bit sampling. The second generation of FEC are concatenated codes which are, as the name suggests, a junction of more than one type of coding. At last, a special form of concatenated codes are Turbo Codes and Low Density Parity Check (LDPC), based on soft decisions and iterative decoding. [27]

Nowadays, turbo codes are often used in communication systems as they are considered the most powerful codes, almost achieving Shannon's theoretical limit. [28]

2.7.2 Automatic Repeat Request

In an Automatic Repeat Request (ARQ) system the receiver, through an error-detecting code with a certain retransmission protocol, discards an erroneously received data packet if an error is detected and requests to the transmitter, using control messages, a retransmission of the data. This process is repeated as many times as necessary until the data packet is successfully received.

The error detection is possible due to the introduction of redundant bits in the data burst (like the FEC method mentioned before), which will be tested by the receiver. In case of correspondence with the expected data, the receiver informs the transmitter side of the success in the operation. Otherwise, an error is detected and the data is discarded, being requested the correspondent retransmission to the sender.

The main advantages of ARQ schemes lie in the low complexity and high reliability offered. Nevertheless, as data error rates increases, the system throughput substantially reduces due to the need of more redundant bits in the data packet as well as the number of retransmission requests increases.

2.7.3 Diversity Techniques

Diversity techniques refers to a kind of schemes where the method for improving the reliability of a message signal is to use two or more communication channels with different characteristics. This type of technique plays an important role when the communication channel presents severe interference effects and error bursts occurs leading to poor reception reliability. These problems could be avoided by combining multiple versions of the same signal, received in different time intervals or different frequencies.

Time diversity consists on the transmission of multiple versions of the same signal at different time instants [29]. Usually, it works by the BS demanding data retransmissions from a MT when the message is received with data errors. Automatic Repeat Request (ARQ) and Hybrid-ARQ schemes can be considered as a subset of the time diversity class, which will be explored in the following section.
In frequency diversity the signal is transmitted using multiple frequency channels or spread over a defined bandwidth. This method, widely used in nowadays wireless communication systems as SC equalization (section 2.4), spread spectrum methods (CDMA) or Multi-Carrier systems like OFDM, presents the problem of non-linear frequency response, essentially due to the occurrence of fading and ISI in the communication channel. The methods presented before exploit and minimize these limitations through an efficient equalization with good results, being chosen for the LTE/WiMax 3GPP standards.
Finally, in spatial diversity the signal is transmitted through different propagation paths. This means, particularly in wireless communication, that the transmitter or the receiver terminals (in some cases both of them) use multiple antennas dealing with the signal. A well known example of spatial diversity is the Multiple Input Multiple Output (MIMO) scheme, a standard for LTE and 3GPP WiMax, where both the transmitter and the receiver use multiple antennas to improve communication performance. The different copies of the message are then combined in order to improve communication performance. [30]

2.7.4 Hybrid-ARQ schemes

Hybrid-ARQ schemes are a combination of FEC and ARQ techniques, both explained in the previous subsections, consisting of a FEC subsystem contained in an ARQ system. Embracing FEC as a function of an ARQ system reduces the frequency of retransmissions by correcting some error patterns which occurs more often. Thus,

the system throughput may be increased as these errors are corrected and, with this combination done in a proper way, the disadvantages of both techniques can be overcome [31]. This approach opens the door to a more reliable system than a FEC only and also a higher throughput system than ARQ only.

The H-ARQ schemes can be divided into two categories: Type-I Hybrid ARQ and Type-II Hybrid ARQ [31]. Hybrid ARQ techniques are currently used in 3GPPs High-Speed Downlink Packet Access (HSDPA), High-Speed Uplink Packet Access (HSUPA) and LTE. Furthermore, since the work done in this thesis relies on Hybrid-ARQ architectures, an overview will be given about this topic.

Type-I Hybrid-ARQ schemes

The Type-I Hybrid ARQ protocol is the simplest of hybrid protocols. In this technique, each data packet is encoded for error correction and error detection, suitable for both FEC and ARQ schemes. The message estimation and the error detection parity bits are output to an FEC decoder, which tests it for error detection to determine if the message should be accepted or rejected due to errors. It is possible to achieve better performance with this protocol when the message is long and/or the signal strength is low.

The crossover point in terms of performance between ARQ protocols and Type I H-ARQ protocols happens in cases where signal strength is high. In these cases, this hybrid protocol type does not improve the efficiency, because a strong signal allows the delivery of free error messages.

Type-II Hybrid-ARQ schemes

Type-II Hybrid ARQ protocols are mainly based in incremental redundancy, since this scheme takes into account the channel conditions, adapting itself to interference and/or noise present in it. It is an adaptive scheme by behaving like a pure ARQ when the channel presents a good behavior and while the channel becomes noisy,

extra parity-check bits are added to the codeword.

In this protocol, a message in its first transmission is coded with parity-check bits for error detection only, as in a pure ARQ scheme, forming a codeword. If the receiver detects an error in the respective codeword, it saves the erroneous word and requests a retransmission. Now, the retransmission is not necessarily the original codeword, as is in type-I scheme, but can be a block of parity-check bits formed based on the original codewords and an error-correcting code. After this block of parity-check bits has been received, it is used to correct the errors presented in the previous stored codeword. If it does not succeed, a second retransmission is requested. The second retransmission may be either a repetition of the first and original codeword or another block of parity-check bits, depending on the retransmission strategy and the type of error-correcting code to be used.

The main goal of Type-II H-ARQ protocols is to work with the efficiency given by plain ARQ protocols in strong signals and to obtain the improvement of type I H-ARQ when the quality of the signal is lower.

Code Combining and Diversity Combining

Costelo et al [11] defined two main categories to classify the Type-II Hybrid ARQ family, commonly known and referred as packet combining systems: Code-Combining (CC) and Diversity-Combining (DC) systems. In code-combining systems, the packets are concatenated to form noise-corrupted codewords from increasingly longer and lower rate codes. In diversity-combining systems, the individual symbols from multiple, identical copies of a packet are combined to create a single packet with more reliable constituent symbols. These identical copies are obtained by straightforward retransmissions. DC systems are generally suboptimal with respect to CC systems, but are simpler to implement [11]. DC techniques can easily be extended to SC-FDE schemes and provide significant improvements in terms of delay and throughput performance, as will be proved through this

dissertation [32].

2.8 Chapter Overview

The current chapter described a comprehensive bibliography concerning the theme of this thesis. Section 2.1 overviews phase modulation methods, such as BPSK and QPSK, the most commonly used technique for high frequency data transmission. Section 2.2 describes the support pulses used to eliminate ISI, namely the Nyquist's derivative Root-Raised Cosine. In section 2.3 it is explained the essential pulse design regarding this dissertation, the Faster-than-Nyquist pulse shape, a technique that requires less bandwidth than the Nyquist bandwidth, with satisfactory results. Section 2.4 has some comments concerning single-carrier modulation techniques, SC-FDE, and the advantages of its use in uplink communication. In Section 2.5 it is presented the IB-DFE receiver structure for single-carrier transmission, an iterative block that provides much better performance than conventional frequency domain equalization with low complexity design. Section 2.6 briefs traditional MAC schemes and their respective taxonomy. Centralized MAC schemes are appropriate to coordinate MTs actions within the wireless channel, though the MAC scheme should be adequate for strict QoS requirements for a given number of MTs; so a structured network where MTs contend for their access seems appropriate for asymmetric traffic loads. Finally, Section 2.7 overviews error control coding and it is concluded that turbo-coding can achieve near Shannon capacity, though its complexity might be unsuitable for energy-constrained devices. It also presents alternative or complementary techniques to error-coding, named diversity techniques. These techniques can be used on various domains: time, frequency and space. The use of these techniques depends on various requirements: bandwidth, delay, or complex transmitter/receiver structures. From these diversity techniques,

it is possible to achieve not only lower complexity design but also increased efficiency that, combined with the Faster-than-Nyquist signaling explored in this dissertation, creates a technique that explores bandwidth usage with acceptable data transmission error rates.

Chapter 3

Iterative FDE for Faster-than-Nyquist Signaling

In the previous chapter was shown that block transmission techniques employing FDE equalization are suitable in a wireless broadband context, in order to handle multi-path dispersive channels. Typically, the receiver for SC-FDE schemes is a linear FDE. Being recognized that non-linear equalizers outperform linear equalizers [19], in this chapter it is presented an IB-DFE receiver specially designed to cope with the overall ISI inherent to both FTN signaling and severely time-dispersive multi-path channels. Bandwidth efficiency is here obtained by the use of FTN signaling for the uplink of broadband wireless systems, employing SC-FDE schemes and taking advantage of the additional bandwidth employed by the root-raised cosine pulse for additional diversity.

The work presented in this chapter was proposed for publication in the *2014 IEEE 80th Vehicular Technology Conference* (VTC2014-Fall).

The chapter is organized as follows: Section 3.1 introduces the ISI problem when implementing FTN signaling with a root-raised cosine pulse shape; section 3.2 describes the pulse shape and the bandwidth diversity technique in use; in section 3.3 a detailed analysis on the IB-DFE receiver is presented; and in section 3.4

performance results on the BER are discussed.

3.1 Motivation

The minimum bandwidth for a ISI-free transmission, according to the assumption of the Nyquist theorem, is half the symbol rate: [13]

$$W = \frac{R_s}{2} = \frac{1}{2T_s}\,. \tag{3.1}$$

As discussed in section 2.2 raised cosine pulses (and root-raised cosine pulses) satisfy Nyquist's criterion. A raised cosine pulse can be mathematically described as (subsection 2.2.3)

$$p(t) = \left(sinc\left(\frac{t}{T_s}\right)\right)\left(\frac{cos\left(\frac{\pi\alpha t}{T_s}\right)}{1-\frac{4\alpha^2t^2}{T_s^2}}\right) \tag{3.2}$$

in the time domain, and represented by (2.16) in the frequency domain. This solution is usually adopted in nowadays wireless communication systems as presents a much simpler practical implementation than the Nyquist's ideal *sinc* pulse, that would require a filter with ideal rectangular shape. The inconvenience on this solution is that, although are simpler to implement, these pulses have a slightly higher bandwidth (typically with roll-off between 0.25 and 0.5). This bandwidth increase is regarded as an unavoidable price when designing wireless systems, known to have significant power and bandwidth constraints.

Following this line of thought, a question arises - the possibility of still achieving optimum asymptotic performance with a bandwidth below the minimum Nyquist band. By employing the so-called Faster-than-Nyquist (FTN) signaling (see section 2.3) the transmission bandwidth can be reduced to around 80% without compromising the minimum Euclidean distance between binary sequences, where

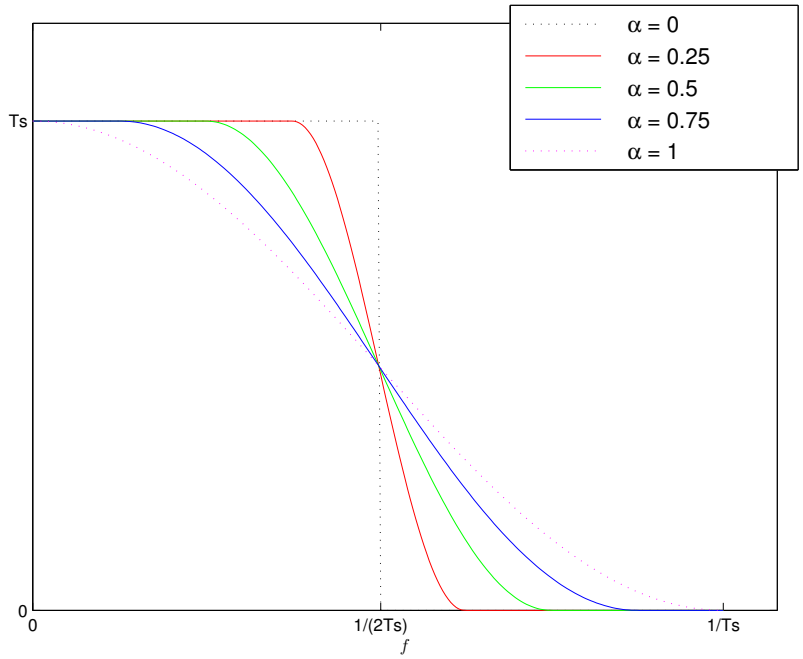

Figure 3.1: Raised cosine pulse in the frequency domain for different roll-off values.

the pulse for FTN occupies only

$$\beta W = (1 - \Delta_f)\, W \tag{3.3}$$

of the Nyquist bandwidth. However, as a drawback of this approach, the ISI inherent to FTN combined with the ISI associated to multi-path time-dispersive effects in the communication channel leads to interference values that are impossible to handle by conventional FTN receivers [4]. In Figure 3.2 it is possible to observe the BER associated to each pulse shape discussed before. It is noticeable the degradation of the BER when the FTN pulse is implemented, corroborating the previous interference statement. To cope with this problem, it is proposed the replacement of the linear FDE by a non-linear FDE [10] - the IB-DFE - in order to improve the performance of the SC-FDE uplink of mobile communications.

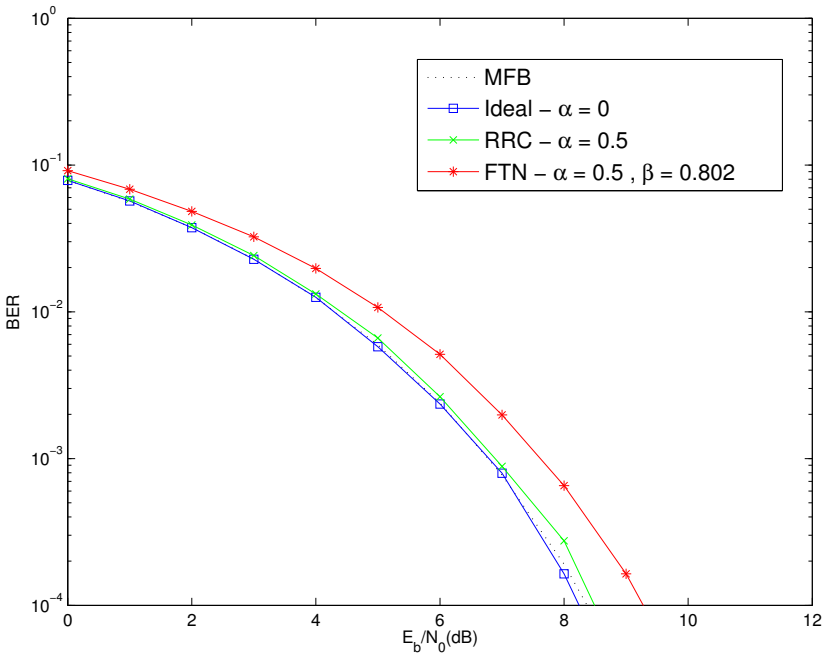

Figure 3.2: BER of Ideal Nyquist signaling ($\alpha = 0$), square-root raised-cosine pulse ($\alpha = 0.5$) and FTN signaling ($\beta = 0.802$) in a AWGN channel assuming linear equalization.

3.2 System Characterization

Let us assume a SC-FDE scheme with a IB-DFE receiver, using FTN signaling. A raised cosine pulse, for a roll-off factor α, symbol transmission time T_s (with bandwidth $W = 1/T_s$) and a FTN factor $\beta = (1 - \Delta_f)$, where $\beta \leq 1$, is often characterized in the frequency domain as

$$R(f,\beta,\alpha,T_s) = \begin{cases} T_s & , \quad 0 \leq |f| \leq \beta\frac{1-\alpha}{2T_s} \\ \frac{T_s}{2}\left\{1 + cos\left[\frac{\pi T_s}{\alpha}\left(|f| - \frac{1-\alpha}{2T_s}\right)\right]\right\} & , \quad \beta\frac{1-\alpha}{2T_s} \leq |f| \leq \beta\frac{1+\alpha}{2T_s} \\ 0 & , \quad |f| > \beta\frac{1+\alpha}{2T_s} \end{cases} \tag{3.4}$$

So, assuming a *normalized* root-raised cosine pulse for a carrier frequency F_c results

$$P^{\dagger}(f, F_c, \beta, \alpha, T_s) = \sqrt{\frac{A^2}{T_s}|R(f - F_c, \beta, \alpha, T_s)|}. \tag{3.5}$$

Figure 3.3 displays (3.5) with a roll-off $\alpha = 0.5$ for a bandwidth $W = 1/T_s$, in the frequency domain, for Nyquist and FTN signaling, where the pulse for FTN occupies only $\beta W = (1 - \Delta_f)W = 0.802W$ of the Nyquist bandwidth. As observed in this

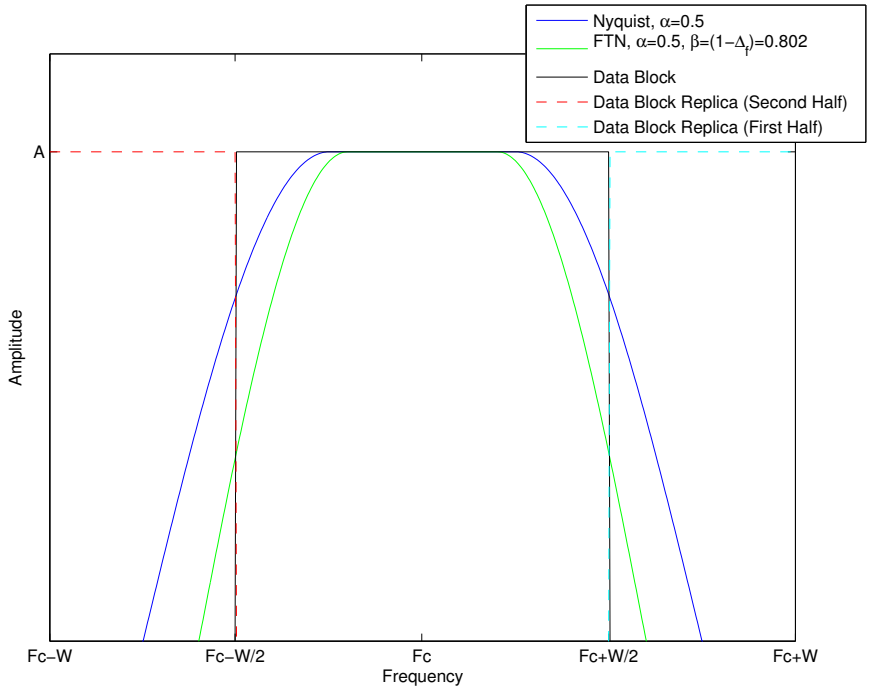

Figure 3.3: Root-raised cosine, $P^{\dagger}(f)$, in the frequency domain for a roll-off $\alpha = 0.5$ for Nyquist and FTN signaling.

example, the FTN pulse, although being smaller in bandwidth than the Nyquist pulse, it is capable of modulating a signal in the entire W bandwidth due to the extra bandwidth provided by the root-raised cosine. So, as already mentioned in section 2.3, it is possible to observe that FTN signaling only requires $2\beta W$ of bandwidth if the roll-off α extends a total bandwidth of $2W$.

3.2.1 Bandwidth Diversity

In both Nyquist and FTN types of signaling, it is possible to take advantage of the additional bandwidth from the root raised cosine pulse outside of $[F_c - W/2, F_c + W/2]$, using it as additional diversity to diminish packet errors. With the additional bandwidth that can be re-used in the intervals $[F_c - \beta W, F_c - W/2[$ and $]F_c + W/2, F_c + \beta W]$, with $0.5 < \beta \leq 1$ (which depends on the shape of (3.2)), the SC-FDE data block can be partially replicated in those intervals. For Nyquist signaling, the first half of the data block can fill the interval $]F_c + W/2, F_c + W]$ and the second half the interval $[F_c - W, F_c - W/2[$ as shown in Figure 3.3; for FTN the first half would be associated to $]F_c + W/2, F_c + \beta W]$ and the second half to $[F_c - \beta W, F_c - W/2[$.

It should be noted though that the amount of diversity used is dependent of the root raised cosine roll-off α, the FTN factor $\beta = (1 - \Delta_f)$ and the channel response for the additional bandwidth. It is more relevant near $-W/2$ and $W/2$, where the amplitude of the additional diversity is higher.

Assuming a data block sent by a MT, $[a_0, ..., a_{M-1}]$, and its respective DFT, $[A_0, ..., A_k, ..., A_{M-1}]$, where the M sub-carriers are distributed for the entire W bandwidth. For each symbol A_k there are sent two replicas, one modulated by the root-raised cosine pulse, $P^{\dagger}_{k,1}$, and the other from its additional bandwidth, $P^{\dagger}_{k,2}$. For the sake of simplicity $P^{\dagger}(f, F_c, \beta, \alpha, T_s)$ will be treated as $P^{\dagger}(f)$, so

$$P^{\dagger}_{k,i} = \begin{cases} P^{\dagger}(-W/2 + k/W) & , \quad i = 1 \\ P^{\dagger}(W/2 + k/W) & , \quad i = 2 \wedge \left\{ \lfloor \frac{\beta - 0.5}{M} \rfloor \leq k \leq \frac{M}{2} \right\} \\ P^{\dagger}(-W/2 + k/W) & , \quad i = 2 \wedge \left\{ \frac{M}{2} < k \leq \lfloor \frac{\beta - 0.5}{M} \rfloor - 1 \right\} \end{cases} \tag{3.6}$$

Assuming that K is an integer that amounts the redundancy used for bandwidth

diversity gain, where $K = \{1, 2\}$, for a MT that send L transmissions the received signals at the BS for a given symbol are, in frequency domain,

$$\mathbf{Y}_k = \mathbf{H}_{k,K}^T A_k + \mathbf{N}_{k,K}\,, \tag{3.7}$$

where $\mathbf{H}_{k,K} = \left[\mathbf{H}_{k,K}^{(1)}, ..., \mathbf{H}_{k,K}^{(L)}\right]$ and $\mathbf{N}_{k,K} = \left[\mathbf{N}_{k,K}^{(1)}, ..., \mathbf{N}_{k,K}^{(L)}\right]^T$ are the channel response multiplied by the root-raised cosine pulse and the channel noise respectively. Furthermore, expanding $\mathbf{H}_k^{(l)}$ and $\mathbf{N}_k^{(l)}$, for an l-th transmission results

$$\begin{aligned}
\mathbf{H}_{k,1}^{(l)} &= H_{k,1}^{(l)\,\dagger}\, P_{k,l,1}^{\dagger}\,,\\
\mathbf{H}_{k,2}^{(l)} &= \left[H_{k,1}^{(l)\,\dagger}\, P_{k,l,1}^{\dagger}\,,\, H_{k,2}^{(l)\,\dagger}\, P_{k,l,2}^{\dagger}\right]\,,\\
\mathbf{N}_{k,1}^{(l)} &= N_{k,1}^{(l)}\,,\\
\mathbf{N}_{k,2}^{(l)} &= \left[N_{k,1}^{(l)}\,,\, N_{k,2}^{(l)}\right]\,,
\end{aligned} \tag{3.8}$$

where $H_{k,1}^{(l)\,\dagger}$ and $H_{k,2}^{(l)\,\dagger}$ are respectively the channel response for the main bandwidth and outside bandwidth of the root-raised cosine pulse for the l-th transmission.

3.3 IB-DFE Receiver Analysis

The present section describes the IB-DFE receiver design for a QPSK modulation. A BER and Packet Error Rate (PER) analytical model is proposed for the prefix-assisted Direct-Sequence Code Division Multiples Access (DS-CDMA) system that is largely based on the analytical PER model from [33]. Perfect channel estimation and perfect synchronization conditions are assumed.

Regarding the IB-DFE receiver operation, it decodes packets in an iterative manner, removing channel noise and ISI up to N_{iter} iterations. It should be noted that the matched filter operation at the BS is already implicit within the IB-DFE equalization

scheme, since the receiver already works with the $\mathbf{H}_k$ channel realizations and the symbol estimates from these realizations.

A data symbol estimation at the output of the IB-DFE receiver for iteration $i < N_{iter}$ is

$$\tilde{A}_k^{(i)} = \mathbf{F}_k^{(i)^T}\mathbf{Y}_k - B_k^{(i)}\bar{A}_k^{(i-1)}, \tag{3.9}$$

where

$$\mathbf{F}_{k,K}^{(i)\ T} = \left[\mathbf{F}_{k,K}^{(i,1)^T}, \ldots, \mathbf{F}_{k,K}^{(i,L)^T}\right], \tag{3.10}$$

are the feedforward coefficients, where for an l-th transmission

$$\begin{aligned}\mathbf{F}_{k,1}^{(i,l)^T} &= F_{k,1}^{(i,l)},\\ \mathbf{F}_{k,2}^{(i,l)^T} &= \left[F_{k,1}^{(i,l)}, F_{k,2}^{(i,l)}\right],\end{aligned} \tag{3.11}$$

and $\mathbf{B}_k^{(i)}$ is the feedback coefficient from (2.40). $\bar{A}_k^{(i-1)}$ is the soft-decision estimate from the previous iteration, where

$$\begin{aligned}\bar{A}_k^{(i-1)} &\simeq \rho^{(i-1)}\hat{A}_k^{(i-1)},\\ \hat{A}_k^{(i-1)} &= \rho^{(i-1)} + \Delta_k.\end{aligned} \tag{3.12}$$

$\rho^{(i-1)}$ is a correlation coefficient and Δ_k is a zero-mean error value. For the first iteration, $i = 1$, $\bar{A}_k^{(i-1)}$ and $\rho^{(i-1)}$ are null values. For more information on the calculus of $\rho^{(i-1)}$, $\bar{A}_k^{(i-1)}$ and $\hat{A}_k^{(i-1)}$ for QPSK constellations refer to[17].

Assuming that R_A, $\mathbf{R}_N$ and R_Δ, are respectively, the correlation of $\mathbf{A}_k$, $\mathbf{N}_k$ and $\mathbf{\Delta}_k$, and considering that σ_A^2 is the symbol's variance and σ_N^2 is the noise's variance then

$$R_A = \mathbb{E}\left[|A_k|^2\right] = 2\sigma_A^2, \tag{3.13}$$

$$\mathbf{R}_N = \mathbb{E}\left[\mathbf{N}_k\mathbf{N}_k^H\right] = 2\sigma_N^2\mathbf{I}_{K\times L}, \tag{3.14}$$

$$R_\Delta = \mathbb{E}\left[|\Delta_k|^2\right] \simeq 2\sigma_A^2\left(1-\rho^{(i-1)^2}\right). \tag{3.15}$$

For R_Δ calculus refer to [34].

The Mean Square Error (MSE), $MSE_{k,p}^{(i)}$, of A_k for an i-th iteration, as in [33], is

$$\begin{aligned} MSE_k^{(i)} &= \mathbb{E}\left[\left|A_k - \tilde{A}_k^{(i)}\right|^2\right] = \\ &= \alpha_k^{(i)^*} R_A \alpha_k^{(i)} + \mathbf{F}_{k,K}^{(i)^H}\mathbf{R}_N\mathbf{F}_{k,K}^{(i)} + \beta_k^{(i)^*} R_\Delta \beta_k^{(i)}, \end{aligned} \tag{3.16}$$

where

$$\alpha_k^{(i)} = \mathbf{F}_{k,K}^{(i)}\mathbf{H}_{k,K}^T - B_k^{(i)}\rho^{(i-1)^2} - 1, \tag{3.17}$$

$$\beta_k^{(i)} = B_k^{(i)}\rho^{(i-1)}. \tag{3.18}$$

To compute the optimal coefficients, $\mathbf{F}_{k,K}^{(i)}$ and $B_k^{(i)}$, under the MMSE criterion and constrained to $\gamma_p^{(i)} = \frac{1}{M}\sum_{k=0}^{M-1}\sum_{l=1}^{L}\sum_{j=1}^{K} F_{k,j}^{(i,l)} {H_{k,j}}^{(l)^\dagger} P_{k,j}^\dagger = 1$ is formally equivalent to the Lagrange function applied to (3.16), where $\mathcal{L}_k^{(i)} = MSE_k^{(i)} + \left(\gamma_p^{(i)} - 1\right)\lambda_p^{(i)}$. Therefore the gradient operation is applied to $\mathcal{L}_{k,p}^{(i)}$ where

$$\nabla\mathcal{L}_k^{(i)} = \nabla\left(MSE_k^{(i)} + \left(\gamma_p^{(i)} - 1\right)\lambda_p^{(i)}\right). \tag{3.19}$$

The Lagrange multipliers in (3.19) ensure a maximum signal to interference plus noise ratio. Evaluating the following set of equations

$$\begin{cases} \nabla_{\mathbf{F}_{k,K}^{(i)}} \mathcal{L} = 0 \\ \nabla_{B_k^{(i)}} \mathcal{L} = 0 \\ \nabla_{\lambda_p^{(i)}} \mathcal{L} = 0 \end{cases}, \tag{3.20}$$

$\nabla_{\mathbf{F}_{k,K}^{(i)}} \mathcal{L} = 0$ is

$$\begin{aligned} &\mathbf{H}_{k,K}^H R_A \mathbf{H}_{k,K} \mathbf{F}_k^{(i)} - \mathbf{H}_{k,K}^H R_A {\rho^{(i-1)}}^2 B_k^{(i)} - \dots \\ &\dots - \mathbf{H}_{k,K}^H R_A + \mathbf{R}_N \mathbf{F}_{k,K}^{(i)} + \frac{1}{M} \mathbf{H}_{k,K}^H \lambda_p^{(i)} = 0, \end{aligned} \tag{3.21}$$

$\nabla_{\mathbf{B}_{k,p}^{(i)}} \mathcal{L} = 0$ is

$$\left({\rho^{(i-1)}}^2 R_A + R_\Delta \right) \mathbf{B}_k^{(i)} = R_A \mathbf{H}_{k,K} \mathbf{F}_{k,K}^{(i)} - R_A, \tag{3.22}$$

and $\nabla_{\lambda_p^{(i)}} \mathcal{L}$ is $\gamma_p^{(i)} = 1$. So the optimal coefficients are

$$\begin{cases} B_k^{(i)} = \mathbf{H}_{k,K} \mathbf{F}_{k,K}^{(i)} - 1 \\ \mathbf{F}_{k,K}^{(i)} = \mathbf{\Lambda}_k^{(i)} \mathbf{H}_{k,K}^H \mathbf{\Theta}_k^{(i)} \end{cases}, \tag{3.23}$$

where

$$\mathbf{\Lambda}_k^{(i)} = \left(\mathbf{H}_{k,K}^H \left(1 - {\rho^{(i-1)}}^2 \right) \mathbf{H}_{k,K} + \frac{\sigma_N^2}{\sigma_S^2} \mathbf{I}_{K \times L} \right)^{-1}, \tag{3.24}$$

$$\mathbf{\Theta}_k^{(i)} = \left(1 - {\rho^{(i-1)}}^2 \right) - \frac{\lambda_p^{(i)}}{2 \sigma_A^2 M}. \tag{3.25}$$

From (3.16), and using the optimal $\mathbf{F}_k^{(i)}$ and $B_{k,p}^{(i)}$ coefficients from (3.23), it is possible to compute the MMSE. Defining

$$\sigma_p^{2(i)} = \frac{1}{M^2} \sum_{k=0}^{M-1} MSE_k^{(i)}, \tag{3.26}$$

and the Gaussian error function, $\Phi(x)$, the estimated BER at the ith iteration of the IB-DFE receiver for a QPSK constellation is

$$BER^{(i)} \simeq \Phi\left(\frac{1}{\sigma_p{}^{(i)}}\right). \tag{3.27}$$

Since a severely time dispersive channel with multipath propagation is being considered, bit errors can be considered independent. Therefore, for an uncoded system with independent and isolated errors, the PER for a fixed packet size of M bits is

$$PER^{(i)} \simeq 1 - \left(1 - BER^{(i)}\right)^M. \tag{3.28}$$

3.4 Performance Results

The current section presents the system performance results concerning the proposed SC-FDE with IB-DFE receiver for Faster-than-Nyquist signaling, as well as the correspondent MFB, for an Additive White Gaussian Noise (AWGN) and a multi-path time-dispersive channel such as the one in [35]. It will be presented a set of performance results concerning the impact of the total ISI in the BER and its variation according to different roll-off and FTN factors, as well as the verification of the impact of bandwidth diversity implementation in the proposed system.

The results were obtained through *Monte Carlo* simulations, assuming that a MT sends data packets to the BS with $M = 256$ QPSK symbols, for a total of 1000

Monte Carlo rands, except for Figure 3.4 with 10000 - each data symbol lasts for $4\mu s$ and the SC-FDE CP has the equivalent duration of 20% of the data block. It is also assumed perfect synchronization and channel estimation. All performance results are expressed as function of E_b/N_0, where E_b is the energy of the transmitted bits and N_0 is the power spectral density (PSD) of the channel noise.

A problem that could be associated to FTN signaling is that the higher overlapping between pulses might lead to higher envelope fluctuations than in conventional Nyquist signaling, and consequently a higher difficulty to amplify the signal. To evaluate how serious this problem is, Figure 3.4 presents the complementary cumulative distribution of the PMEPR of the transmitted signals (defined as in [36]) for FTN ($\beta = \{0.7; 0.802\}$) and Nyquist signaling ($\beta = 1$), with square-root raised-cosine pulses with $\alpha = \{0; 0.5; 1.0\}$ in a multi-path time-dispersive channel. In general, the PMEPR is slightly higher with FTN than in conventional Nyquist signaling, although the difference is smaller than 1dB - for values above 7dB, the probability tends asymptotically to 0. For a FTN factor of $\beta = 0.802$, it is possible to achieve a lower PMEPR for the interval]5,7[. This could occur due to the fact that the bandwidth needed to modulate the signals is enough for a lower amplitude than $\beta = 1$, while for $\beta = 0.7$ an higher envelope is needed to transmit data due to its even lower amplitude, mainly at the edges of the required bandwidth.

Figure 3.5 portrays the BER of FTN ($\beta = \{0.7; 0.802\}$) and Nyquist signaling ($\beta = 1$) for $\alpha = \{0; 0.2; 0.5; 1\}$ in a AWGN channel without bandwidth diversity and assuming linear equalization, i.e. the number of iterations of the IB-DFE receiver is $N_{iter} = 1$. It is possible to observe that the system performance is mostly affected by lower values of the FTN factor β, especially if the roll-off α presents a low value. This means that the pulse bandwidth in use is smaller for a FTN scenario. This results also confirm the Mazo's limit [3], as presents best results for a FTN factor of $\beta = 0.802$. For $\beta = 1$ the system performance almost achieves the MFB

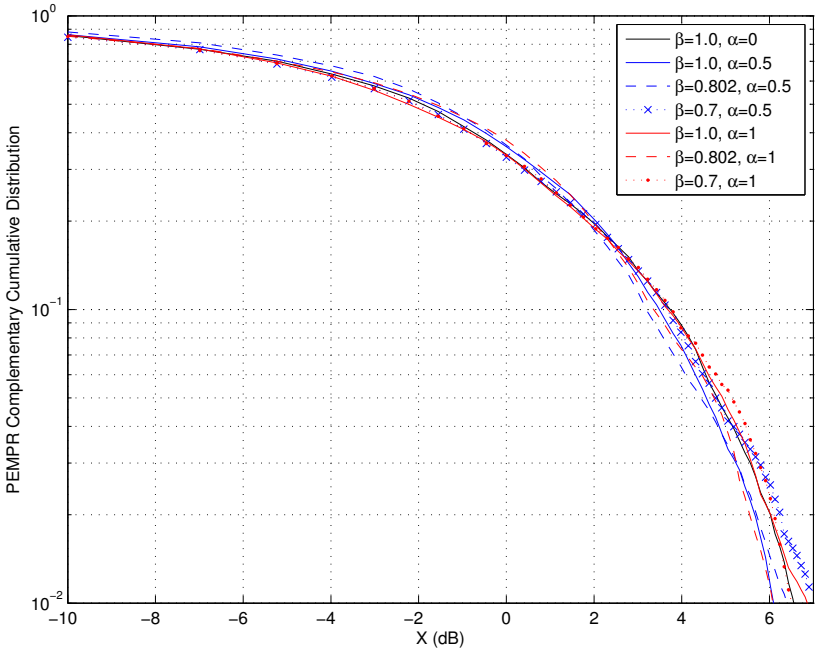

Figure 3.4: Complementary comulative distribution of the PMEPR for FTN ($\beta = \{0.7; 0.802\}$) and Nyquist signaling($\beta = 1$) for $\alpha = \{0; 0.5; 1\}$.

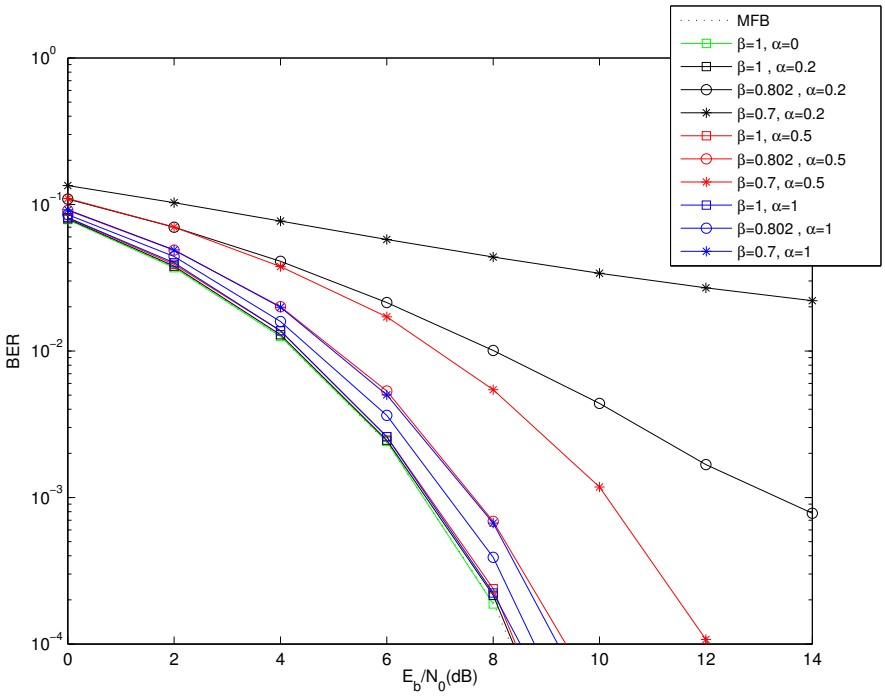

Figure 3.5: BER of FTN ($\beta = \{0.7; 0.802\}$) and Nyquist signaling ($\beta = 1$) for $\alpha = \{0; 0.2; 0.5; 1\}$ in a AWGN channel assuming linear equalization.

performance, regardless of α.

The performance of the proposed IB-DFE receiver, in oposition to a linear equalization, is analysed in Figure 3.6 which portrays the BER of FTN ($\beta = \{0.7; 0.802\}$) and Nyquist signaling ($\beta = 1$) for a roll-off factor of $\alpha = 0.5$ in a multi-path dispersive channel for several iterations up to $N_{iter} = 4$.

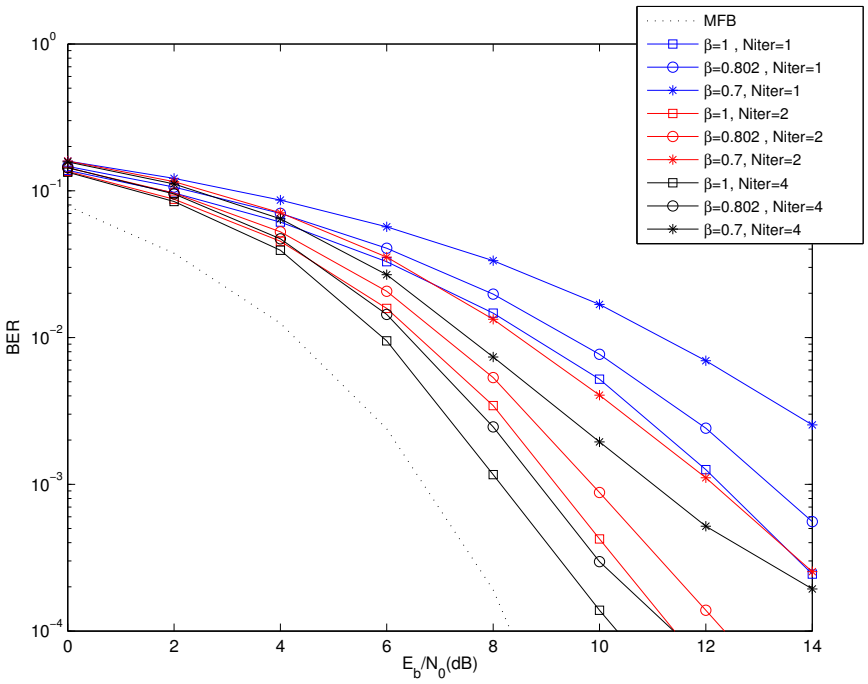

Figure 3.6: BER of FTN ($\beta = \{0.7; 0.802\}$) and Nyquist signaling ($\beta = 1$) for $\alpha = 0.5$ in a multi-path dispersive channel for up to $N_{iter} = 4$ iterations.

As it is possible to observe, the IB-DFE equalization technique is able to diminish the channel interference for each subsequent iteration, with the BER successively approaching the MFB performance. As expected, lower values of the FTN factor β slightly degrade the system performance. Nevertheless, the performance for $\beta = 0.802$ with 4 iterations is almost similar to $\beta = 1$ for 2 iterations - this way it is possible to achieve a similar performance to Nyquist signaling at the cost of a higher number of iterations.

In Figures 3.7 and 3.8, the performance of bandwidth diversity, as described in

section 3.2.1 is observed. Figure 3.7 portrays the BER of FTN ($\beta = \{0.7; 0.802\}$) and Nyquist signaling ($\beta = 1$) for $\alpha = 0.5$ in a multi-path dispersive channel with and without bandwidth diversity ($K = \{1; 2\}$) for $N_{iter} = 4$ iterations. It is possible to observe that, with the addiction of bandwidth diversity to the pulse modulation, there is a higher energy gain of 2 to 3 dB. Furthermore, it is possible to diminish channel interference for a smaller bandwidth where $\beta = 0.7$, especially for $E_b/N_0 =]0, 8[$ dB, when compared with the Nyquist pulse $\beta = 1$ without any diversity gain.

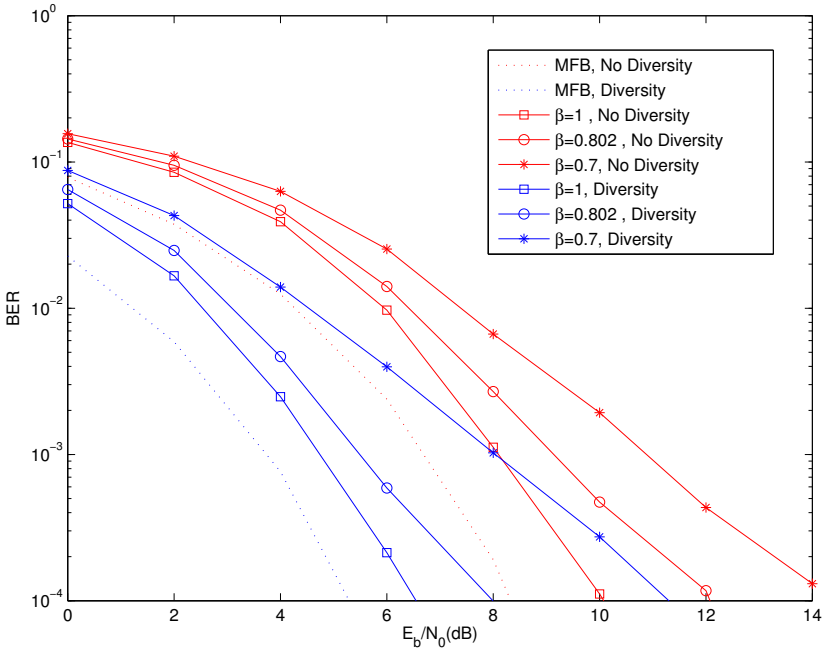

Figure 3.7: BER of FTN ($\beta = \{0.7; 0.802\}$) and Nyquist signaling ($\beta = 1$) for $\alpha = 0.5$ in a multi-path dispersive channel with and without bandwidth diversity for $N_{iter} = 4$ iterations.

In Figure 3.8 it is observed the BER performance of FTN ($\beta = \{0.7; 0.802\}$) and Nyquist signaling ($\beta = 1$) for $\alpha = \{0; 0.2; 0.5; 1\}$ in a multi-path dispersive channel with bandwidth diversity gain for $N_{iter} = 4$ iterations.

As shown in this figure, it is possible to achieve a better performance by increasing the roll-off factor, achieving similar results to a roll-off $\alpha = 0$ and still with a smaller bandwidth than Nyquist signaling ($\beta = 1$).

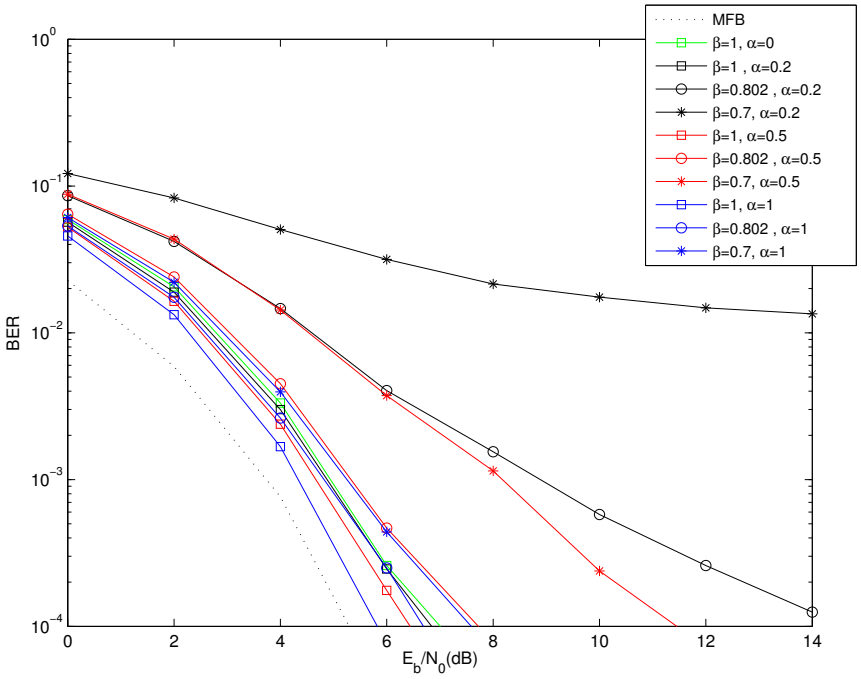

Figure 3.8: BER of FTN ($\beta = \{0.7; 0.802\}$) and Nyquist signaling ($\beta = 1$) for $\alpha = \{0; 0.2; 0.5; 1\}$ in a multi-path dispersive channel with diversity for $N_{iter} = 4$ iterations.

3.5 Conclusions

Faster-than-Nyquist signaling was proposed in this chapter for a SC-FDE context at the uplink, where the BS takes advantage of the full bandwidth diversity from the root-raised cosine pulse using the IB-DFE technique for equalization. The design of a SC-FDE system with FTN signaling allows a higher spectrum efficiency, however it is expected a worser performance in terms of the BER. Performance results show that the proposed system achieves similar results to a orthogonal pulse, for a higher roll-off factor and a smaller bandwidth. As the number of iterations at the IB-DFE increases, the performance becomes higher and the proposed technique presents itself suitable for multi-path time-dispersive channels. In the next chapters higher-layer models will be proposed.

Chapter 4

H-ARQ Time Division Multiple Access Model

TDMA presents itself as a static centralized MAC scheme, since each time slot is assigned to a MT. This type of scheme can be useful in certain conditions - when the channel is fully loaded MTs always have a packet to transmit at each TDMA frame - especially for rigid QoS requirements. However, the employment of conventional ARQ techniques can result in high transmission delay and degradation of the channel throughput for difficult conditions such as multi-path time-dispersive effects. Besides, the MT will use a higher transmission power to overcome such problems, which will result in reduced battery life.

Furthermore, in a time-dispersive channel, reception errors can be bothersome either due to poor channel conditions or a low SNR. To cope with channel errors, a BS can ask for additional copies of the same packet, but those copies might have errors since channel conditions might not vary for subsequent retransmissions leading to a throughput degradation. Fortunately, the use of H-ARQ [11] can be useful in such conditions, especially when employing Diversity Combining (DC) H-ARQ [1], since it uses the individual copies from each symbol, received at the BS, to create a packet with better reliability with appropriate equalization techniques.

In this chapter, an efficient H-ARQ with TDMA technique that takes into account the characteristics of the adopted FTN scheme is proposed for a SC-FDE system employing FTN signaling. It is considered the use of the IB-DFE receiver studied in the previous section.

The work presented in this chapter was published in [12].

The proposed system is presented in section 4.1; section 4.2 introduces the MAC analytical model; section 4.3 performs the system simulations on the proposed receiver and section 4.4 comments on the chapter's conclusions.

4.1 System Characterization

The IB-DFE receiver presented so far can be used with any MAC protocol that only allows single packet reception. A simple TDMA system is considered to illustrate the advantages of using H-ARQ and FTN. For a wireless network of J MTs, a TDMA frame is composed of J slots, each one assigned for each user. For the sake of simplicity each slot carries one data packet.

Given the shorter bandwidth of the FTN pulse, it is possible to reduce the bandwidth per TDMA slot for the same roll off factor. Therefore, it is possible to increase the number of slots available for a given bandwidth by a factor $1/\beta$ - the trade off is a slight PER increase. The bandwidth reduction using a FTN pulse is illustrated in Figure 4.1.

4.2 Analytical Model

This section analyses how β influences the performance of a TDMA system using H-ARQ and FTN, based on the analysis in [37]. The section is organized as follows: the

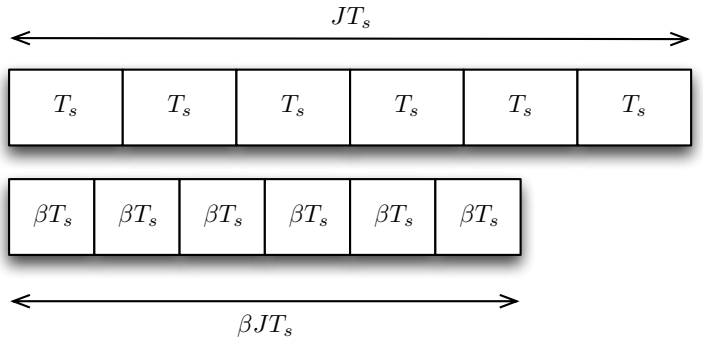

Figure 4.1: Bandwidth efficiency for FTN signaling in a TDMA system.

MAC reception probabilities are described in section 4.2.1, the system's saturated throughput is characterized in section 4.2.2, the expended Energy per Useful Packet (EPUP) is described in section 4.2.3 and the throughput gain is calculated in section 4.2.4.

4.2.1 Reception Probabilities

Assuming a PER denoted by $\epsilon_p^{(l)}$, with $0 \leq \epsilon_p^{(l)} \leq 1$, where l, $1 \leq l \leq L$, is the maximum number of H-ARQ transmissions for a given packet and p is a fixed number of iterations of the IB-DFE receiver. The probability $\epsilon_p^{(l)}$ depends on the successful reception of every bit, assuming that each bit is independent and identically distributed (i.i.d.). Assuming a fixed size of M bits per packet, then

$$\epsilon_p^{(l)}(\beta) = \left(1 - BER_p^{(l)}(\beta)\right)^M, \tag{4.1}$$

with $BER_p^{(l)}$ as the bit error probability for the same conditions mentioned before. The probability of having $x-1$ failed transmissions is denoted by

$$Q_x = \prod_{l=1}^{x-1} \epsilon_p^{(l)}(\beta). \tag{4.2}$$

Both $\epsilon_p^{(l)}$ and Q_x will be used in the remaining subsections.

4.2.2 Throughput

The expected number of slots used to transmit one data packet when employing FTN signaling is reduced by a factor of β. Therefore, the expected service time used, for a maximum of L transmissions is

$$\mathbb{E}\left[N\right](\beta) = \sum_{i=1}^{L} \left(i\left(1-\epsilon_p^{(i)}(\beta)\right)Q_i\right) + L\,Q_{L+1}. \tag{4.3}$$

The saturation throughput per slot (i.e. the maximum throughput per slot) is given by [37]

$$S_{sat}(\beta) = \frac{1-Q_{L+1}}{J\ \mathbb{E}\left[N\right](\beta)}. \tag{4.4}$$

The total channel capacity is the aggregated throughput of all MTs, given by $J\ S_{sat}(\beta)$, for a fixed bandwidth.

4.2.3 Energy Comsumption

Another relevant parameter is the average energy spent per each packet correctly received, named EPUP and denoted by Φ. Cui et al [38] proposed an energy model for uncoded M-QAM. However, this model does not take into account the acknowledgement costs that depend on the MAC layer design.

The EPUP measures the average transmitted energy for a correctly received packet. FTN contributes to the reduction of the energy spent transmitting a packet in each slot, $E_p(\beta)$, but it also contributes to the increase in the number of re-transmissions. The EPUP can be calculated as in [37], where

$$\Phi(\beta) = \frac{\mathbb{E}[N](\beta) E_p}{1 - \prod_{i=1}^{R} \epsilon_p^{(i)}(\beta)}. \tag{4.5}$$

E_p, assuming that the circuit consumption of the mobile devices is negligible, is approximately calculated as

$$E_p \approx (1 + \beta_T) G_1 d^{\kappa} M_l M E_b, \tag{4.6}$$

where β_T is the ratio of the transmission power over the amplifier's power; M_l is the link margin gain compensating the hardware process variations and other additive noise; G_1 is the gain factor at a distance of $d = 1$ m; κ is the characteristic power-path loss. β_T is computed as $\beta_T = (\nu_P/\varpi_P - 1)$ with ϖ_P as the drain efficiency of the radio frequency power amplifier and ν_P as the peak-to-average-power ratio where $\nu_P = 3(\sqrt{2^{B_e}} - 1/\sqrt{2^{B_e}} + 1)$. Although ϖ_P increases with the transmitted power [39], for the sake of simplicity a constant value is considered for $\varpi_P = 0.35$. B_e is approximately equal to the number of bits per symbol for an M-QAM constellation [38]. $\kappa = 3.5$ and $G_1 = 30dB$ will be assumed. Also, for an AWGN channel the power spectral density is $N_0 = -174$ dBm/Hz for a given bandwidth B. The energy per bit is proportional to the slot duration, thus $E_p^{(2)}/E_p^{(1)} = 1/\beta - 1$.

4.2.4 Throughput Gain

To illustrate the advantages of the proposed system, it is interesting to model the throughput gain, denoted by G_{FTN}, which compares the throughput of the adopted system with the troughput of a conventional TDMA system with $\beta = 1$. Assuming

$S_{sat}^{N} = S_{sat}(1)$, the throughput gain can be defined as

$$G_{FTN}(\beta) = \frac{S_{sat}(\beta)}{S_{sat}^{N}} = \frac{\left(1 - Q_{L+1}\right) \ \mathbb{E}[N](\beta = 1)}{\left(1 - \prod_{i=1}^{L} \epsilon_{p}^{(i)}(\beta = 1)\right) \ \mathbb{E}[N](\beta)}. \tag{4.7}$$

4.3 Model Performance

The current section presents the model performance results, for an AWGN and a multi-path time-dispersive channels such as the one in [35]. The results were obtained through *Monte Carlo* simulations, assuming that a MT sends data packets to the BS with $M = 256$ QPSK symbols, for a total of 1000 simulations - each data symbol lasts for $4\mu s$ and the SC-FDE Cyclic Prefix (CP) has the equivalent duration of 20% of the data block. For each figure the lines illustrate the theoretical performance of the proposed PER model and the markers the simulations' results, except for the last two figures that only show the theoretical performance of the presented system. Table 4.1 presents the simulation parameters used in the EPUP computation.

Parameter	Value
ϖ_P	0.35
N	256
G_1	30 dB
d	1 Km
B_e	2
κ	3.5
M_l	40 dB
B	2.5 MHz
N_0	-174 dBm/Hz

Table 4.1: Simulation parameters.

Initially, is shown the influence of the maximum number of retransmissions L and the number of iterations of the IB-DFE receiver. Figure 4.2 illustrates the PER

for Nyquist signaling ($\beta = 1$) with $\alpha = 0.5$ and $L = \{1; 2; 4\}$ up to $N_{iter} = 4$ iterations without bandwidth diversity, i.e. assuming $K = 1$. The PER model follows with good accuracy the simulations' results and, as expected, the system results show that, with an increasing number of iterations and H-ARQ transmissions the performance is greatly enhanced.

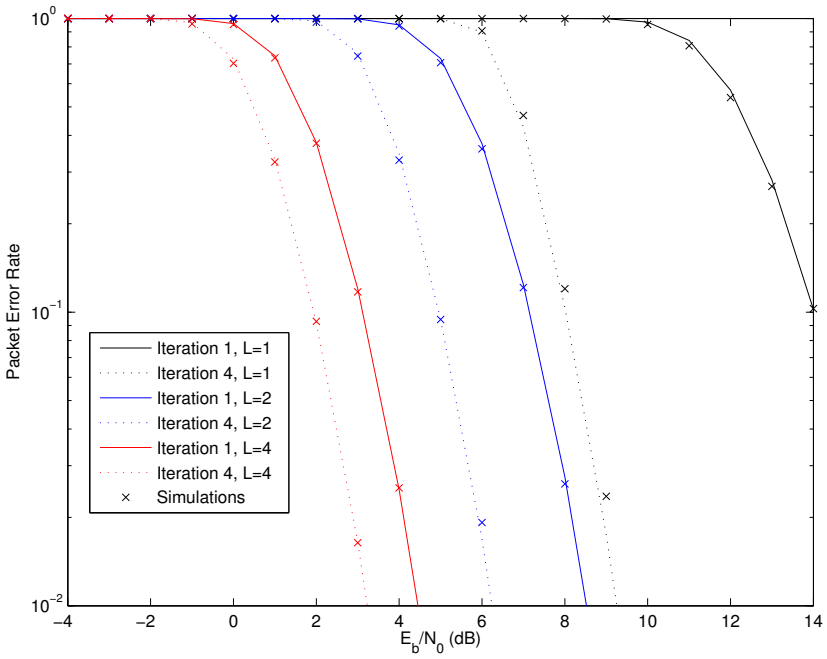

Figure 4.2: PER for $\beta = 1$ with $\alpha = 0.5$ and $L = \{1; 2; 4\}$ up to $N_{iter} = 4$ iterations without bandwidth diversity ($K = 1$).

Figure 4.3 presents the PER for $\beta = \{0.7; 0.802; 1\}$ with $\alpha = 0.5$ and $L = \{1; 4\}$ up to $N_{iter} = 4$ iterations without bandwidth diversity ($K = 1$). As expected, in terms of the system performance, results show that with an increasing number of iterations the overall performance between different values of β becomes smaller, meaning that it is possible to achieve a similar performance to Nyquist signaling with a reduction of the bandwidth up to 30%. Furthermore, the addition of more transmissions also aids the performance of the proposed system with FTN signaling, since the additional redundancy helps to reduce ISI errors.

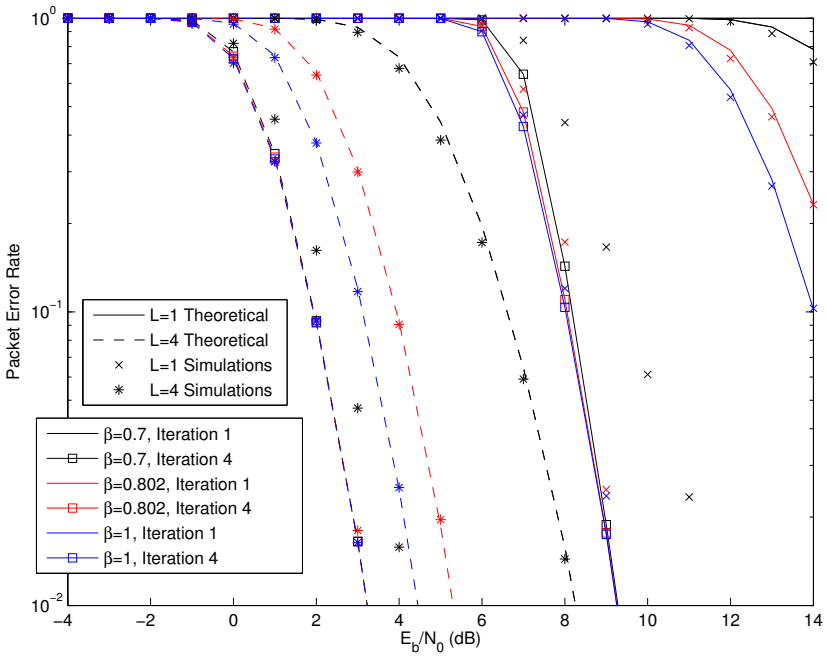

Figure 4.3: PER for $\beta = \{0.7; 0.802; 1\}$ with $\alpha = 0.5$ and $L = \{1; 4\}$ up to 4 iterations without bandwidth diversity ($K = 1$).

As explained in section 3.2.1, the use of bandwidth diversity is an important enhancement to the IB-DFE equalization technique, as it takes advantage of the additional bandwidth provided by the root-raised cosine pulse. In Figure 4.4 it is illustrated the PER for $\beta = 1$ with $\alpha = 0.5$ and $L = \{1, 2, 4\}$ for $N_{iter} = 4$ iterations with and without bandwidth diversity ($K = \{1; 2\}$). Once again, it is observed that the addition of bandwidth diversity ($K = 2$) enhances the system performance for a lower number of transmissions; the increase of H-ARQ transmissions also aids to diminish the amount of errors introduced by the channel. The PER model accurately follows the performance of the simulations' results.

Figure 4.5 portrays the PER for $\beta = \{0.7; 0.802; 1\}$ with $\alpha = 0.5$ and $L = \{1; 4\}$ for $N_{iter} = 4$ iterations with and without bandwidth diversity ($K = \{1; 2\}$). This time, the PER model achieves the system results with greater accuracy for a higher number of transmissions, as well as for the inclusion of bandwidth diversity, except for a lower number of packet transmissions and a smaller bandwidth diversity. As

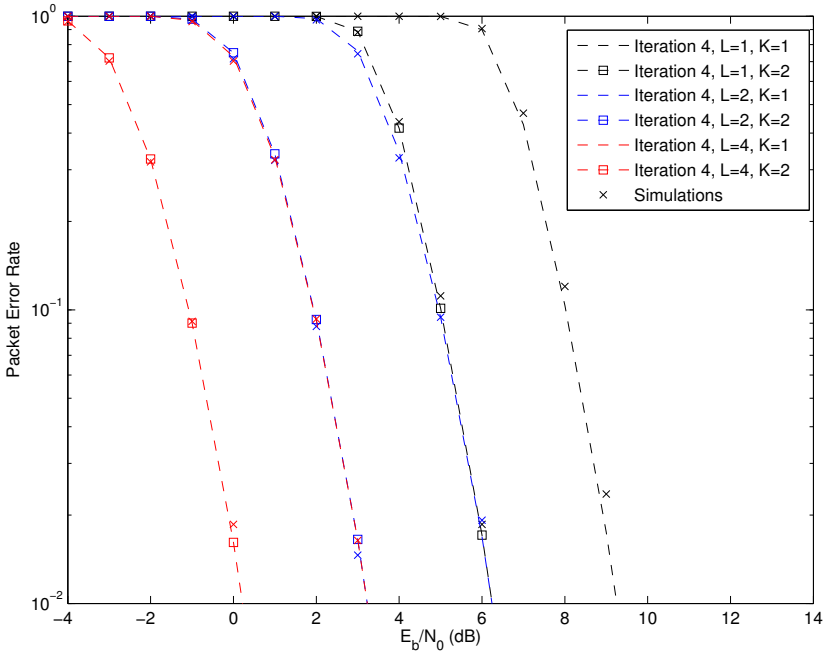

Figure 4.4: PER for $\beta = 1$ with $\alpha = 0.5$ and $L = \{1; 2; 4\}$ up to 4 iterations with(out) bandwidth diversity ($K = \{1; 2\}$).

expected, the system performs better with the addition of bandwidth diversity and, in this case, it is noticeable that the employment of FTN signaling achieves almost similar results to Nyquist signaling as long as the BS employs a high number of iterations. In addition, the use of DC H-ARQ also aids the proposed system to recover from packet errors introduced by FTN signaling, especially ISI errors.

The maximum achievable rate of successful packet delivery over the communication channel is depicted in Figure 4.6, which illustrates the saturated throughput (i.e. assuming that there is always a packet to transmit) for $\beta = \{0.7; 0.802; 1\}$ with $\alpha = 0.5$ and $L = \{1; 4\}$ for $N_{iter} = 4$ iterations with and without bandwidth diversity ($K = \{1; 2\}$). As expected, it is possible to achieve the maximum system capacity, with a lower E_b/N_0 ratio, by employing a higher number of system transmissions and/or bandwidth diversity ($K = 2$). As previously discussed, it is possible to diminish the number of necessary transmissions to achieve the same performance as to $K = 1$ when employing bandwidth diversity (e.g. $\{L = 1, K = 2\}$ achieves the

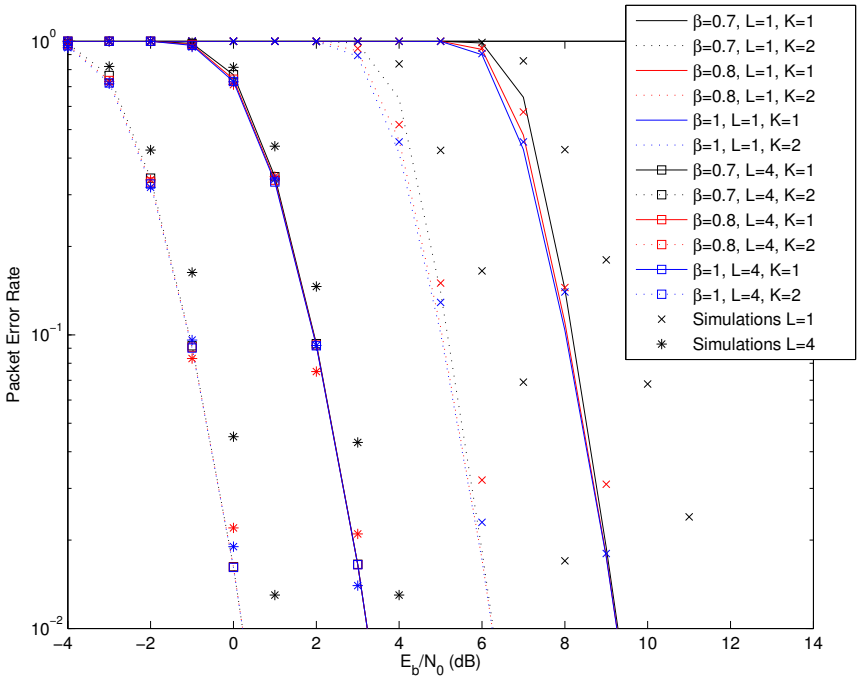

Figure 4.5: PER for $\beta = \{0.7; 0.802; 1\}$ with $\alpha = 0.5$ and $L = \{1; 4\}$ and 4 iterations with(out) bandwidth diversity ($K = \{1; 2\}$).

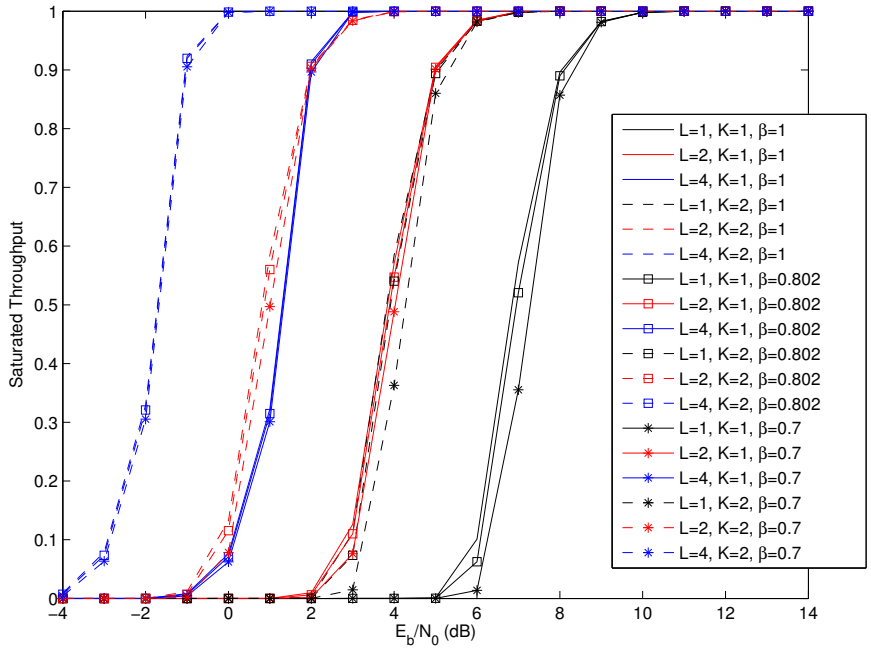

Figure 4.6: Saturated throughput for $\beta = \{0.7; 0.802; 1\}$ with $\alpha = 0.5$ and $L = \{1; 2; 4\}$ and 4 iterations with(out) bandwidth diversity ($K = \{1; 2\}$).

same performance as $\{L = 2, K = 1\}$).

In terms of energy consumption, Figure 4.7 shows the EPUP (Φ) results for $\beta = \{0.7; 0.802; 1\}$ with $\alpha = 0.5$ and $L = \{1; 4\}$ for $N_{iter} = 4$ iterations with and without bandwidth diversity ($K = \{1; 2\}$). As observed in Figure 4.6, it is possible to achieve a lower Φ value by employing a higher number of system transmissions and/or bandwidth diversity ($K = 2$) and reduce the number of necessary transmissions to achieve the same performance as to $K = 1$ when employing bandwidth diversity.

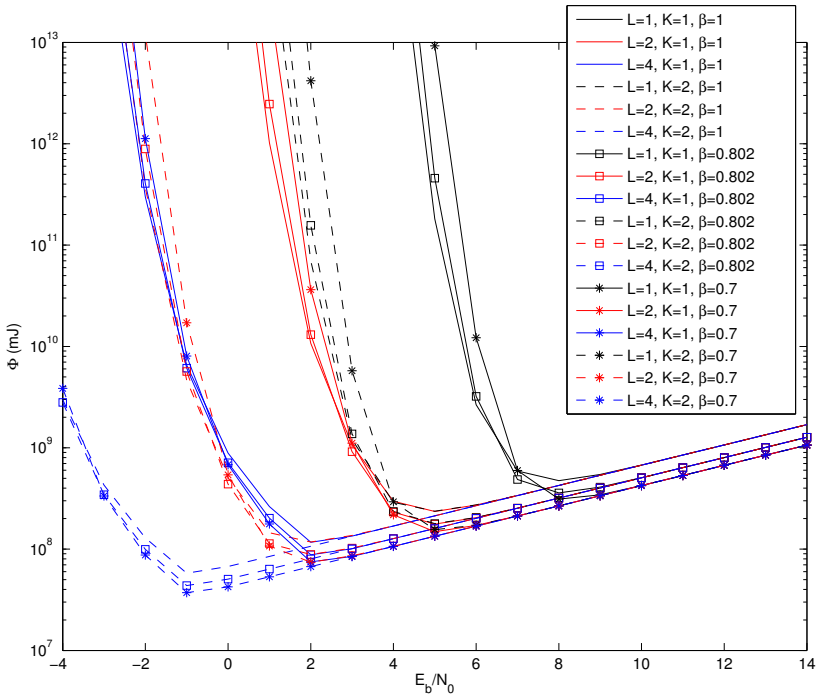

Figure 4.7: EPUP for FTN ($\beta = \{0.7; 0.802\}$) and Nyquist signaling ($\beta = 1$), both with with $\alpha = 0.5$ and $L = \{1; 2; 4\}$ for 4 iterations with(out) bandwidth diversity ($K = \{1; 2\}$).

4.4 Conclusions

A FTN PER model was proposed in this chapter for a SC-FDE context at the uplink, where the BS takes advantage of the full bandwidth diversity from the root-

raised cosine pulse using the IB-DFE technique for equalization and DC H-ARQ to enhance packet reception. A simple H-ARQ with TDMA technique was assumed and its performance with the variation of the FTN factor β was observed. Results show that the PER model achieves similar results to the simulated values and that it is possible to achieve similar results to Nyquist signaling by employing the IB-DFE technique with additional bandwidth diversity and additional transmissions from DC H-ARQ. In the following chapter it will be considered a different approach, where the reduction of the transmission slot time will be re-explored and combined with a scheduled access H-ARQ technique.

Chapter 5

Scheduled Access H-ARQ for Faster-than-Nyquist Signaling

As presented in subsection 2.7.4, the implementation of a H-ARQ technique improves the overall performance of a Multiple Access (MA) scheme, as the ability of combining different versions of a given packet at the BS will improve the throughput, delay and energy per useful packet. It is known that in a MAC scheme employing H-ARQ, the E_b/N_0 ratio of a data packet, for a given PER requirement, decreases for an increasing number of retransmissions [38]; the combination of stored packets at the BS leads to a lower energy transmission on subsequent retransmissions. Quaglieri et al [40] reveals that there is a performance trade-off between energy efficiency and throughput when employing H-ARQ techniques.

It was mentioned in the previous chapter that in FTN signaling it is possible to take advantage of the shorter bandwidth of the FTN pulse for an equal roll-off factor. Therefore, it is possible to increase the number of slots available for a given bandwidth by a factor $1/\beta$. However, a different approach can be implemented - the residual information stored in the side bands of the FTN pulse can be immediately retransmitted whenever a packet is received with errors. Such technique can achieve a Nyquist signaling equivalent performance.

In this chapter, an efficient H-ARQ with SA-FTN (Scheduled Access with Faster-than-Nyquist) technique is proposed for a SC-FDE system employing FTN signaling. It is considered the using of the IB-DFE receiver studied in chapter 3 with minor modifications regarding the bandwidth diversity technique. The chapter studies how the employment of different slot durations aid the use of FTN signaling in schedule access.

The work presented in this chapter was proposed for publication in the *2015 IEEE 81st Vehicular Technology Conference* (VTC2015-Spring).

A MAC protocol based on a SA system using H-ARQ and FTN signaling is characterized in section 5.1; section 5.2 presents an analytical model, as well as a MATLAB® simulation script for the proposed system; in section 5.3 the system simulation results on the proposed receiver are depicted; lastly, section 5.4 comments the chapter's conclusions.

5.1 System Description

In the system hereupon described it is considered the use of FTN signaling for the uplink of broadband wireless systems employing SC-FDE schemes. Although the IB-DFE receiver described in chapter 3 is especially designed to cope with the strong overall ISI levels, it still presents some performance degradation when compared with Nyquist-rate signaling, which increases as we increase the transmission rate. To cope with such degradation, it is considered an H-ARQ scheme especially designed to deal with FTN signals.

The wireless channel is composed by a BS that coordinates the MTs assuming a scheduled access, using two control data channels: an uplink shared control channel

is used to transmit block transmission requests; a downlink shared control channel is used to broadcast the slot allocation map in the uplink data channel.

The data slots of the uplink data channel are allocated to individual MTs and can be of two sizes: large slots, corresponding to the FTN symbol separation factor β with duration

$$T_1 = \beta\, T_s, \tag{5.1}$$

where T_s refers to the TDMA with $\beta = 1$ data symbol duration; and short slots, corresponding to the residual information $(1 - \beta)$,

$$T_2 = (1 - \beta)\, T_s, \tag{5.2}$$

and required to have Nyquist rate signal information. The two different data block are ilustrated in Figure 5.1.

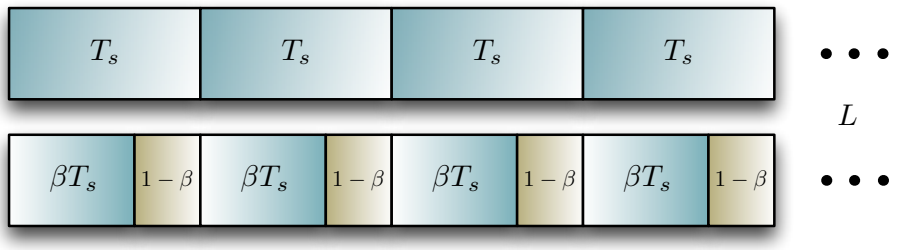

Figure 5.1: Slot duration for long and short blocks, in comparison with TDMA.

The effective bandwidth used is longer due to the root-raised cosine used is both kinds of slots with a roll-off α. Up to L consecutive transmissions on a long and short slots can be used for a single data block. FTN signaling is used in the first transmission of a given packet. In case of a reception error, the complementary signal information pruned using FTN is transmitted, allowing the receiver to combine them

and achieve a Nyquist signalling equivalent performance. If both transmissions fail, the procedure may be repeated up to L times - then, the packet is dropped. After each new fragment is received, a H-ARQ approach is used [33] to reduce the error rate. Thus, the channel data slot's duration will depend on what is being transmitted: the initial FTN fragment of the block's signal, with slot time T_1, or the complementary fragment, with slot time T_2. This new approach requires a scheduled access uplink channel, where the base station (BS) defines the sequence and type of the access slots assigned to each MT. On the other hand, given a high success rate of the initial FTN transmission, it is possible to achieve a bandwidth efficiency gain of up to $1/\beta$.

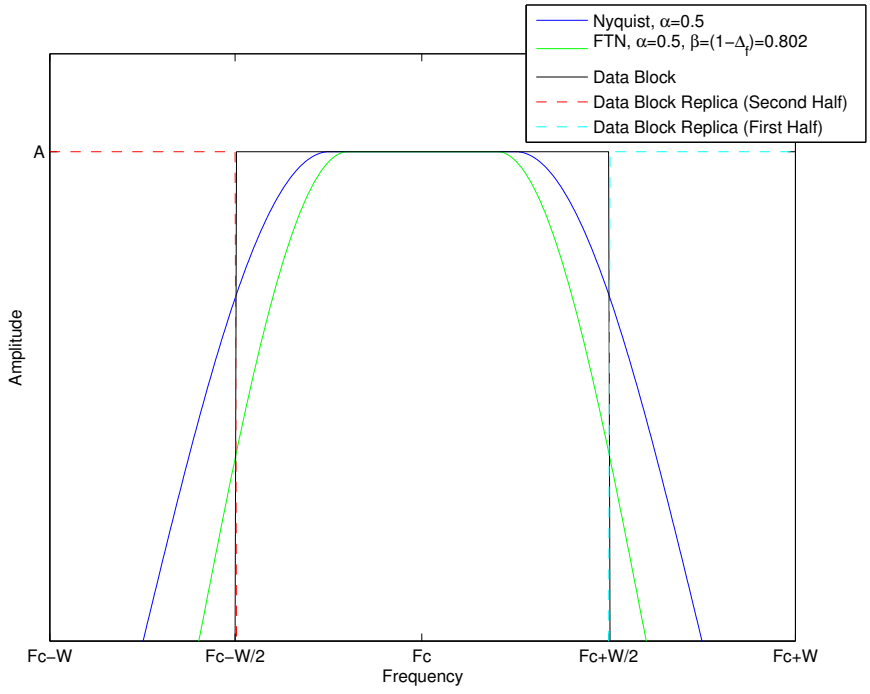

Figure 5.2: Data block and respective side replicas, for a roll-off of $\alpha = 0.5$ for Nyquist and FTN signaling.

5.1.1 Bandwidth Diversity

In previous chapters, bandwidth diversity was assumed considering data blocks of constant duration (see subsection 3.2.1). In this new approach, however, the two blocks have distinct length, which leads to new channel responses for each j-th transmission.

Therefore, assuming an identical data block sent by a MT, $[a_0, \ldots, a_{M-1}]$, and its respective DFT, $[A_0, \ldots, A_k, \ldots, A_{M-1}]$, the main difference is that the two replicas sent for each symbol A_k, one modulated by the root-raised cosine pulse, $P_{k,1}^{(j)\dagger}$, and the other one from its additional bandwidth, $P_{k,2}^{(j)\dagger}$, are now different for each j-th slot, where $j = 1$ stands for the transmission in a long slot and $j = 2$ in a short slot, so

$$P_{k,i}^{(j)\dagger} = \begin{cases} P^{(j)\dagger}(-W/2 + k/W) & , \quad i = 1 \\ P^{(j)\dagger}(W/2 + k/W) & , \quad i = 2 \wedge \left\{ \lfloor \frac{\beta - 0.5}{M} \rfloor \leq k \leq \frac{M}{2} \right\} \\ P^{(j)\dagger}(-W/2 + k/W) & , \quad i = 2 \wedge \left\{ \frac{M}{2} < k \leq \lfloor \frac{\beta - 0.5}{M} \rfloor - 1 \right\} \end{cases} . \tag{5.3}$$

Assuming, as in section 3.2.1, that K comprehends the values $\{1, 2\}$, which amounts the bandwidth diversity used by the proposed system and for a MT that sends L transmissions in long slots and L transmissions in L short slots, the received signals at the BS for a given symbol are now

$$\mathbf{Y}_k = \mathbf{H}_{k,K}^T A_k + \mathbf{N}_{k,K}, \tag{5.4}$$

where $\mathbf{H}_{k,K} = \left[\mathbf{H}_{k,K}^{(1,1)}, \mathbf{H}_{k,K}^{(1,2)}, \ldots, \mathbf{H}_{k,K}^{(L,1)}, \mathbf{H}_{k,K}^{(L,2)} \right]$ are the channel response multiplied by the root-raised cosine pulses of the long and short slots and $\mathbf{N}_{k,K} =$

$\left[\mathbf{N}_{k,K}^{(1,1)}, \mathbf{N}_{k,K}^{(1,2)}, \ldots, \mathbf{N}_{k,K}^{(L,1)}, \mathbf{N}_{k,K}^{(L,2)}\right]^T$ is the channel noise. Furthermore, expanding now $\mathbf{H}_k^{(l,j)}$ and $\mathbf{N}_k^{(l,j)}$, for an l-th transmission and j-th slot results

$$\begin{aligned}
\mathbf{H}_{k,1}^{(l,1)} &= {H_{k,1}^{(l)}}^{\dagger} P_{k,1}^{(1)\dagger}, \\
\mathbf{H}_{k,1}^{(l,2)} &= {H_{k,1}^{(l)}}^{\dagger} P_{k,1}^{(2)\dagger}, \\
\mathbf{H}_{k,2}^{(l,1)} &= \left[{H_{k,1}^{(l)}}^{\dagger} P_{k,1}^{(1)\dagger}, {H_{k,2}^{(l)}}^{\dagger} P_{k,2}^{(1)\dagger}\right], \\
\mathbf{H}_{k,2}^{(l,2)} &= \left[{H_{k,1}^{(l)}}^{\dagger} P_{k,1}^{(2)\dagger}, {H_{k,2}^{(l)}}^{\dagger} P_{k,2}^{(2)\dagger}\right], \\
\mathbf{N}_{k,1}^{(l,j)} &= N_{k,1}^{(l,j)}, \\
\mathbf{N}_{k,2}^{(l,j)} &= \left[N_{k,1}^{(l,j)}, N_{k,2}^{(l,j)}\right],
\end{aligned}$$

where ${H_{k,1}^{(l,j)}}^{\dagger}$ and ${H_{k,2}^{(l,j)}}^{\dagger}$ are respectively the channel response for the main bandwidth and outside bandwidth of the root-raised cosine pulse for the l-th transmission and j-th slot. $P_{k,i}^{(1)\dagger}$ and $P_{k,i}^{(2)\dagger}$ are raised cosine shapes with band βW and $(1-\beta)W$, respectively (without loss of generality, we assume the same roll-off). Since the frequency-domain samples at the edge of the band were eliminated or faced strong attenuation due to FTN filtering, it is desirable to give more power to those samples at the second transmission attempt. This can be achieved by a cyclic shift of length $M/2$ on the set of A_k, which is formally equivalent to make a similar but reversed shift on ${H_{k,2}^{(l,j)}}^{\dagger}$ and $P_k^{(2)\dagger}$.

The lack of transmission in a short slot, due to success at the first attempt in a long block, is modeled by ${H_{k,K}^{(l,2)}}^{\dagger} = 0$.

5.2 Analytical Performance Model

This section analyses how β influences the performance of the scheduled transmission system using H-ARQ and FTN. Several metrics are studied:

the MAC reception success and failure probabilities in section 5.2.1; the transmission's mean service time in section 5.2.2; the throughput in section 5.2.3; and the expended EPUP in section 5.2.4. It is considered a saturated system with J MTs, i.e., where J MTs always have packets to transmit. For simplicity, it is assumed that each packet is carried by one block.

5.2.1 MAC Reception Probabilities

Assuming that the probability of receiving a packet with an error (i.e. PER) at the BS is denoted by $\epsilon_p^{(l,j)}$, with $0 \leq \epsilon_p^{(l,j)} \leq 1$, where l, $1 \leq l \leq L$, is the number of retransmission transmissions for a given packet, p is a fixed number of iterations of the IB-DFE receiver with $j = 1$ for the long slot and $j = 2$ for the short slot. The probability $\epsilon_p^{(l,j)}$ depends on the successful reception of every bit, assuming that each bit is independent and identically distributed (i.i.d.). Assuming a fixed size of M bits per packet, then

$$\epsilon_p^{(l,j)}(\beta) = \left(1 - BER_p^{(l,j)}(\beta)\right)^M, \tag{5.5}$$

where $BER_p^{(l,j)}$ is the bit error probability for the same conditions mentioned before. The probability of having $x - 1$ failed transmissions is now denoted by

$$Q_x = \prod_{l=1}^{x-1} \epsilon_p^{(l,1)}\, \epsilon_p^{(l,2)}(\beta), \tag{5.6}$$

where $\epsilon_p^{(l,1)}$ represents the PER for the transmission of the long slot and $\epsilon_p^{(l,2)}$ the PER for the subsequent retransmission of the short slot considering the use of bandwidth diversity presented in subsection 5.1.1. When the long and short slots are combined, the receiver has approximately the same information as when Nyquist signaling is

used. Therefore, the PER for l packet retransmissions in the long and short slots can be approximated by the PER of a Nyquist rate signaling with l retransmissions calculated in [12]. Both $\epsilon_p^{(l,j)}$ and Q_x will be used in the remaining subsections.

5.2.2 Packet's Mean Service Time

The expended time to transmit one data packet in a conventional TDMA with H-ARQ system can be decreased when employed SA-FTN with H-ARQ, as the slot time is reduced by a factor of β. If the packet reception in a long slot transmission ($j = 1$) is not successful and a second transmission ($j = 2$) is required, using a slot time of $(1-\beta)$, the total packet's expected service time becomes equal to the service time of a single transmission in conventional TDMA systems.

Thus, the expected time (measured in number of Nyquist slots, i.e. long slots for $\beta = 1$) used to transmit one data packet, for a maximum of L transmissions is

$$\mathbb{E}[\tau] = L\, Q_{L+1} + \sum_{i=1}^{L} \left(\Big((i - 1 + \beta)\left(1 - \epsilon_p^{(i,1)}\right) + i\epsilon_p^{(i,1)}\left(1 - \epsilon_p^{(i,2)}\right) \Big) Q_i \right). \tag{5.7}$$

5.2.3 Throughput

Let S_{sat} be the saturation throughput per slot (i.e. the maximum throughput per slot), measured in packets per Nyquist slots. It is limited by the packet's average service time and success probability, and is given by

$$S_{sat}(\beta) = \frac{1 - Q_{L+1}}{J\ \mathbb{E}[N](\beta)}. \tag{5.8}$$

The total channel capacity is the aggregated throughput of all MTs, given by $J\, S_{sat}(\beta)$, for a fixed bandwidth.

5.2.4 Energy Comsumption

The EPUP, denoted by Φ, measures the average transmitted energy for a correctly received packet. It depends on the expected number of long slots and short slots used to transmit a packet and the packet's error rate, and can be calculated as

$$\Phi(\beta) = \frac{\mathbb{E}\left[N^{(1)}\right] E_p^{(1)} + \mathbb{E}\left[N^{(2)}\right] E_p^{(2)}}{1 - \prod_{i=1}^{R} \epsilon_p^{(i,1)} \epsilon_p^{(i,2)}} \,. \tag{5.9}$$

where

$$\mathbb{E}\left[N^{(1)}\right] = \sum_{i=1}^{L} i(1-\epsilon_p^{(i,1)})Q_L + L\epsilon_p^{(L,1)}Q_{L+1} \,, \tag{5.10}$$

$$\mathbb{E}\left[N^{(2)}\right] = \sum_{i=1}^{L} i\epsilon_p^{(i,1)}(1-\epsilon_p^{(i,2)})Q_L + L\epsilon_p^{(L,1)}\epsilon_p^{(L,2)}Q_{L+1} \,. \tag{5.11}$$

FTN reduces the energy spent transmitting a packet in each slot, $E_p^{(j)}(\beta)$ (where j denotes the slot duration), but it also contributes to the increase in the number of re-transmissions. Therefore, the total energy considering the transmission in the long and the short slots is higher or equal to the energy per packet in with Nyquist signaling rate, i.e. $E_p^{(N)} \leq E_p^{(1)} + E_p^{(2)}$. E_p, assuming that the circuit consumption of the mobile devices is negligible, is approximately calculated as

$$E_p \approx (1+\beta_T) G_1 d^{\kappa} M_l M E_b. \tag{5.12}$$

where β_T is the ratio of the transmission power over the amplifier's power; M_l is the link margin gain compensating the hardware process variations and other additive noise; G_1 is the gain factor at a distance of $d = 1$ m; κ is the characteristic power-path loss. β_T is computed as $\beta_T = (\nu_P/\varpi_P - 1)$ with ϖ_P as the drain efficiency of the radio frequency power amplifier and ν_P as the peak-to-average-power ratio

where $\nu_P = 3(\sqrt{2^{B_e}} - 1/\sqrt{2^{B_e}} + 1)$. Remaining transmission channel conditions are assumed from subsection 4.2.3, as well as from the values in Table 5.1.

5.2.5 Simulation

A simple scheduled access H-ARQ with FTN signaling protocol simulator was implemented using the MATLAB® software, in order to validate the analytical model. It computes J slots in a 10000 frames simulation and processes the mean service time and the throughout of the proposed system by increasing the slot time (long or short blocks) when a transmission fails. PER results from the previous chapter are used, however, this time for a bandwidth diversity regarding the different block time for a j-th transmission.

The MATLAB® script is presented below, in a reduced yet understandable form.

```
sentPackets = 0;
successfulPackets = 0;


for t=1:Nframes %--For Nframes
    for s=1:J %--For J users
        f = queue(s);
        top = f(1); %--The packet at the top of the queue
        presentTime = presentTime + T1; %--Long block
        serviceTime(top) = serviceTime(top) + T1;
        sucess=[rand(1)>PER_T1(Ltransmission(top))]; %--PER for the
        %long block
        if(sucess == 1) %--Packet successfully received
            queue_fifo(top,'get'); %--Remove packet from queue
            queue(s) = queue(s) - 1;
            sentPackets = sentPackets + 1;
            successfulPackets = successfulPackets + 1;
```

```
        else %--Packet received with error
            presentTime = presentTime + T2; %--Short block
            serviceTime(top) = serviceTime(top) + T2;
            sucess=[rand(1)>PER_T2(Ltransmission(top))]; %--PER for
            %the short block
            if(sucess == 1)
                queue_fifo(top,'get'); %--Remove packet from queue
                queue(s) = queue(s) - 1;
                sentPackets = sentPackets + 1;
                successfulPackets = successfulPackets + 1;
            else %--Packet received with error
                Ltransmission(top) = Ltransmission(top) + 1;
                if(Ltransmission(top) > L)
                %--Packet reached transmissions limit
                    queue_fifo(top,'get'); %--Remove packet from queue
                    queue(s) = queue(s) - 1;
                    sentPackets = sentPackets + 1;
                end
            end;
        end;
    end;
end;
```

After the J slots cycle is completed, the mean service time is calculated taking into account the service time from all the successfully received packets. Therefore, the saturated throughput of the system is calculated dividing the packet's success probability (i.e. number of received packets divided by the number of total transmitted packets) by the mean service time of the system.

```
meanServiceTime = mean(serviceTime);
satThroughput = (successfulPackets / sentPackets) / meanServiceTime;
```

In the following section, both analytical model and MATLAB® simulation results will be presented and discussed.

5.3 Performance Results

In the current section it is presented the SA-FTN with H-ARQ system model performance analysis concerning the proposed SC-FDE with IB-DFE receiver for FTN signaling, considering the PER, mean service time, throughput and EPUP for an AWGN channel. The results were obtained through *Monte Carlo* simulations. It is assumed that a MT sends a data packet to the BS with $M = 256$ QPSK symbols, for a total of 1000 simulations - each data symbol lasts for $4\mu s$ and the SC-FDE CP duration is 20% of the data block. It is also assumed perfect synchronization and channel estimation. All performance results are expressed as function of E_b/N_0, where E_b is the energy of the transmitted bits and N_0 is the power spectral density (PSD) of the channel noise. Table 5.1 lists the parameters configuration for the SA-FTN with H-ARQ energy model.

Simulated results were obtained through a set of tests executed in the MATLAB® software, for a number of 10000 slots assuming a saturated system with a MT ($J = 1$) always with packets to transmit, in order to compare and validate the protocol performance for simulation results and analytical model. For each figure the lines illustrate the theoretical performance of the proposed H-ARQ with FTN system model and the markers the simulation results, except for the first two and last figure that only show the theoretical performance of the system.

Figures 5.3 and 5.4 depict the PER performance ($\epsilon^{(l,j)}$) of the H-ARQ FTN system respectively for $\beta = 0.802$ and $\beta = 0.7$, for $\alpha = 0.5$ for $N_{iter} = 4$ iterations. The

Parameter	Value
ϖ_P	0.35
N	256
G_1	30 dB
d	1 km
B_e	2
κ	3.5
M_l	40 dB
B	2.5 MHz
N_0	-174 dBm/Hz

Table 5.1: Simulation parameters.

figures show that the $\epsilon^{(l,j)}$ decreases when the number of retransmissions increases, although the decrease for a short slot is small for $\beta = 0.802$. As expected, the effect of the short slots is more relevant for $\beta = 0.7$, especially for $L = 1$.

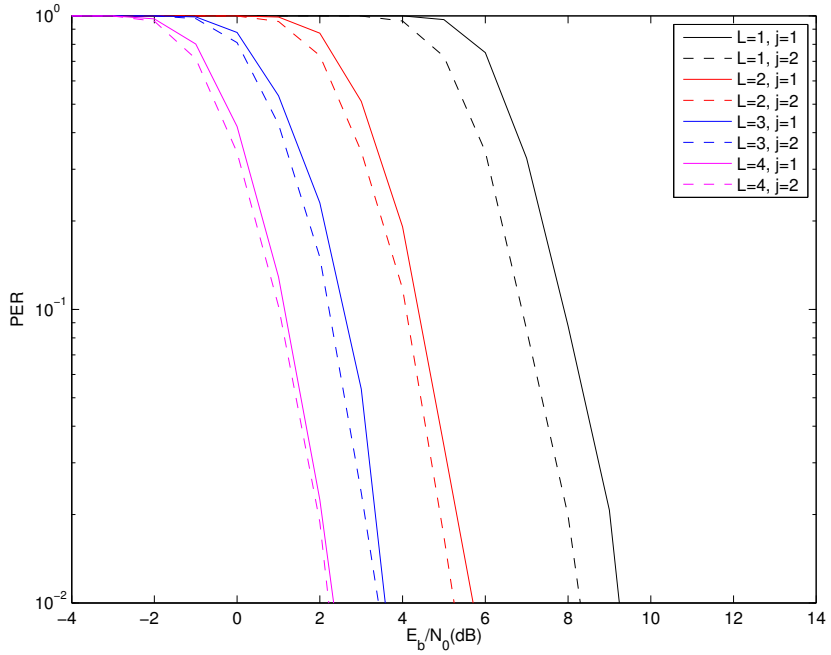

Figure 5.3: Packet Error Rate (PER) of H-ARQ FTN ($\beta = 0.802$) and Nyquist signaling ($\beta = 1$) for $\alpha = 0.5$ and $N_{iter} = 4$ iterations.

The next set of figures illustrate the system level performance of H-ARQ FTN for $\beta = \{0.7; 0.802; 1\}$ with $\alpha = 0.5$, $L = \{1; 2; 4\}$, $N_{iter} = 4$ iterations and using FTN bandwidth diversity ($K = 2$). Figure 5.5 shows the expected service time ($\mathbb{E}[\tau]$)

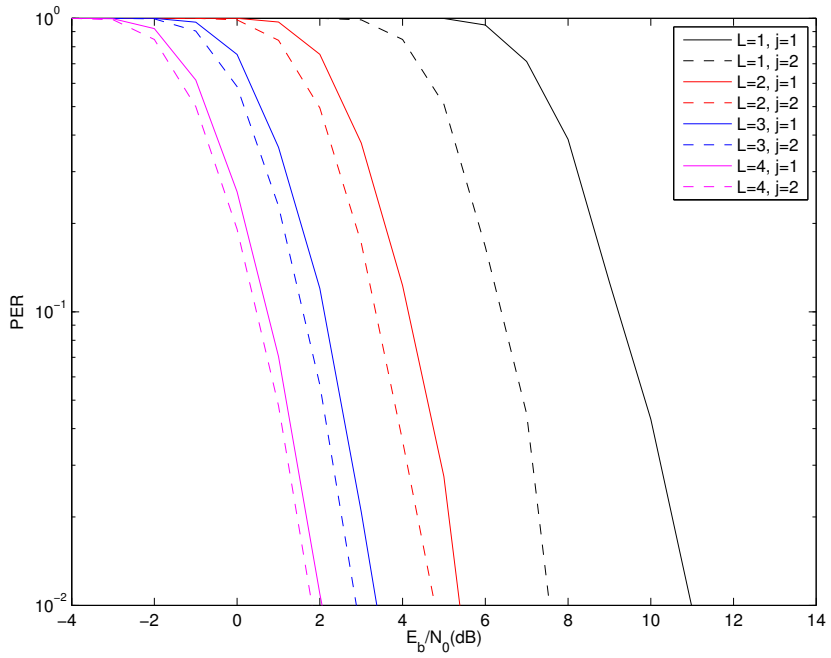

Figure 5.4: Packet Error Rate (PER) of H-ARQ FTN ($\beta = 0.7$) and Nyquist signaling ($\beta = 1$) for $\alpha = 0.5$ and $N_{iter} = 4$ iterations.

evolution with the average E_b/N_0. It is possible to depict that the average service time increases with the decreasing of E_b/N_0, up to the maximum L retransmissions number limit. It also shows that for high E_b/N_0 values FTN uses mainly the first long slot, leading to shorter service times for FTN than using Nyquist signaling rate. The service time model follows with good accuracy the simulation results.

Figure 5.6 depicts the total saturated throughput (JS_{sat}) and shows that H-ARQ FTN effectively contributes to increase the network capacity for low E_b/N_0 values, by combining the signal received in multiple slots for each packet. Due to the lower PER after the transmission in the long slot, H-ARQ FTN with $\beta = 0.802$ achieves a better throughput in these cases. For E_b/N_0 values above 8 dB, the shorter service time for $\beta = 0.7$ achieves the highest network capacity. The FTN bandwidth redundancy contributes decisively to let $\beta = 0.7$ beat the performance using the "Mazo's limit", i.e. $\beta = 0.802$. Once again, the throughput model accurately overlap the simulation results, which confirms the validity of the analytical model.

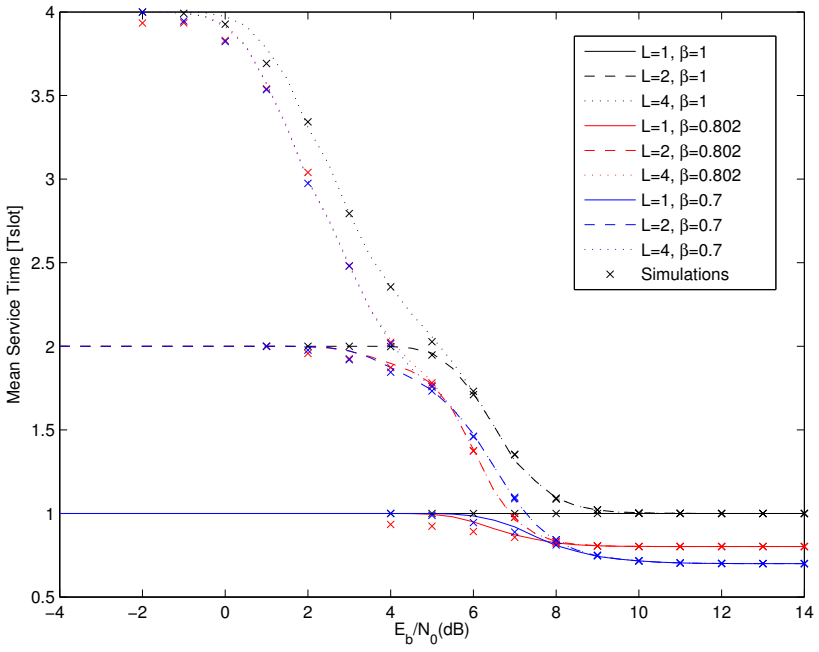

Figure 5.5: Expected service time (τ) performance for $\beta = \{0.7; 0.802; 1\}$ with $\alpha = 0.5$ and $L = \{1; 2; 4\}$ for $N_{iter} = 4$ iterations.

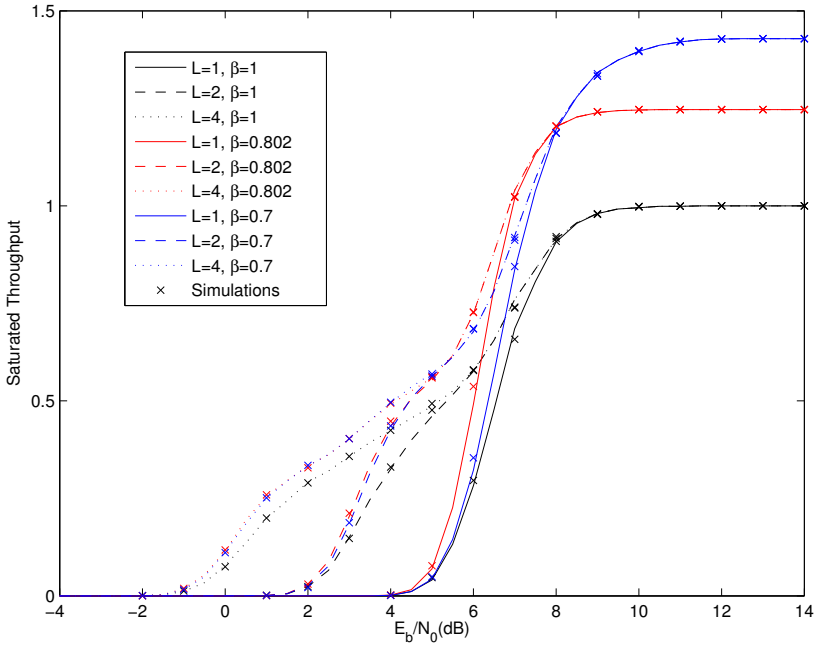

Figure 5.6: Saturated system throughput for $\beta = \{0.7; 0.802; 1\}$ with $\alpha = 0.5$ and $L = \{1; 2; 4\}$ for $N_{iter} = 4$ iterations.

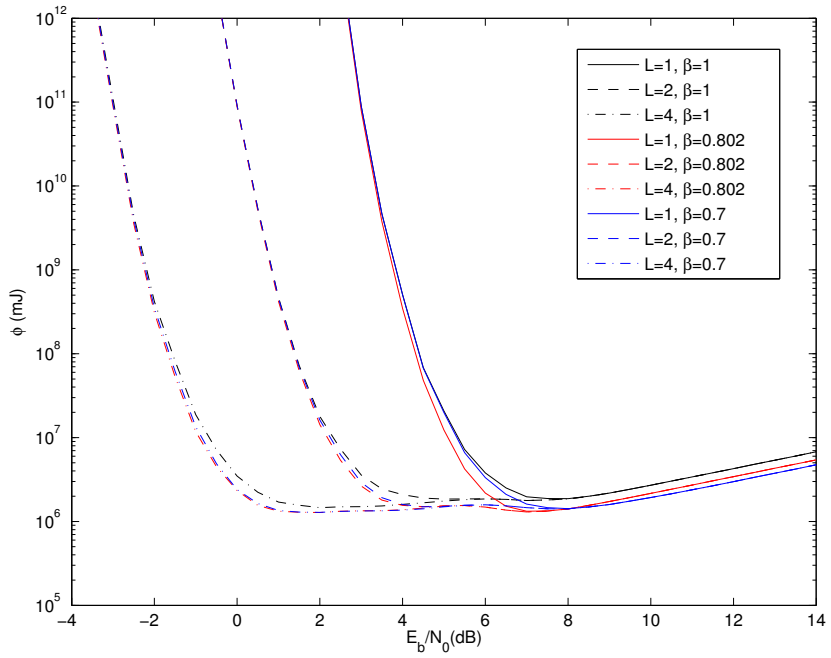

Figure 5.7: EPUP (Φ) for $\beta = \{0.7; 0.802; 1\}$ with $\alpha = 0.5$ and $L = \{1; 2; 4\}$ for $N_{iter} = 4$ iterations.

Similar conclusions can be taken from the EPUP (Φ) results, depicted in figure 5.7. The H-ARQ system with $L = 4$ is energy efficient for a broad range of E_b/N_0 values for all configurations, although it is bandwidth limited for E_b/N_0 below 7 dB for all β values. The lowest EPUP is achieved for $E_b/N_0 = 2$dB, with a saturation rate of 35% of the Nyquist rate system. The best energy performance occurs for the lowest E_b/N_0 that satisfies the data rate requirements, in the range between 2 dB and 8 dB.

5.4 Conclusions

In the present chapter it is considered an iterative FDE receiver combined with a H-ARQ technique, both especially designed for FTN signaling. It is also presented a simple, yet accurate analytical model for the proposed technique and a

simple simulation script that illustrates a basic scheduled access H-ARQ for a single user taking into account the two different block sizes ($j = [1, 2]$).

The performance results showed that we can have significant throughput gains, while maintaining essentially the receiver complexity of conventional Nyquist-rate schemes, even for severely time-dispersive channels. The analytical model follows with accuracy the simulation results. It is observed that, with this approach, and given the high success rate of the initial FTN transmission, it is possible to achieve a bandwidth efficiency gain up to $1/\ \beta$.

Chapter 6

Conclusions

This document proposed the use of FTN signaling, a technique that allows a significant increase on the spectral efficiency and specially interesting for implementation on broadband wireless systems. However, FTN signaling is not usually considered, mainly because it requires complex receivers, able to cope with the resulting ISI levels over time-dispersive channels. In this thesis, as it is considered the use of a IB-DFE receiver specially designed to deal with the overall interference. Results show that it is possible to achieve significant error rate performance and throughput gains, while maintaining essentially the receiver complexity of conventional Nyquist-rate schemes, even for severe interference conditions.

This chapter resumes this dissertation in the following way: section 6.1 states the final conclusions on this thesis and section 6.2 enumerates some topics for future work.

6.1 Final Considerations

Throughout this thesis, simulation results showed that the use of FTN signaling allied to a IB-DFE receiver design with additional bandwidth diversity employment

achieves similar results to a conventional system. In chapter 3, such techniques were discussed and its performance analyzed. These results emerged by means of several BER performance simulations regarding the different specificities of the proposed receiver - number of iterations, bandwidth diversity, retransmissions - and for different β and α values.

Chapter 4 proposed a FTN PER model regarding the receiver design of chapter 3, as well as an efficient H-ARQ technique using TDMA. The use of Hybrid ARQ proved itself as a useful technique in order to cope with interference conditions and consequent channel errors, specially when employing Diversity Combining (DC) to create a packet with better reliability. Results regarding the proposed model confirms the capability of the IB-DFE design with bandwidth diversity. In terms of system throughput and energy consumption simulations, the model also achieves a remarkable efficiency.

Finally, in chapter 5 it is proposed a scheduled access H-ARQ approach, with time slots of variable duration, specially designed to deal with FTN signals. It implements a protocol where a first transmission of a block, with duration β, is attempted. In case of error, the complementary signal information pruned using FTN is transmitted, in a total of L retransmission transmissions. It is achieved a Nyquist signaling equivalent performance by combining successive data packets, at the sime time that a bandwidth efficiency gain is obtained for a factor of up to $1/\beta$. Also, model simulation results presented significant throughput gains, corroborated by a simple script simulating a scheduled access system.

6.2 Future Work

In this dissertation, it was considered perfect time synchronization and channel estimation. Therefore, a logic improvement would be to analyze the impact of synchronization and channel estimation techniques in the overall performance of the proposed system. As complementary work, it is possible to identify the following subjects:

- Delay analysis of the H-ARQ with FTN systems described in chapters 4 and 5;
- Simulation for more than one MT ($J > 1$) in the MAC environment of chapter 5;
- Model performance and simulation results for a non-saturated system in chapters 4 and 5;

Appendix

Appendix A

Publications

In this appendix are presented the articles submitted in international conferences:

- **Chapter 4**

  "A High Throughput H-ARQ Technique with Faster-than-Nyquist Signaling"- The work presented in this chapter was published in the *2014 International Conference on Telecommunications and Multimedia* (TEMU) [12].

- **Chapter 5**

  "A Hybrid ARQ Scheme for Faster than Nyquist Signaling with Iterative Frequency-Domain Detection"- The work presented in this chapter was submitted for the *2015 IEEE 81st Vehicular Technology Conference* (VTC2015-Spring).

A High Throughput H-ARQ Technique with Faster-than-Nyquist Signaling

F. Ganhão[(1,2)], B. Cunha[(1)], L. Bernardo[(1,2)], R. Dinis[(1,2)], R. Oliveira[(1,2)]
[(1)] CTS, Uninova, Dep.^{o} de Eng.^{a} Electrotécnica, Faculdade de Ciências e Tecnologia, FCT,
Universidade Nova de Lisboa, 2829-516 Caparica, Portugal
[(2)] Instituto de Telecomunicações, Lisboa, Portugal

***Abstract*—Current wireless communication systems rely on the assumptions of the Nyquist theorem. Faster-Than-Nyquist (FTN) assumes that a bandwidth below the Nyquist bandwidth can be used with minimum loss, however the existing receivers are too complex. Single Carrier with Frequency-Domain Equalization (SC-FDE) has been proposed to handle multipath dispersive broadband channels, however the uplink of SC-FDE can be severely affected by deep-fades and/or poor channel conditions. To cope with such difficulties Diversity Combining (DC) Hybrid ARQ is a viable technique, since it combines the several packet copies sent by a Mobile Terminal to create reliable packet symbols at the receiver. This paper proposes a simple SC-FDE Packet Error Rate analytical model using FTN signaling, based on the Iterative Block with Decision Feedback Equalization technique, which achieves a performance similar to Nyquist signaling.**

***Index Terms*—SC-FDE, IB-DFE, Multipacket Reception, Packet Combining, Analytical Performance.**

I. Introduction

The design of future broadband wireless systems presents considerable challenges since those systems are expected to have high power and spectral efficiencies over channels with strong time-dispersive effects [1], [2]. It is well known that high power and spectral efficiency are conflicting goals since the increase in one is achieved at the decrease of the other.

Furthermore, in a time-dispersive channel, reception errors can be bothersome either due to poor channel conditions or a low Signal-to-Noise Ratio (SNR). To cope with channel errors, a BS can ask for additional copies of the same packet, but those copies might have errors since channel conditions might not vary for subsequent retransmissions leading to a throughput degradation. Fortunately the use of Hybrid Automatic Repeat reQuest (H-ARQ) [3] can be useful in such conditions, especially when employing Diversity Combining (DC) H-ARQ [1], since it uses the individual copies from each symbol, received at the BS, to create a packet with better reliability with appropriate equalization techniques.

A bandlimited transmission without Inter-Symbol Interference (ISI) is possible by employing pulses that satisfy the Nyquist criterion, with the most popular ones being the so-called raised-cosine pulses (actually square-root raised-cosine pulses are employed in this paper; using a matched filter results in raised-cosine pulses). The maximum spectral efficiency is associated to the minimum bandwidth, corresponding to pulses with an ideal rectangular spectrum (i.e. roll-off factor 0). Due to implementation difficulties, the roll-off is usually required to be above 0.25, which reduces the system's spectral efficiency.

A less known fact is that it is possible to achieve optimum asymptotic performance with a bandwidth below the minimum Nyquist band. In fact, by employing the so-called Faster-Than-Nyquist (FTN) signaling the transmission band can be reduced to around 80% without compromising the minimum Euclidean distance between different binary sequences, in spite of the inherent high ISI levels [4]. This remarkable result was almost completely ignored for over 30 years mainly because the optimum receiver with FTN signaling was too complex. However, due to spectrum scarcity and advances in signal processing there is a renewed interest in FTN (see [5] and references within).

FTN signaling is particularly interesting for broadband wireless systems. However, this means that the ISI inherent to FTN signaling is combined with the ISI associated to multipath time-dispersive effects, which leads to much higher ISI levels that cannot be handled by conventional FTN receivers (even the simplified receivers from [6], [7] are too complex). Block transmission techniques combined with Frequency-Domain Equalization (FDE) such as Orthogonal Frequency Division Multiplexing (OFDM) [2] and Single-Carrier with FDE (SC-FDE) [8] are widely recognized as the best candidates for the downlink and uplink, respectively [9], [10]. Although a linear FDE is suitable for OFDM, it is far from optimum for SC-FDE. In that case, the most promising FDE is the so-called IB-DFE (Iterative Block Decision-Feedback Equalizer) [11].

In this paper, an efficient H-ARQ technique is proposed for a SC-FDE system employing FTN signaling using the IB-DFE receiver to cope with the strong ISI inherent to FTN signaling over severely time-dispersive channels. This paper studies how the employment of bandwidth diversity and the redundancy of additional transmissions aid the use of FTN signaling, since its use can degrade the system performance.

The paper is organized as follows: section II characterizes the proposed SC-FDE system with FTN signaling; section III describes the IB-DFE receiver architecture; section IV performs the system simulations on the proposed receiver and section V comments this paper's conclusions.

This work was supported by the FCT/MEC projects CTS PEst-OE/EEI/UI0066/ 2011; IT PEst-OE/EEI/LA0008/ 2013; MPSat PTDC/EEA-TEL/099074/2008; OPPORTUNISTIC-CR PTDC/EEA-TEL/115981/ 2009; ADCOD PTDC/EEA-TEL/099973/2008 and Femtocells PTDC/EEA-TEL/120666/2010; Ciência 2008 Post-Doctoral Research grant as well as grant SFRH/BD/66105/2009.

II. System Characterization

The design of a SC-FDE system with FTN signaling allows a higher spectrum efficiency, though it should be expected a worser performance in terms of the bit error rate. A raised cosine pulse, for a roll-off α, symbol transmission time T_s (bandwidth $W = 1/T_s$) and an FTN factor $\beta = (1 - \Delta_f)$, where $\beta \leq 1$, is often characterized in the frequency domain as

$$R(f,\beta,\alpha,T_s) = \ldots$$
$$\begin{cases} T_s & 0 \leq |f| \leq \beta\frac{1-\alpha}{2T_s} \\ \frac{T_s}{2}\left(1+\cos\left(\frac{\pi T_s}{\alpha}\left(|f|-\frac{1-\alpha}{2T_s}\right)\right)\right) & \beta\frac{1-\alpha}{2T_s} \leq |f| \leq \beta\frac{1+\alpha}{2T_s} \\ 0 & |f| > \beta\frac{1+\alpha}{2T_s} \end{cases}.$$

So, assuming a *normalized* root-raised cosine pulse for a carrier frequency of F_c results

$$P^{\dagger}(f,F_c,\beta,\alpha,T_s) = \sqrt{\frac{A^2}{T_s}|R(f-F_c,\beta,\alpha,T_s)|}, \quad (1)$$

Figure 1 displays (1) with a roll-off $\alpha = 0.5$ for a bandwidth $W = 1/T_s$, in the frequency domain, for Nyquist and FTN signaling, where the pulse for FTN occupies only $\beta W = (1 - \Delta_f)W = 0.802W$ of the Nyquist bandwidth. As observed in this example the FTN pulse, although being smaller in bandwidth than the Nyquist pulse, it is capable of modulating a signal in the entire W bandwidth due to the extra bandwidth provided by the root-raised cosine. So based on this picture, it is possible to observe that FTN signaling only requires $2\beta W$ of bandwidth if the roll-off α extends a bandwidth total of $2W$.

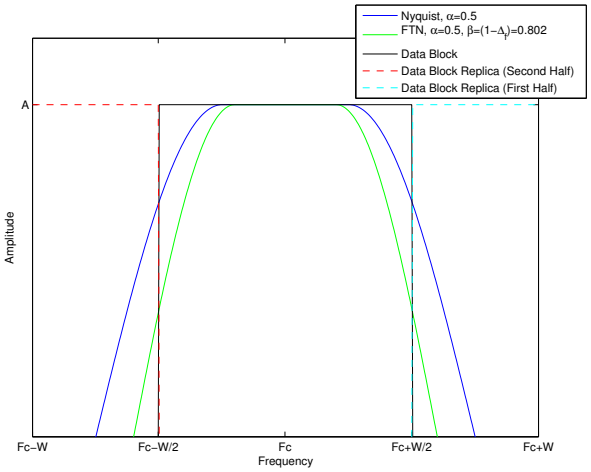

Figure 1. Root-raised cosine, $P^{\dagger}(f)$, in the frequency domain for a roll-off $\alpha = 0.5$ for Nyquist and FTN signaling, where $\beta = 0.802W$ for FTN.

In both types of signaling it is possible to take advantage of the additional bandwidth from the root raised cosine pulse outside of $[F_c - W/2, F_c + W/2]$, using it as additional diversity to diminish packet errors. With the additional bandwidth that can be re-used in the intervals $[F_c - \beta W, F_c - W/2[$ and $]F_c + W/2, F_c + \beta W]$, with $1/2 < \beta \leq 1$ (which depends on the shape of (1)), the SC-FDE data block can be partially replicated in those intervals. For Nyquist signaling, the first half of the data block can fill the interval $]Fc+W/2, Fc+W]$ and the second half the interval $[Fc - W, Fc - W/2[$ as demonstrated in Figure 1; for FTN the first half would be associated to $]Fc + W/2, Fc + \beta W]$ and second one to $[Fc - \beta W, Fc - W/2[$.

It should be noted though that the amount of diversity depends on α, $\beta = (1 - \Delta_f)$ value and the channel response for the additional bandwidth. It is more relevant near $-W/2$ and $W/2$, where the amplitude of the additional diversity is higher.

A data block sent by a MT is denoted by $[a_0, \ldots, a_{M-1}]$ and its respective Discrete Fourier Transform (DFT) by $[A_0, \ldots, A_k, \ldots, A_{M-1}]$, where M sub-carriers are distributed for the entire W bandwidth. For each symbol A_k there are two replicas for an l-th packet transmission, one modulated by the root-raised cosine pulse, $P^{\dagger}_{k,l,1}$, and the other one from its additional bandwidth, $P^{\dagger}_{k,2}$. So for an l-th transmission, where for the sake of simplicity $P^{\dagger}(f,F_c,\beta,\alpha,T_s)$ will be treated as $P^{\dagger}(f)$, results

$$P^{\dagger}_{k,l,i} = \ldots$$
$$\begin{cases} P^{\dagger}(-W/2 + k/W) & i = 1 \\ P^{\dagger}(W/2 + k/W) & i = 2 \wedge \left\{\lfloor\frac{\beta-0.5}{M}\rfloor \leq k \leq \frac{M}{2}\right\} \\ P^{\dagger}(-W/2 + k/W) & i = 2 \wedge \left\{\frac{M}{2} < k \leq \lfloor\frac{\beta-0.5}{M}\rfloor - 1\right\} \end{cases}.$$

Assuming that K is an integer that amounts the redundancy used for bandwidth diversity gain, where $K = \{1, 2\}$, so for a MT that sends L transmissions, the received signals at the BS for a given symbol are

$$\mathbf{Y}_k = \mathbf{H}^T_{k,K} A_k + \mathbf{N}_{k,K},$$

where $\mathbf{H}_{k,K} = \left[\mathbf{H}^{(1)}_{k,K}, \ldots, \mathbf{H}^{(L)}_{k,K}\right]$ and $\mathbf{N}_{k,K} = \left[\mathbf{N}^{(1)}_{k,K}, \ldots, \mathbf{N}^{(L)}_{k,K}\right]^T$ are the channel response multiplied by the root-raised cosine pulse and the channel noise respectively. Furthermore, expanding $\mathbf{H}^{(l)}_k$ and $\mathbf{N}^{(l)}_k$, for an l-th transmission results

$$\begin{aligned} \mathbf{H}^{(l)}_{k,1} &= {H^{(l)}_{k,1}}^{\dagger} P^{\dagger}_{k,l,1}, \\ \mathbf{H}^{(l)}_{k,2} &= \left[{H^{(l)}_{k,1}}^{\dagger} P^{\dagger}_{k,l,1}, {H^{(l)}_{k,2}}^{\dagger} P^{\dagger}_{k,l,2}\right], \\ \mathbf{N}^{(l)}_{k,1} &= N^{(l)}_{k,1}, \\ \mathbf{N}^{(l)}_{k,2} &= \left[N^{(l)}_{k,1}, N^{(l)}_{k,2}\right], \end{aligned}$$

where ${H^{(l)}_{k,1}}^{\dagger}$ and ${H^{(l)}_{k,2}}^{\dagger}$ are respectively the channel response for the main bandwidth and outside bandwidth of the root-raised cosine pulse for the l-th transmission.

III. IB-DFE Receiver Analysis

This section describes the IB-DFE receiver design for a Quadrature Phase Shift Keying (QPSK) modulation. The Packet Error Rate (PER) analytical model is largely based on the model from [12]. Perfect channel estimation and perfect synchronization conditions are assumed.

Regarding the IB-DFE receiver operation, it decodes packets in an iterative manner, removing channel noise and ISI interference up to N_{iter} iterations. It should be noted that the matched filter operation at the BS is already implicit within the IB-DFE equalization scheme, since the receiver already works with the $\mathbf{H}_k$ channel realizations and the symbol estimates from these realizations.

A data symbol estimation at the output of the IB-DFE receiver for iteration $i < N_{iter}$ is

$$\tilde{A}_k^{(i)} = {\mathbf{F}_k^{(i)}}^T \mathbf{Y}_k - B_k^{(i)} \bar{A}_k^{(i-1)}, \tag{2}$$

where

$${\mathbf{F}_{k,K}^{(i)}}^T = \left[{\mathbf{F}_{k,K}^{(i,1)}}^T, \ldots, {\mathbf{F}_{k,K}^{(i,L)}}^T \right], \tag{3}$$

are the feedforward coefficients, where for an l-th transmission

$$\begin{aligned} {\mathbf{F}_{k,1}^{(i,l)}}^T &= F_{k,1}^{(i,l)}, \\ {\mathbf{F}_{k,2}^{(i,l)}}^T &= \left[F_{k,1}^{(i,l)}, F_{k,2}^{(i,l)} \right]. \end{aligned} \tag{4}$$

and $\mathbf{B}_k^{(i)}$ is the feedback coefficient. $\bar{A}_k^{(i-1)}$ is the soft-decision estimate from the previous iteration, where

$$\begin{aligned} \bar{A}_k^{(i-1)} &\simeq \rho^{(i-1)} \hat{A}_k^{(i-1)}, \\ \hat{\mathbf{A}}_k^{(i-1)} &= \rho^{(i-1)} + \Delta_k. \end{aligned}$$

$\rho^{(i-1)}$ is a correlation coefficient and Δ_k is a zero-mean error value. For the first iteration, $i = 1$, $\bar{A}_k^{(i-1)}$ and $\rho^{(i-1)}$ are null values. For more information on the calculus of $\rho^{(i-1)}$, $\bar{A}_k^{(i-1)}$ and $\hat{A}_k^{(i-1)}$ for QPSK constellations refer to [13].

Assuming that R_A, $\mathbf{R}_N$ and R_Δ, are respectively, the correlation of $\mathbf{A}_k$, $\mathbf{N}_k$ and $\mathbf{\Delta}_k$, and considering that σ_A^2 is the symbol's variance and σ_N^2 is the noise's variance then

$$R_A = \mathbb{E}\left[|A_k|^2 \right] = 2\sigma_A^2, \tag{5}$$

$$\mathbf{R}_N = \mathbb{E}\left[\mathbf{N}_k \mathbf{N}_k^H \right] = 2\sigma_N^2 \mathbf{I}_{K \times L}, \tag{6}$$

$$R_\Delta = \mathbb{E}\left[|\Delta_k|^2 \right] \simeq 2\sigma_A^2 \left(1 - {\rho^{(i-1)}}^2 \right). \tag{7}$$

For R_Δ calculus refer to [14].

The Mean Square Error (MSE), $MSE_{k,p}^{(i)}$, of A_k for an i-th iteration, as in [12], is

$$\begin{aligned} MSE_k^{(i)} &= \mathbb{E}\left[\left| A_k - \tilde{A}_k^{(i)} \right|^2 \right] \\ &= {\alpha_k^{(i)}}^* R_A \alpha_k^{(i)} + {\mathbf{F}_{k,K}^{(i)}}^H \mathbf{R}_N \mathbf{F}_{k,K}^{(i)} + \ldots \\ &\ldots + \quad {\beta_k^{(i)}}^* R_\Delta \beta_k^{(i)}. \end{aligned} \tag{8}$$

where

$$\alpha_k^{(i)} = \mathbf{F}_{k,K}^{(i)} \mathbf{H}_{k,K}^T - B_k^{(i)} {\rho^{(i-1)}}^2 - 1, \tag{9}$$

$$\beta_k^{(i)} = B_k^{(i)} \rho^{(i-1)}. \tag{10}$$

To compute the optimal coefficients, $\mathbf{F}_{k,K}^{(i)}$ and $B_k^{(i)}$, under the MMSE criterion and constrained to $\gamma_p^{(i)} = \frac{1}{M} \sum_{k=0}^{M-1} \sum_{l=1}^{L} \sum_{j=1}^{K} F_{k,j}^{(i,l)} {H_{k,j}^{(l)}}^\dagger P_{k,j}^\dagger = 1$ is formally equivalent to the Lagrange function applied to (8), where $\mathcal{L}_k^{(i)} = MSE_k^{(i)} + \left(\gamma_p^{(i)} - 1 \right) \lambda_p^{(i)}$. Therefore the gradient operation is applied to $\mathcal{L}_{k,p}^{(i)}$ where

$$\nabla \mathcal{L}_k^{(i)} = \nabla \left(MSE_k^{(i)} + \left(\gamma_p^{(i)} - 1 \right) \lambda_p^{(i)} \right). \tag{11}$$

The Lagrange multipliers in (11) ensure a maximum signal to interference plus noise ratio. Evaluating the following set of equations

$$\begin{cases} \nabla_{\mathbf{F}_{k,K}^{(i)}} \mathcal{L} = 0 \\ \nabla_{B_k^{(i)}} \mathcal{L} = 0 \\ \nabla_{\lambda_p^{(i)}} \mathcal{L} = 0 \end{cases}, \tag{12}$$

$\nabla_{\mathbf{F}_{k,K}^{(i)}} \mathcal{L} = 0$ is

$$\begin{aligned} &\mathbf{H}_{k,K}^H R_A \mathbf{H}_{k,K} \mathbf{F}_k^{(i)} - \mathbf{H}_{k,K}^H R_A {\rho^{(i-1)}}^2 B_k^{(i)} - \ldots \\ &\ldots - \mathbf{H}_{k,K}^H R_A + \mathbf{R}_N \mathbf{F}_{k,K}^{(i)} + \frac{1}{M} \mathbf{H}_{k,K}^H \lambda_p^{(i)} = 0, \end{aligned} \tag{13}$$

$\nabla_{\mathbf{B}_{k,p}^{(i)}} \mathcal{L} = 0$ is

$$\begin{aligned} &\left({\rho^{(i-1)}}^2 R_A + R_\Delta \right) \mathbf{B}_k^{(i)} = \ldots \\ &\ldots = R_A \mathbf{H}_{k,K} \mathbf{F}_{k,K}^{(i)} - R_A, \end{aligned} \tag{14}$$

and $\nabla_{\lambda_p^{(i)}} \mathcal{L}$ is $\gamma_p^{(i)} = 1$. So the optimal coefficients are

$$\begin{cases} B_k^{(i)} = \mathbf{H}_{k,K} \mathbf{F}_{k,K}^{(i)} - 1 \\ \mathbf{F}_{k,K}^{(i)} = \mathbf{\Lambda}_k^{(i)} \mathbf{H}_{k,K}^H \mathbf{\Theta}_k^{(i)} \end{cases}, \tag{15}$$

where

$$\mathbf{\Lambda}_k^{(i)} = \left(\mathbf{H}_{k,K}^H \left(1 - {\rho^{(i-1)}}^2 \right) \mathbf{H}_{k,K} + \frac{\sigma_N^2}{\sigma_S^2} \mathbf{I}_{K \times L} \right)^{-1},$$

$$\mathbf{\Theta}_k^{(i)} = \left(1 - {\rho^{(i-1)}}^2 \right) - \frac{\lambda_p^{(i)}}{2\sigma_A^2 M}.$$

From (8), and using the optimal $\mathbf{F}_k^{(i)}$ and $B_{k,p}^{(i)}$ coefficients from (15), it is possible to compute the MMSE. Defining

$${\sigma_p^2}^{(i)} = \frac{1}{M^2} \sum_{k=0}^{M-1} MSE_k^{(i)}, \tag{16}$$

and the Gaussian error function, $\Phi(x)$, the estimated Bit Error Rate (BER) at the ith iteration for a QPSK constellation is

$$BER^{(i)} \simeq \Phi\left(\frac{1}{{\sigma_p}^{(i)}} \right). \tag{17}$$

Since a severely time dispersive channel with multipath propagation is being considered, bit errors can be considered independent, therefore for an uncoded system with independent and isolated errors, the Packet Error Rate (PER) for a fixed packet size of N bits is

$$PER^{(i)} \simeq 1 - \left(1 - BER^{(i)}\right)^{N}. \quad (18)$$

IV. Performance Results

The current section presents the proposed system performance results, for an Additive White Gaussian Noise (AWGN) and a multipath time-dispersive channel such as the one in [17]. The results were obtained through *Monte Carlo* simulations, assuming that a MT sends data packets to the BS with $M = 256$ QPSK symbols, for a total of 1000 simulations - each data symbol lasts for $4\mu s$ and the SC-FDE Cyclic Prefix (CP) has the equivalent duration of 20% of the data block. For each figure the lines illustrate the theoretical performance of the proposed PER model and the markers the simulations' results.

Figure 2 presents the PER for $\beta = 1$ with $\alpha = 0.5$ and $L = \{1, 2, 4\}$ up to 4 iterations without bandwidth diversity ($K = 1$). The PER model follows with good accuracy the simulations' results and as expected the system results show that with an increasing number of iterations and H-ARQ transmissions the performance is greatly enhanced.

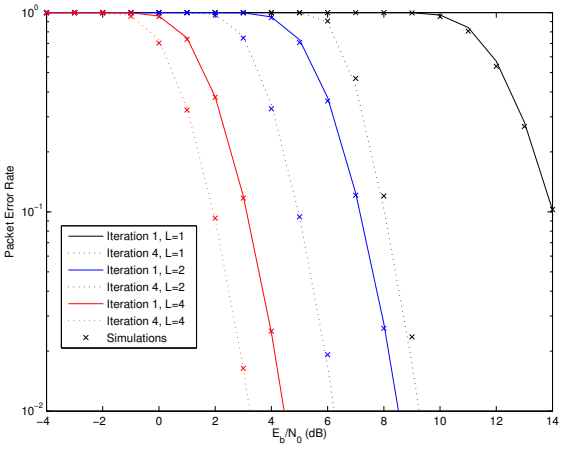

Figure 2. PER for $\beta = 1$ with $\alpha = 0.5$ and $L = \{1; 2; 4\}$ up to 4 iterations without bandwidth diversity ($K = 1$).

Figure 3 presents the PER for $\beta = 1$ with $\alpha = 0.5$ and $L = \{1, 2, 4\}$ for 4 iterations with/out bandwidth diversity ($K = \{1; 2\}$). Once more the PER model accurately follows the performance of the simulations' results, where the addition of bandwidth diversity ($K = 2$) enhances the system performance for a lower number of transmissions; the increase of H-ARQ transmissions also aids to diminish the amount of errors introduced by the channel.

Figure 4 illustrates the PER for $\beta = \{0.7; 0.802; 1\}$ with $\alpha = 0.5$ and $L = \{1; 4\}$ up to 4 iterations without bandwidth

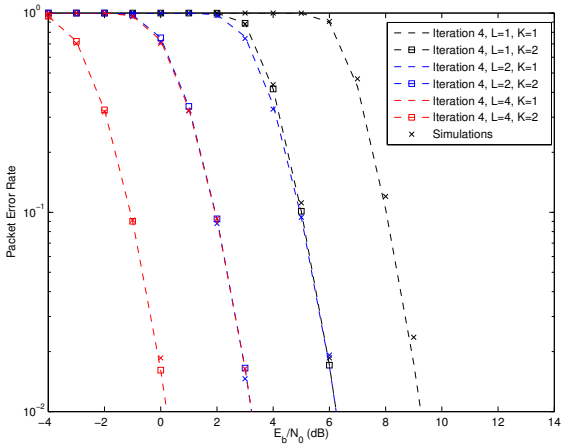

Figure 3. PER for $\beta = 1$ with $\alpha = 0.5$ and $L = \{1; 2; 4\}$ up to 4 iterations with(out) bandwidth diversity ($K = \{1; 2\}$).

diversity ($K = 1$). In this figure the PER analytical model has a higher difficulty to portray the system results for a lower number of packet transmissions when $\beta < 1$, otherwise it can portray with good accuracy the simulations' results. In terms of the system performance as the number of iterations increases the overall performance between different values of β becomes smaller, meaning that it is possible to achieve a similar performance to Nyquist signaling with a reduction of the bandwidth up to 30%. Furthermore the inclusion of more transmissions also aids the performance of the proposed system with FTN signaling, since the additional redundancy helps to reduce ISI erros.

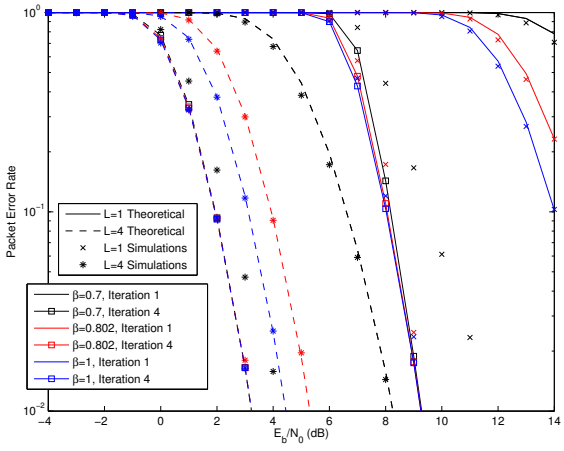

Figure 4. PER for $\beta = \{0.7; 0.802; 1\}$ with $\alpha = 0.5$ and $L = \{1; 4\}$ up to 4 iterations without bandwidth diversity ($K = 1$).

Figure 5 portrays the PER for $\beta = \{0.7; 0.802; 1\}$ with $\alpha = 0.5$ and $L = \{1; 4\}$ and 4 iterations with(out) bandwidth diversity ($K = \{1; 2\}$). The PER model can portray the system results with greater accuracy for a higher number

of transmissions, as well as for the inclusion of bandwidth diversity, except for a lower number of packet transmissions and a smaller bandwidth diversity. As expected, the system performs better with the addition of bandwidth diversity and in this case it is quite noticeable that the employment of FTN signaling achieves almost similar results to Nyquist signaling as long as the BS employs a high number of iterations. In addition the use of DC H-ARQ also aids the proposed system to recover from packet errors introduced by FTN signaling, especially ISI errors.

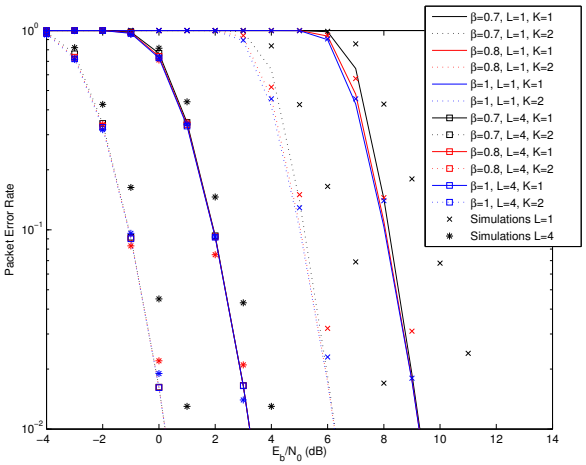

Figure 5. PER for $\beta = \{0.7; 0.802; 1\}$ with $\alpha = 0.5$ and $L = \{1; 4\}$ and 4 iterations with(out) bandwidth diversity ($K = \{1; 2\}$).

V. Conclusions

An FTN PER model was proposed in this paper for a SC-FDE context at the uplink, where the BS takes advantage of the full bandwidth diversity from the root-raised cosine pulse using the IB-DFE technique for equalization and DC H-ARQ to enhance packet reception. Results show that the PER model achieves similar results to the simulated values and that it is possible to achieve similar results to Nyquist signaling by employing the IB-DFE technique with additional bandwidth diversity and additional transmissions from DC H-ARQ. For future work, the authors plan to extend the analytical model and propose higher-layer models that characterize a bandwidth efficient system.

References

[1] M. Pereira, L. Bernardo, R. Oliveira, P. Carvalho, P. Pinto, "Performance of Diversity Combining ARQ Error Control in a TDMA SC-FDE System," Communications, IEEE Transactions on , vol.60, no.3, pp.735–746, March 2012

[2] L. Cimini, "Analysis and simulation of a digital mobile channel using orthogonal frequency division multiplexing," IEEE Trans. Commun., vol. 33, no. 7, July 1985.

[3] D. Costello, J. Hagenauer, H. Imai and S. Wicker, "Applications of error-control coding," *in IEEE Transactions on Information Theory*, vol.44, no.6, pp.2531-2560, October 1998.

[4] J. Mazo, "Faster-than-Nyquist signaling", Bell Syst. Tech. J., vol. 54, pp. 1451-1462, Oct. 1975.

[5] J. Anderson, F. Rusek, V. Owall, "Faster-Than-Nyquist Signaling", IEEE Proceedings, Vol. 101, No. 8, pp. 1817-1830, Aug. 2013.

[6] J. Anderson and A. Prlja, "Turbo equalization and an M-BCJR algorithm for strongly narrowband intersymbol interference", in Proc. Int. Symp. Inf. Theory Appl., Taichung, Taiwan, pp. 261-266, Oct. 2010.

[7] A. Prlja and J. Anderson, "Reduced-complexity receivers for strongly narrowband intersymbol interference introduced by faster-than-Nyquist signaling", IEEE Trans. Commun., vol. 60, no. 9, pp. 2591-2601, Sep. 2012.

[8] H. Sari, G. Karam and I. Jeanclaude, "An Analysis of Orthogonal Frequency-division Multiplexing forMobile Radio Applications," In Proc. IEEE Vehic. Tech. Conf., VTC-94, pp. 1635-1639, Stockholm, June 1994.

[9] A. Gusmão, R. Dinis, J. Conceiçao and N. Esteves, "Comparison of two modulation choices for broadband wireless communications," *in Proceedings of 2000 IEEE Vehicular Technology Conference Spring*, vol.2, pp.1300-1305, 2000.

[10] D. Falconer, S. Ariyavisitakul, A. Benyamin-Seeyar and B. Eidson, "Frequency domain equalization for single-carrier broadband wireless systems," *in IEEE Communications Magazine*, vol.40, no.4, pp.58-66, April 2002.

[11] N. Benvenuto, R. Dinis, D. Falconer and S. Tomasin, "Single Carrier Modulation With Nonlinear Frequency Domain Equalization: An Idea Whose Time Has Come–Again," *in Proceedings of the IEEE*, vol.98, no.1, pp.69-96, January 2010.

[12] F. Ganhão, R. Dinis, L. Bernardo, R. Oliveira, "Analytical BER and PER Performance of Frequency-Domain Diversity Combining, Multipacket Detection and Hybrid Schemes," *in IEEE Transactions in Communications*, vol. 60, n. 8, August 2012.

[13] N. Benvenuto and S. Tomasin, "Block iterative DFE for single carrier modulation," *in Electronics Letters*, vol.38, no.19, pp. 1144-1145, 12 September 2002.

[14] R. Dinis, P. Silva and A. Gusmão, "IB-DFE receivers with space diversity for CP-assisted DS-CDMA and MC-CDMA systems," *in European Transactions on Telecommunications*, vol. 18, pp. 791–802, June 2007.

[15] F. Ganhão, M. Pereira, L. Bernardo, R. Dinis, N. Souto, J. Silva, R. Oliveira and P. Pinto, "Energy per useful packet optimization on a TDMA HAP channel," *in Proc. of 2010 IEEE Vehicular Technology Conference Fall*, September 2010.

[16] S. Cui, A. Goldsmith, and A. Bahai, "Energy-constrained modulation optimization," IEEE Transactions on Wireless Communications, vol. 4, no. 5, pp. 2349–2360, Sept. 2005.

[17] J. Medbo and P. Schramm, "Channel models for HIPERLAN/2 in different indoor scenarios," *ETSI BRAN 3ERI085B*, pp. 1-8, 1998.

A Hybrid ARQ Scheme for Faster than Nyquist Signaling with Iterative Frequency-Domain Detection

R. Dinis[(1,2)], B. Cunha[(1)], F. Ganhão[(1,2)], L. Bernardo[(1,2)], R. Oliveira[(1,2)], P. Pinto[(1,2)]
[(1)] CTS, Uninova, Dep.^{o} de Eng.^{a} Electrotécnica, Faculdade de Ciências e Tecnologia, FCT,
Universidade Nova de Lisboa, 2829-516 Caparica, Portugal
[(2)] Instituto de Telecomunicações, Lisboa, Portugal

***Abstract*—FTN (Faster Than Nyquist) signaling allows capacity gains but requires substantially complex equalization schemes, even for an ideal AWGN (Additive White Gaussian Noise) channel. Extending conventional FTN receivers for severely time-dispersive channels is not an option, since the receiver complexity becomes prohibitively high. In this paper we address the design of a receiver for FTN signaling over severely time-dispersive channels. To cope with the severe ISI (Inter-Symbol Interference) associated to the combined effects of FTN signaling and the time-dispersive channel we consider an iterative FDE scheme (Frequency-Domain Equalization) combined with a HARQ (Hybrid Automatic Repeat reQuest) especially designed taking into account the characteristics of FTN signals. We also present a simple, yet accurate model for the performance evaluation, considering multiple retransmissions per block. Our performance results show that we can have significant throughput gains, while maintaining essentially the receiver complexity of conventional, Nyquist-rate signaling schemes, even for severely time-dispersive channels.** [1]

***Index Terms*—Faster Than Nyquist, SC-FDE, IB-DFE, Packet Combining, Hybrid ARQ, Analytical Performance.**

I. Introduction

It is well-known that the minimum bandwidth for a transmission without ISI (Inter-Symbol Interference), also known as Nyquist bandwidth, is half the symbol rate [1]. This can be achieved by employing sinc pulses. Since symbol-spaced pulses are orthogonal, a relatively simple receiver based on a matched filter can have optimum performance, identical to the one achieved when an isolated pulse is transmitted. However, to overcome the implementation difficulties inherent to the use of a sinc pulse (i.e., filter with ideal rectangular shape), most communication systems employ square-root raised cosine pulses which are simpler to implement, although have a slightly higher bandwidth (typically will roll-off between 0.25 and 0.5). This extra bandwidth is generally regarded as an unavoidable price that we have to pay when designing communication systems in general and wireless communication systems in particular, which are known to have significant power and bandwidth constraints.

[1]This work was supported by the FCT/MEC projects ADIN PTDC/EEI-TEL/2990/2012; CTS PEst-OE/EEI/UI0066/2011; IT PEst-OE/EEI/LA0008/2013; MANY2COMWIN EXPL/EEI-TEL/0969/2013; and EnAcoMIMOCo EXPL/EEI-TEL/2408/2013.

A lesser known result is the fact that we can still have optimum asymptotic performance with a bandwidth below the minimum Nyquist bandwidth. In fact, for binary signaling we can reduce the symbol separation by a factor up to 0.802 without asymptotic performance degradation, which is usually known as "Mazo's limit" [2]. The same phenomenon occurs with other pulse shapes [3], as well as two-dimensional and/or multicarrier systems [4], [5]. Since the radio spectrum is a scarce and expensive resource, FTN signaling seems an interesting choice, especially for broadband wireless systems, since it allows significant increase on the spectral efficiency. However, FTN signaling is usually not considered because FTN signaling requires complex receivers able to cope with the resulting ISI levels [6], [7], even when reduced-complexity receivers are employed [8], [9]. The receiver complexity increases substantially if we consider FTN signaling over severely time-dispersive channels, where the ISI inherent to FTN signaling is combined with the ISI associated to multipath time-dispersive effects.

Block transmission techniques combined with FDE (Frequency-Domain Equalization) such as OFDM (Orthogonal Frequency Division Multiplexing) [10] and SC-FDE (Single-Carrier with FDE) [11] have demonstrated that OFDM is suitable for the downlink transmission (i.e., the transmission from the BS (Base Station) to the UE (User Equipment)), while SC-FDE is preferable for the uplink (i.e., the transmission from the UE to the BS) [12], [13]. Since for OFDM schemes the detection is performed at the subcarrier level, a linear FDE is appropriate for OFDM. This is not the case of SC-FDE, where we can improve significantly the performance by employing a nonlinear FDE [14]. The most promising nonlinear FDE is the IB-DFE (Iterative Block Decision-Feedback Equalizer) [15], which is an iterative FDE. Although IB-DFE-based equalizers are sub-optimum receivers they have two main advantages: their complexity is independent of the ISI levels (and the ISI span) and their performance can be very good, even approaching the MFB (Matched Filter Bound) [16].

In this paper we consider the use of FTN signaling for the uplink of broadband wireless systems employing SC-FDE schemes. We present an IB-DFE receiver especially designed to cope with the overall ISI inherent to both FTN signaling

and severely time-dispersive multipath channels. Although our receiver is able to cope with the strong ISI levels, it still has some performance degradation when compared with Nyquist-rate signaling, and the degradation increases as we increase the rate. To cope with this degradation, we consider a HARQ scheme especially designed to the specifics of the FTN signals. FTN signaling is used in the first transmission of a block. In case of an error, the complementary signal information pruned using FTN is transmitted, allowing the receiver to combine them and achieve a Nyquist signaling equivalent performance. If both transmissions fail, the procedure may be repeated up to L times, before dropping the block. After each new failed transmission, a HARQ approach is used [17] to reduce the error rate. Thus, the channel data slot's duration will depend on what is being transmitted: the initial FTN signal, or the complementary one. This new approach requires a scheduled access uplink channel, where the base station (BS) defines the sequence and type of the slots assigned to each mobile terminal (MT). On the other hand, given a high success rate of the initial FTN transmission, it is possible to achieve a bandwidth efficiency gain of up to $1/\beta$.

This paper is organized as follows: section II characterizes the proposed SC-FDE system with FTN signaling; section III describes the IB-DFE receiver architecture; section IV analyses the medium access control performance; section V performs the system simulations on the proposed receiver and section VI presents the paper's conclusions.

II. System Characterization

This paper assumes a scheduled access uplink data channel coordinated by the BS, using two control channels: an uplink shared control channel is used to transmit block transmission requests; a downlink shared control channel is used to broadcast the slot allocation map in the uplink data channel. The data slots of the uplink data channel are allocated to individual MTs and can be of two sizes: large slots (corresponding to the FTN symbol separation factor β) and short slots (corresponding to the residual information $(1-\beta)$, required to have Nyquist rate signal information). The effective bandwidth used is larger due to the root-raised cosine used in both kinds of slots with a roll-off α. Up to L consecutive transmissions on a long and short slots can be used for a single data block.

The design of a SC-FDE system with FTN signaling allows a higher spectrum efficiency when only long slots are used, though it should be expected a worse performance in terms of the bit error rate, which is compensated by the complementary transmission of short slots.

A raised cosine pulse, for a roll-off α, symbol transmission time T_s (bandwidth $W = 1/T_s$) and a FTN factor $\beta = (1 - \Delta_f)$, where $\beta \leq 1$ is often characterized in the frequency domain as

$$R(f,\beta,\alpha,T_s) = \ldots$$
$$\begin{cases} T_s & 0 \leq |f| \leq \beta\frac{1-\alpha}{2T_s} \\ \frac{T_s}{2}\left(1+\cos\left(\frac{\pi T_s}{\alpha}\left(|f|-\frac{1-\alpha}{2T_s}\right)\right)\right) & \beta\frac{1-\alpha}{2T_s} \leq |f| \leq \beta\frac{1+\alpha}{2T_s} \\ 0 & |f| > \beta\frac{1+\alpha}{2T_s} \end{cases}.$$

So, assuming a *normalized* root-raised cosine pulse for a carrier frequency of F_c results

$$P^{\dagger}(f,F_c,\beta,\alpha,T_s) = \sqrt{\frac{A^2}{T_s}|R(f-F_c,\beta,\alpha,T_s)|}. \quad (1)$$

Figure 1 displays (1) with a roll-off $\alpha = 0.5$ for a bandwidth $W = 1/T_s$, in the frequency domain, for Nyquist and FTN signaling, where the pulse for FTN occupies only $\beta W = (1-\Delta_f)W = 0.802W$ of the Nyquist bandwidth. As observed in this example the FTN pulse, although being smaller in bandwidth than the Nyquist pulse, is capable of modulating a signal in the entire W bandwidth due to the extra bandwidth provided by the root-raised cosine. So, based on this picture, it is possible to observe that FTN signaling only requires $2\beta W$ of bandwidth if the roll-off α extends a total bandwidth of $2W$.

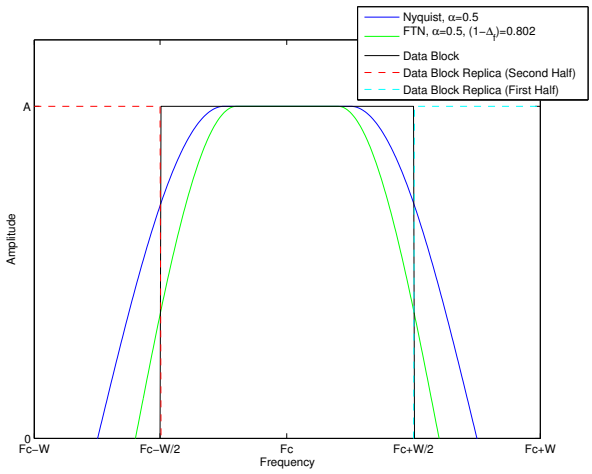

Figure 1. Root-raised cosine, $P^{\dagger}(f)$, in the frequency domain for a roll-off $\alpha = 0.5$ for Nyquist and FTN signaling.

In both types of signaling it is possible to take advantage of the additional bandwidth from the root raised cosine pulse outside of $[F_c - W/2, F_c + W/2]$, using it as additional diversity to diminish packet errors. With the additional bandwidth that can be re-used in the intervals $[F_c - \beta W, F_c - W/2[$ and $]F_c + W/2, F_c + \beta W]$, with $1/2 < \beta \leq 1$ (which depends on the shape of (1)), the SC-FDE data block can be partially replicated in those intervals. For Nyquist signaling, the first half of the data block can fill the interval $]Fc+W/2, Fc+W]$ and the second half the interval $[Fc - W, Fc - W/2[$ as demonstrated in Figure 1; for FTN the first half would be

associated to $]Fc + W/2, Fc + \beta W]$ and second one to $[Fc - \beta W, Fc - W/2[$.

It should be noted though that the amount of diversity used is dependent on the root-raised cosine roll-off α, the $\beta = (1 - \Delta_f)$ value and the channel response for the additional bandwidth. It is more relevant near $-W/2$ and $W/2$, where the amplitude of the additional diversity is higher.

Assuming a data block sent by a MT, $[a_0, \ldots, a_{M-1}]$, and its respective Discrete Fourier Transform (DFT), $[A_0, \ldots, A_k, \ldots, A_{M-1}]$, where M sub-carriers are distributed for the entire W bandwidth of one slot (large or short). For each symbol A_k and for a slot j there are two replicas sent, one modulated by the root-raised cosine pulse, $P_{k,1}^{(j)\dagger}$, and the other one from its additional bandwidth, $P_{k,2}^{(j)\dagger}$. For the sake of simplicity $P^{(j)\dagger}(f, F_c, \beta, \alpha, T_s)$ will be treated as $P^{(j)\dagger}(f)$, so

$$P_{k,i}^{(j)\dagger} = \ldots$$
$$\begin{cases} P^{(j)\dagger}(-W/2 + k/W) & i = 1 \\ P^{(j)\dagger}(W/2 + k/W) & i = 2 \wedge \left\{ \lfloor \frac{\beta - 0.5}{M} \rfloor \leq k \leq \frac{M}{2} \right\} \\ P^{(j)\dagger}(-W/2 + k/W) & i = 2 \wedge \left\{ \frac{M}{2} < k \leq \lfloor \frac{\beta - 0.5}{M} \rfloor - 1 \right\} \end{cases}.$$

Assuming that K is an integer that amounts the redundancy used for bandwidth diversity gain, where $K = \{1, 2\}$, so for a MT that sends L transmissions in long slots and L transmissions in L short slots, the received signals at the BS for a given symbol are

$$\mathbf{Y}_k = \mathbf{H}_{k,K}^T A_k + \mathbf{N}_{k,K},$$

where $\mathbf{H}_{k,K} = \left[\mathbf{H}_{k,K}^{(1,1)}, \mathbf{H}_{k,K}^{(1,2)}, \ldots, \mathbf{H}_{k,K}^{(L,1)}, \mathbf{H}_{k,K}^{(L,2)}\right]$ is the channel response multiplied by the root-raised cosine pulses of the long and short slots and $\mathbf{N}_{k,K} = \left[\mathbf{N}_{k,K}^{(1,1)}, \mathbf{N}_{k,K}^{(1,2)}, \ldots, \mathbf{N}_{k,K}^{(L,1)}, \mathbf{N}_{k,K}^{(L,2)}\right]^T$ is the channel noise. Furthermore, expanding $\mathbf{H}_k^{(l,j)}$ and $\mathbf{N}_k^{(l,j)}$, for an l-th transmission and j-th slot ($j = 1$ stands for the transmission in a long slot and $j = 2$ in a short slot) results

$$\begin{aligned} \mathbf{H}_{k,1}^{(l,1)} &= {H_{k,1}^{(l)}}^{\dagger} P_{k,1}^{(1)\dagger}, \\ \mathbf{H}_{k,1}^{(l,2)} &= {H_{k,1}^{(l)}}^{\dagger} P_{k,1}^{(2)\dagger}, \\ \mathbf{H}_{k,2}^{(l,1)} &= \left[{H_{k,1}^{(l)}}^{\dagger} P_{k,1}^{(1)\dagger}, {H_{k,2}^{(l)}}^{\dagger} P_{k,2}^{(1)\dagger}\right], \\ \mathbf{H}_{k,2}^{(l,2)} &= \left[{H_{k,1}^{(l)}}^{\dagger} P_{k,1}^{(2)\dagger}, {H_{k,2}^{(l)}}^{\dagger} P_{k,2}^{(2)\dagger}\right], \\ \mathbf{N}_{k,1}^{(l,j)} &= N_{k,1}^{(l,j)}, \\ \mathbf{N}_{k,2}^{(l,j)} &= \left[N_{k,1}^{(l,j)}, N_{k,2}^{(l,j)}\right], \end{aligned}$$

where ${H_{k,1}^{(l,j)}}^{\dagger}$ and ${H_{k,2}^{(l,j)}}^{\dagger}$ are respectively the channel response for the main bandwidth and outside bandwidth of the root-raised cosine pulse for the l-th transmission and j-th slot. $P_{k,i}^{(1)\dagger}$ and $P_{k,i}^{(2)\dagger}$ are raised cosine shapes with band βW and $(1-\beta)W$, respectively (without loss of generality, we assume the same roll-off). Since the frequency-domain samples at the edge of the band were eliminated or faced strong attenuation due to FTN filtering, it is desirable to give more power to those samples at the second transmission attempt. This can be achieved by a cyclic shift of length $M/2$ on the set of A_k, which is formally equivalent to make a similar but reversed shift on ${H_{k,2}^{(l,j)}}^{\dagger}$ and $P_k^{(2)\dagger}$.

The lack of transmission in a short slot is modeled by ${H_{k,K}^{(l,2)}}^{\dagger} = 0$.

III. IB-DFE Receiver Analysis

This section describes the IB-DFE receiver design for a Quadrature Phase Shift Keying (QPSK) modulation. The Packet Error Rate (PER) analytical model is largely based on the model from [17]. Perfect channel estimation and perfect synchronization conditions are assumed.

Regarding the IB-DFE receiver operation, it decodes packets in an iterative manner, removing channel noise and ISI interference up to N_{iter} iterations. It should be noted that the matched filter operation at the BS is already implicit within the IB-DFE equalization scheme, since the receiver already works with the $\mathbf{H}_k$ channel realizations and the symbol estimates from these realizations.

A data symbol estimation at the output of the IB-DFE receiver for iteration $i < N_{iter}$ is

$$\tilde{A}_k^{(i)} = {\mathbf{F}_k^{(i)}}^T \mathbf{Y}_k - B_k^{(i)} \bar{A}_k^{(i-1)}, \tag{2}$$

where

$${\mathbf{F}_{k,K}^{(i)}}^T = \left[{\mathbf{F}_{k,K}^{(i,1)}}^T, \ldots, {\mathbf{F}_{k,K}^{(i,L)}}^T\right], \tag{3}$$

are the feedforward coefficients, where for an l-th transmission

$$\begin{aligned} {\mathbf{F}_{k,1}^{(i,l)}}^T &= F_{k,1}^{(i,l)}, \\ {\mathbf{F}_{k,2}^{(i,l)}}^T &= \left[F_{k,1}^{(i,l)}, F_{k,2}^{(i,l)}\right]. \end{aligned} \tag{4}$$

and $\mathbf{B}_k^{(i)}$ is the feedback coefficient. $\bar{A}_k^{(i-1)}$ is the soft-decision estimate from the previous iteration, where

$$\begin{aligned} \bar{A}_k^{(i-1)} &\simeq \rho^{(i-1)} \hat{A}_k^{(i-1)}, \\ \hat{\mathbf{A}}_k^{(i-1)} &= \rho^{(i-1)} + \Delta_k. \end{aligned}$$

$\rho^{(i-1)}$ is a correlation coefficient and Δ_k is a zero-mean error value. For the first iteration, $i = 1$, $\bar{A}_k^{(i-1)}$ and $\rho^{(i-1)}$ are null values. For more information on the calculus of $\rho^{(i-1)}$, $\bar{A}_k^{(i-1)}$ and $\hat{A}_k^{(i-1)}$ for QPSK constellations refer to [15].

Assuming that R_A, $\mathbf{R}_N$ and R_Δ, are respectively, the correlation of $\mathbf{A}_k$, $\mathbf{N}_k$ and $\mathbf{\Delta}_k$, and considering that σ_A^2 is the symbol's variance and σ_N^2 is the noise's variance then

$$R_A = \mathbb{E}\left[|A_k|^2\right] = 2\sigma_A^2, \tag{5}$$

$$\mathbf{R}_N = \mathbb{E}\left[\mathbf{N}_k \mathbf{N}_k^H\right] = 2\sigma_N^2 \mathbf{I}_{K \times L}, \tag{6}$$

$$R_\Delta = \mathbb{E}\left[|\Delta_k|^2\right] \simeq 2\sigma_A^2 \left(1 - {\rho^{(i-1)}}^2\right). \tag{7}$$

For R_Δ calculus refer to [18].

The Mean Square Error (MSE), $MSE_{k,p}^{(i)}$, of A_k for an i-th iteration, as in [17], is

$$\begin{aligned} MSE_k^{(i)} &= \mathbb{E}\left[\left|A_k - \tilde{A}_k^{(i)}\right|^2\right] \\ &= {\alpha_k^{(i)}}^* R_A \alpha_k^{(i)} + {\mathbf{F}_{k,K}^{(i)}}^H \mathbf{R}_N \mathbf{F}_{k,K}^{(i)} + \dots \\ &\dots + \quad {\beta_k^{(i)}}^* R_\Delta \beta_k^{(i)}. \end{aligned} \tag{8}$$

where

$$\alpha_k^{(i)} = \mathbf{F}_{k,K}^{(i)} \mathbf{H}_{k,K}^T - B_k^{(i)} {\rho^{(i-1)}}^2 - 1, \tag{9}$$

$$\beta_k^{(i)} = B_k^{(i)} \rho^{(i-1)}. \tag{10}$$

To compute the optimal coefficients, $\mathbf{F}_{k,K}^{(i)}$ and $B_k^{(i)}$, under the MMSE criterion and constrained to $\gamma_p^{(i)} = \frac{1}{M}\sum_{k=0}^{M-1}\sum_{l=1}^{L}\sum_{j=1}^{K} F_{k,j}^{(i,l)} H_{k,j}{}^{(l)\dagger} P_{k,j}^{\dagger} = 1$ is formally equivalent to the Lagrange function applied to (8), where $\mathcal{L}_k^{(i)} = MSE_k^{(i)} + \left(\gamma_p^{(i)} - 1\right)\lambda_p^{(i)}$. Therefore the gradient operation is applied to $\mathcal{L}_{k,p}^{(i)}$ and the optimal coefficients are calculated [19],

$$\begin{cases} B_k^{(i)} = \mathbf{H}_{k,K}\mathbf{F}_{k,K}^{(i)} - 1 \\ \mathbf{F}_{k,K}^{(i)} = \mathbf{\Lambda}_k^{(i)} \mathbf{H}_{k,K}^H \mathbf{\Theta}_k^{(i)} \end{cases}, \tag{11}$$

where

$$\mathbf{\Lambda}_k^{(i)} = \left(\mathbf{H}_{k,K}^H \left(1 - {\rho^{(i-1)}}^2\right)\mathbf{H}_{k,K} + \frac{\sigma_N^2}{\sigma_S^2}\mathbf{I}_{K\times L}\right)^{-1},$$

$$\mathbf{\Theta}_k^{(i)} = \left(1 - {\rho^{(i-1)}}^2\right) - \frac{\lambda_p^{(i)}}{2\sigma_A^2 M}.$$

From (8), and using the optimal $\mathbf{F}_k^{(i)}$ and $B_{k,p}^{(i)}$ coefficients from (11), it is possible to compute the MMSE. Defining

$${\sigma_p^2}^{(i)} = \frac{1}{M^2}\sum_{k=0}^{M-1} MSE_k^{(i)}, \tag{12}$$

and the Gaussian error function, $\Phi(x)$, the estimated Bit Error Rate (BER) at the ith iteration for a QPSK constellation is

$$BER^{(i)} \simeq \Phi\left(\frac{1}{{\sigma_p}^{(i)}}\right). \tag{13}$$

Since a severely time dispersive channel with multipath propagation is being considered, bit errors can be considered independent, therefore for an uncoded system with independent and isolated errors, the Packet Error Rate (PER) for a fixed packet size of N bits is

$$PER^{(i)} \simeq 1 - \left(1 - BER^{(i)}\right)^N. \tag{14}$$

When the long and short slots are combined, the receiver has approximately the same information as when Nyquist signaling is used. Therefore, the PER for l packet retransmissions in the long and short slots at the ith iteration can be approximated by the PER of a Nyquist rate signaling with l retransmissions calculated in [19].

IV. Medium Access Control Performance

This section analyses how β influences the performance of the scheduled transmission system using H-ARQ and FTN, considering a saturated system with J MTs, i.e., where J MTs always have packets to transmit. For simplicity, it is assumed that each packet is carried by one block.

A. Throughput

Assume that the PER is denoted by $\epsilon^{(l,j)}$ for an l-th retransmission transmission, with $j = 1$ for the long slot and $j = 2$ for the short slot, with a fixed number of iterations p of the IB-DFE receiver. The expected service time (measured in number of Nyquist slots, i.e. long slots for $\beta = 1$) for one data packet, considering a maximum of L transmissions is

$$\begin{aligned} \mathbb{E}[\tau] = L\prod_{k=1}^{L}\epsilon_p^{(k,1)}\epsilon_p^{(k,2)} + \sum_{i=1}^{L}\Bigg(\Big((i-1+\beta)\left(1-\epsilon_p^{(i,1)}\right) \\ + i\epsilon_p^{(i,1)}\left(1-\epsilon_p^{(i,2)}\right)\Big)\prod_{k=1}^{i-1}\epsilon_p^{(k,1)}\epsilon_p^{(k,2)}\Bigg). \end{aligned} \tag{15}$$

Thus, the saturation throughput (measured in packets per Nyquist slots) can be calculated considering the success rate and the average service time, as

$$S_{sat} = \frac{1 - \prod_{i=1}^{L}\epsilon_p^{(i,1)}\epsilon_p^{(i,2)}}{J\ \mathbb{E}[\tau]}. \tag{16}$$

The total channel capacity is the aggregated throughput of all MTs, given by $J\ S_{sat}$.

B. Energy per Useful Packet

Another relevant parameter is the average energy spent per each packet correctly received, named Energy per Useful Packet (EPUP), denoted by Φ. FTN contributes to the reduction of the energy spent transmitting a packet in each slot, $E_p^{(j)}$ (where j denotes the slot duration), although the total energy considering the transmission in the long and the short slots is higher or equal to the energy per packet with Nyquist signaling rate, i.e. $E_p^{(N)} \leq E_p^{(1)} + E_p^{(2)}$. The EPUP can be calculated considering the expected number of long slots and short slots used to transmit a packet and the error rate, using

$$\Phi(\beta) = \frac{\mathbb{E}\left[N^{(1)}\right]E_p^{(1)} + \mathbb{E}\left[N^{(2)}\right]E_p^{(2)}}{1 - \prod_{i=1}^{R}\epsilon_p^{(i,1)}\epsilon_p^{(i,2)}}. \tag{17}$$

where

$$\begin{aligned} \mathbb{E}\left[N^{(1)}\right] = &\sum_{i=1}^{L} i(1-\epsilon_p^{(i,1)})\prod_{k=1}^{L-1}\epsilon_p^{(k,1)}\epsilon_p^{(k,2)} \\ &+ L\epsilon_p^{(L,1)}\prod_{k=1}^{L}\epsilon_p^{(k,1)}\epsilon_p^{(k,2)}, \end{aligned} \tag{18}$$

$$\begin{aligned} \mathbb{E}\left[N^{(2)}\right] = &\sum_{i=1}^{L} i\epsilon_p^{(i,1)}(1-\epsilon_p^{(i,2)})\prod_{k=1}^{L-1}\epsilon_p^{(k,1)}\epsilon_p^{(k,2)} \\ &+ L\epsilon_p^{(L,1)}\epsilon_p^{(L,2)}\prod_{k=1}^{L}\epsilon_p^{(k,1)}\epsilon_p^{(k,2)}. \end{aligned} \tag{19}$$

Assuming that the circuit consumption of the mobile devices is negligible, the energy per block transmission is calculated as

$$E_p \approx (1+\beta_T) G_1 d^{\kappa} M_l M E_b \,, \tag{20}$$

where β_T is the ratio of the transmission power over the amplifier's; M_l is the link margin gain compensating the hardware process variations and other additive noise; G_1 is the gain factor at a distance of $d = 1$ m; κ is the characteristic power-path loss. β_T is computed as $\beta_T = (\nu_P/\varpi_P - 1)$ with ϖ_P as the drain efficiency of the radio frequency power amplifier and ν_P as the peak-to-average-power ratio where $\nu_P = 3(\sqrt{2^{B_e}} - 1/\sqrt{2^{B_e}} + 1)$. B_e is approximately equal to the number of bits per symbol for an M-QAM constellation [20]. The energy per bit is proportional to the slot duration, thus $E_p^{(2)}/E_p^{(1)} = 1/\beta - 1$.

V. Performance Results

The current section presents the system performance results, for an Additive White Gaussian Noise (AWGN) and a multipath time-dispersive channel such as the one in [21]. The results were obtained through *Monte Carlo* simulations, assuming that a MT sends a data packet to the BS with $M = 256$ QPSK symbols, for a total of 1000 simulations, except for figure 2 with 10000 simulations - each data symbol lasts for $4\mu s$ and the SC-FDE Cyclic Prefix (CP) has the equivalent duration of 20% of the data block.

A problem that could be associated to FTN signaling is that the higher overlapping between pulses might lead to higher envelope fluctuations than in conventional Nyquist signaling and consequently a higher difficulty to amplify the signal. To evaluate how serious this problem is, figure 2 presents the complementary cumulative distribution of the Peak-to-Mean Envelope Power Ratio (PMEPR) of the transmitted signals (defined as in [22]) for FTN ($\beta = \{0.7; 0.802\}$) and Nyquist signaling ($\beta = 1$), with square-root raised-cosine pulses with $\alpha = \{0; 0.5; 1.0\}$. In general, the PMEPR is slightly higher with FTN than in conventional Nyquist signaling, although the difference is smaller than 1dB.

Figures 3 and 4 depict the Bit Error Rate (BER) performance of the FTN signaling for a single slot transmission. Figure 3 portrays the BER of FTN ($\beta = \{0.7; 0.802\}$) and Nyquist signaling ($\beta = 1$) for $\alpha = 0.5$ for several iterations up to $N_{iter} = 4$. It shows that the IB-DFE equalization technique is able to diminish the channel interference for each succeeding iteration, where the BER approaches the Matched-Filter Bound performance (MFB) performance. As observed and expected, lower values of β slightly degrade the system performance, despite that the performance of $\beta = 0.802$ for 4 iterations is almost similar to $\beta = 1$ and 2 iterations - this way it is possible to achieve a similar performance to Nyquist signaling at the cost of a higher number of iterations. Figure 4 portrays the BER of FTN ($\beta = \{0.7; 0.802\}$) and Nyquist signaling ($\beta = 1$) for $\alpha = \{0; 0.2; 0.5; 1.0\}$ for $N_{iter} = 4$ iterations. In terms of errors the system performance is mostly affected by lower values of β, especially if α has a low value,

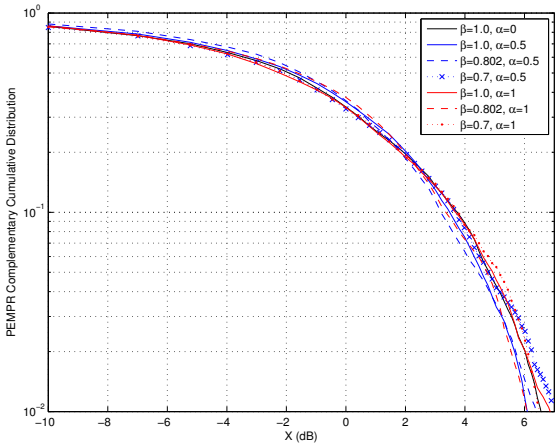

Figure 2. Complementary cumulative distribution of the PMEPR for FTN ($\beta = \{0.7; 0.802\}$) and Nyquist signaling ($\beta = 1$), both with square-root raised-cosine pulses with $\alpha = \{0; 0.5; 1\}$.

which means that the pulse bandwidth in use is smaller for a FTN scenario. For $\beta = 1$, the system performance almost achieves the MFB, regardless of α.

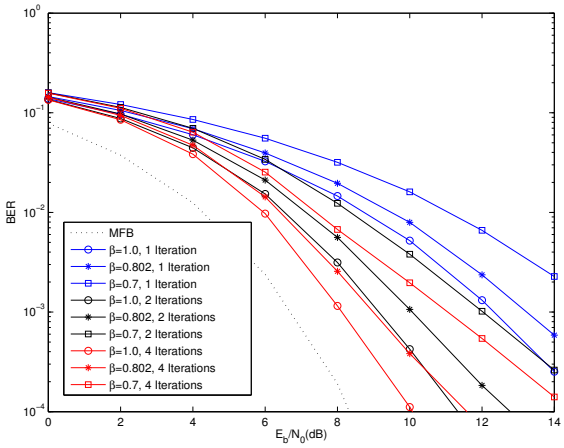

Figure 3. Bit Error Rate (BER) of FTN ($\beta = \{0.7; 0.802\}$) and Nyquist signaling ($\beta = 1$) for $\alpha = 0.5$ for $N_{iter} = 4$ iterations.

Figures 5 and 6 depict the PER performance ($\epsilon^{(l,j)}$) of the HARQ FTN system respectively for $\beta = 0.802$ and $\beta = 0.7$, for $\alpha = 0.5$ with for $N_{iter} = 4$ iterations. They show that the $\epsilon^{(l,j)}$ decreases when the number of retransmissions increases, although the decrease for a short slot is small for $\beta = 0.802$. As expected, the effect of the short slots is more relevant for $\beta = 0.7$, especially for $L = 1$.

The next set of figures illustrate the system level performance of HARQ FTN for $\beta = \{0.7; 0.802; 1\}$ with $\alpha = 0.5$, $L = \{1; 2; 4\}$, 4 iterations and using FTN bandwidth diversity ($K = 2$). Figure 7 depicts the expected service time ($\mathbb{E}[\tau]$) evolution with the average E_b/N_0. It shows that the

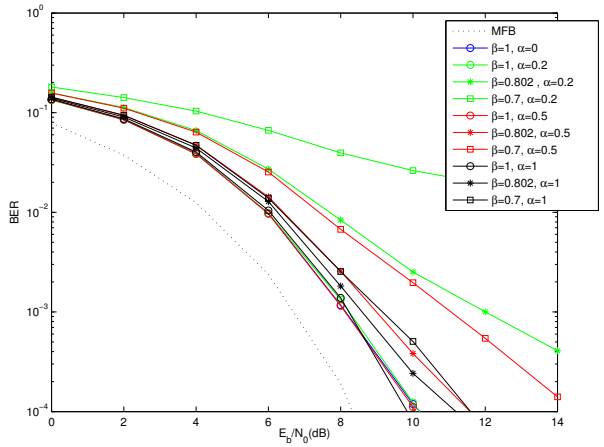

Figure 4. Bit Error Rate (BER) of FTN ($\beta = \{0.7; 0.802\}$) and Nyquist signaling ($\beta = 1$) for $\alpha = \{0; 0.2; 0.5; 1.0\}$ for $N_{iter} = 4$ iterations.

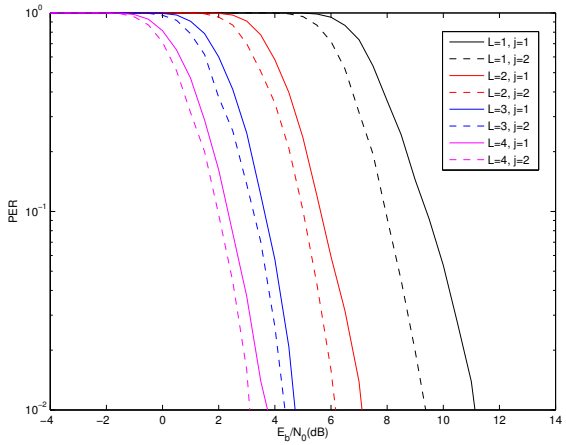

Figure 6. Packet Error Rate (PER) of HARQ FTN ($\beta = 0.7$) and Nyquist signaling ($\beta = 1$) for $\alpha = \{0.5\}$ in a for $\alpha = 0.5$ for $N_{iter} = 4$ iterations.

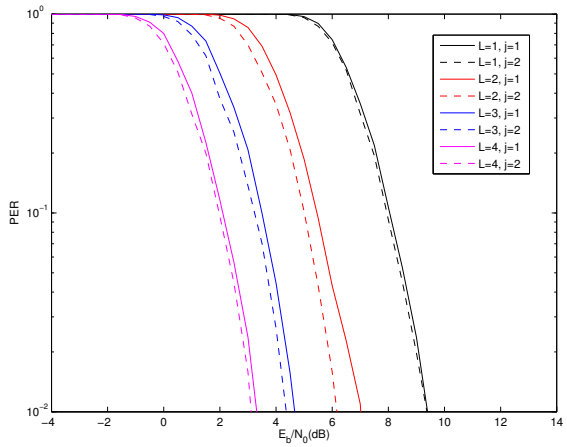

Figure 5. Packet Error Rate (PER) of HARQ FTN ($\beta = 0.802$) and Nyquist signaling ($\beta = 1$) for $\alpha = 0.5$ for $N_{iter} = 4$ iterations.

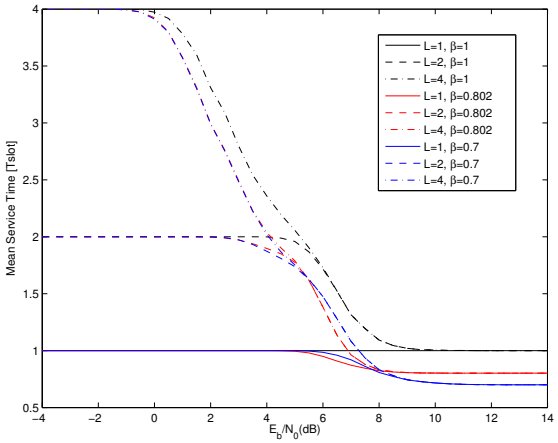

Figure 7. Expected Service Time (τ) for $\beta = \{0.7; 0.802; 1\}$ with $\alpha = 0.5$, $L = \{1; 2; 4\}$ and 4 iterations.

average service time increases when the E_b/N_0 decreases, up to the maximum limit defined by the maximum number of retransmissions defined by L. It also shows that for high E_b/N_0 values FTN uses mainly the first long slot, leading to shorter service times than using Nyquist signaling rate. Figure 8 depicts the total saturated throughput (JS_{sat}) and shows that HARQ FTN effectively contributes to increase the network capacity for low E_b/N_0 values, by combining the signal received in multiple slots for each packet. Due to the lower PER after the transmission in the long slot, HARQ FTN with $\beta = 0.802$ achieves a better throughput in these cases. For E_b/N_0 values above 8 dB, the shorter service time for $\beta = 0.7$ allows achieving the highest network capacity. The FTN bandwidth redundancy contributes decisively to let $\beta = 0.7$ beat the performance using the "Mazo's limit", i.e. $\beta = 0.802$. Similar conclusions can be taken from the EPUP (Φ) results, depicted in figure 9. The HARQ system with $L = 4$ is energy efficient for a broad range of E_b/N_0 values for all configurations, although it is bandwidth limited for E_b/N_0 below 7 dB for all β values. The lowest EPUP is achieved for $E_b/N_0 = 2$dB, with a saturation rate of 35% of the Nyquist rate system. The best energy performance occurs for the lowest E_b/N_0 that satisfies the data rate requirements, in the range between 2 dB and 8 dB.

VI. Conclusions

In this paper we considered SC-FDE schemes for FTN signaling over severely time-dispersive channels. To cope with the strong ISI levels associated to the combined effects of FTN signaling and multipath channel, we considered an iterative FDE receiver combined with a HARQ, both especially designed for FTN signaling. We also presented a simple, yet accurate analytical model for the proposed technique.

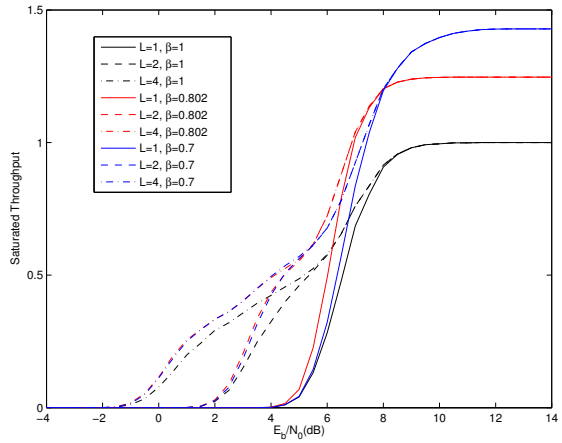

Figure 8. Saturated throughput for $\beta = \{0.7; 0.802; 1\}$ with $\alpha = 0.5$, $L = \{1; 2; 4\}$ and 4 iterations.

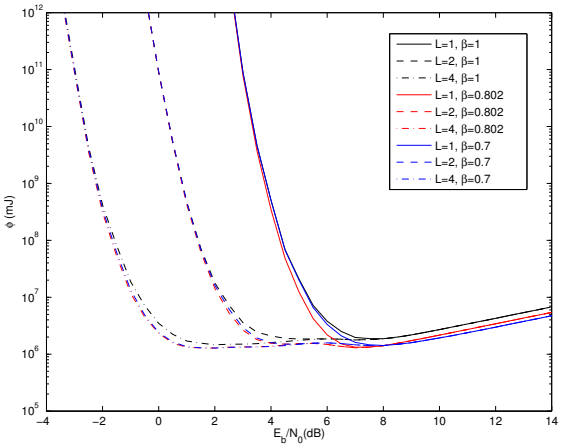

Figure 9. EPUP (Φ) for $\beta = \{0.7; 0.802; 1\}$ with $\alpha = 0.5$, $L = \{1; 4\}$ and 4 iterations.

Our performance results showed that we can have significant throughput gains, while maintaining essentially the receiver complexity of conventional Nyquist-rate schemes, even for severely time-dispersive channels.

REFERENCES

[1] J. Proakis, Digital Communications, 4th ed., ser. McGraw-Hill Series in Electrical and Computer Engineering, McGraw-Hill Higher Education, 2000.

[2] J. Mazo, "Faster-than-Nyquist signaling", *Bell Syst. Tech. J.*, vol. 54, pp. 1451-1462, Oct. 1975.

[3] A. Liveris and C. Georghiades, "Exploiting faster-than-Nyquist signaling", *IEEE Trans. on Communications*, vol. 51, no. 9, pp. 1502-1511, Sep. 2003.

[4] F. Rusek and J. B. Anderson, "The two dimensional Mazo limit", *in Proc. IEEE Int. Symp. Inf. Theory*, Adelaide, Australia, pp. 970-974, Sep. 2005.

[5] F. Rusek and J. B. Anderson, "Multi-stream faster than Nyquist signaling", *IEEE Trans. on Communications*, vol. 57, no. 5, pp. 1329-1340, May 2009.

[6] J. Anderson, F. Rusek, V. Owall, "Faster-Than-Nyquist Signaling", *Proceedings of the IEEE*, vol. 101, no. 8, pp. 1817–1830, Aug. 2013.

[7] A. Modenini, F. Rusek, G. Colavolpe, "Faster-than-Nyquist Signaling for Next Generation Communication Architectures", *in IEEE EUSIPCO'2014*, Lisbon, Portugal, Sep. 2014.

[8] A. Prlja and J. Anderson, "Reduced-complexity receivers for strongly narrowband intersymbol interference introduced by faster-than-Nyquist signaling", *Trans. on Communications*, vol. 60, no. 9, pp. 2591–2601, Sep. 2012.

[9] S. Tomasin, N. Benvenuto, "Fractionally Spaced Non-linear Equalization of Faster Than Nyquist Signals", *in IEEE EUSIPCO'2014*, Lisbon Portugal, Sep. 2014.

[10] L. Cimini, "Analysis and simulation of a digital mobile channel using orthogonal frequency division multiplexing," *Trans. on Communications*, vol. 33, no. 7, July 1985.

[11] H. Sari, G. Karam and I. Jeanclaude, "An Analysis of Orthogonal Frequency-division Multiplexing forMobile Radio Applications," *in Proc. IEEE Vehic. Tech. Conf.*, VTC-94, pp. 1635–1639, Stockholm, June 1994.

[12] D. Falconer, S. Ariyavisitakul, A. Benyamin-Seeyar and B. Eidson, "Frequency domain equalization for single-carrier broadband wireless systems," *IEEE Communications Mag.*, vol.40, no.4, pp.58–66, April 2002.

[13] A. Gusmão, R. Dinis, J. Conceiçao and N. Esteves, "Comparison of two modulation choices for broadband wireless communications," *in Proc. of IEEE Vehic. Tech. Conf. Spring (VTC)*, vol.2, pp.1300–1305, 2000.

[14] N. Benvenuto, R. Dinis, D. Falconer and S. Tomasin, "Single Carrier Modulation With Nonlinear Frequency Domain Equalization: An Idea Whose Time Has Come–Again," *Proceedings of the IEEE*, vol.98, no.1, pp.69–96, January 2010.

[15] N. Benvenuto and S. Tomasin, "Block iterative DFE for single carrier modulation," *Electronics Letters*, vol.38, no.19, pp. 1144–1145, 12 September 2002.

[16] F. Amaral, R. Dinis, P. Montezuma, "Approaching the MFB with Block Transmission Techniques", *European Trans. on Telecommunications*, vol. 23, No. 1, pp. 76 – 86, Feb., 2012.

[17] F. Ganhão, R. Dinis, L. Bernardo, R. Oliveira, "Analytical BER and PER Performance of Frequency-Domain Diversity Combining, Multipacket Detection and Hybrid Schemes," *IEEE Trans. on Communications*, vol. 60, n. 8, pp. 2353 – 2362, Aug. 2012.

[18] R. Dinis, P. Silva and A. Gusmão, "IB-DFE receivers with space diversity for CP-assisted DS-CDMA and MC-CDMA systems," *European Trans. on Telecommunications*, vol. 18, pp. 791–802, June 2007.

[19] F. Ganhão, B. Cunha, L. Bernardo, R. Dinis and R. Oliveira, "A High Throughput H-ARQ Technique with Faster-than-Nyquist Signaling", *in Int. Conf. on Telecommunications & Multimedia*, Heraklion, Greece, Jul. 2014.

[20] S. Cui, A. Goldsmith, and A. Bahai, "Energy-constrained modulation optimization," *IEEE Trans. on Wireless Communications*, vol. 4, no. 5, pp. 2349–2360, Sept. 2005.

[21] J. Medbo and P. Schramm, "Channel models for HIPERLAN/2 in different indoor scenarios," *ETSI BRAN 3ERI085B*, pp. 1-8, 1998.

[22] R. Dinis and A.Gusmão, "A Class of Nonlinear Signal Processing Schemes for Bandwidth-Efficient OFDM Transmission with Low Envelope Fluctuation", *IEEE Trans. on Communications*, vol.52, no.10, pp. 2009–2018, Nov. 2004.

Bibliography

[1] M. Pereira, L. Bernardo, R. Oliveira, P. Carvalho and P. Pinto, "Performance of Diversity Combining ARQ Error Control in a TDMA SC-FDE System", *Communications, IEEE Transactions on*, vol.60, no.3, pp.735–746, March 2012.

[2] L. Cimini, "Analysis and simulation of a digital mobile channel using orthogonal frequency division multiplexing", *IEEE Trans. Commun.*, vol. 33, no. 7, July 1985.

[3] J. Mazo, "Faster-than-Nyquist signaling", *Bell Syst. Tech. J.*, vol. 54, pp. 1451-1462, Oct. 1975.

[4] J. Anderson, F. Rusek and V. Owall, "Faster-Than-Nyquist Signaling", *IEEE Proceedings*, Vol. 101, No. 8, pp. 1817-1830, Aug. 2013.

[5] J. Anderson and A. Prlja, "Turbo equalization and an M-BCJR algorithm for strongly narrowband intersymbol interference", *Proc. Int. Symp. Inf. Theory Appl.*, Taichung, Taiwan, pp. 261-266, Oct. 2010.

[6] A. Prlja and J. Anderson, "Reduced-complexity receivers for strongly narrowband intersymbol interference introduced by faster-than-Nyquist signaling", *IEEE Trans. Commun.*, vol. 60, no. 9, pp. 2591-2601, Sep. 2012.

[7] H. Sari, G. Karam and I. Jeanclaude, "An Analysis of Orthogonal Frequency-division Multiplexing forMobile Radio Applications", *Proc. IEEE Vehic. Tech. Conf.*, VTC-94, pp. 1635-1639, Stockholm, June 1994.

[8] A. Gusmão, R. Dinis, J. Conceição and N. Esteves, "Comparison of two modulation choices for broadband wireless communications", *Proceedings of 2000 IEEE Vehicular Technology Conference Spring*, vol.2, pp.1300-1305, 2000.

[9] D. Falconer, S. Ariyavisitakul, A. Benyamin-Seeyar and B. Eidson, "Frequency domain equalization for single-carrier broadband wireless systems", *IEEE Communications Magazine*, vol.40, no.4, pp.58-66, April 2002.

[10] N. Benvenuto, R. Dinis, D. Falconer and S. Tomasin, "Single Carrier Modulation With Nonlinear Frequency Domain Equalization: An Idea Whose Time Has Come–Again", *Proceedings of the IEEE*, vol.98, no.1, pp.69-96, January 2010.

[11] D. Costello, J. Hagenauer, H. Imai and S. Wicker, "Applications of error-control coding", *in IEEE Transactions on Information Theory*, vol.44, no.6, pp.2531-2560, October 1998.

[12] F. Ganhão, B. Cunha, L. Bernardo, R. Dinis and R. Oliveira, "A High Throughput H-ARQ Technique with Faster-than-Nyquist Signaling", *in Int. Conf. on Telecommunications & Multimedia*, Heraklion, Greece, Jul. 2014.

[13] S. Haykin and M. Moher, *An introduction to Digital and Analog Communications*, pp.245-248, John Wiley and Sons, Hoboken, NJ, USA, 2nd edition, 2007.

[14] G.Forney, "Maximum-likelihood sequence estimation of digital sequences in the presence of intersymbol interference", *Information Theory, IEEE Transactions on*, 18(3):363-378, May 1972.

[15] N. Benvenuto and S. Tomasin, "Block iterative DFE for single carrier modulation", *in Electronics Letters*, vol.38, no.19, pp. 1144-1145, 12 September 2002.

[16] R. Dinis, A. Gusmão and N. Esteves, "On broadband block transmission over strongly frequency-selective fading channels", *n 15th International Conference on Wireless Communications (Wireless 2003)*, pp. 261 - 269, July 2003.

[17] N. Benvenuto and S. Tomasin, "Iterative design and detection of a DFE in the frequency domain", *Communications, IEEE Transactions on*, 53(11):1867 - 1875, Nov 2005.

[18] N. Gusmão, P. Torres, R. Dinis and N. Esteves, "A turbo FDE technique for reduced-cp sc-based block transmission systems", *Communications, IEEE Transactions on*, 55(1):16 - 20, Jan 2007.

[19] J. Proakis, *Digital Communications*, 4th ed., ser. McGraw-Hill Series in Electrical and Computer Engineering, McGraw-Hill Higher Education, 2000.

[20] M. Tuchler and J. Hagenauer, "Turbo Equalization Using Frequency Domain Equalizers", *38th Annual Allerton Conference on Communication*, pp: 1234-1243, Monticello, Illinois, 2000.

[21] M. Tuchler and J. Hagenauer, "Linear Time and Frequency Domain Turbo Equalization", *IEEE VTC'01 (Fall)*, pp: 2773-2777, Atlantic City, USA, 2001.

[22] Larry L. Peterson and Bruce S. Davie, *Computer Networks, Fifth Edition: A Systems Approach*, Morgan Kaufmann Publishers Inc., San Francisco, CA, USA, 5th edition, 2011.

[23] Ajay Chandra V. Gummalla and John O. Limb, "Wireless medium access control protocols", *CIEEE Communications Surveys Tutorials*, 3(2):2-15, quarter 2000.

[24] Phillip M. Feldman, *An Overview and Comparison of Demand Assignment Multiple Access (DAMA) Concepts for Satellite Communications Networks*, MRand Publishing, November 1996.

[25] H. Peyravi, "Medium access control protocols performance in satellite communications", *Communications Magazine, IEEE*, 37(3):62-71, 1999.

[26] Theodore Rappaport, *Wireless Communications: Principles and Practice*, Prentice Hall PTR, Upper Saddle River, NJ, USA, 2nd edition, 2001.

[27] D.J. Costello and Jr. Forney, "G.D. Channel coding: The road to channel capacity", *Proceedings of the IEEE*, 95(6):1150-1177, 2007.

[28] Claude E. Shannon, "A mathematical theory of communication", *The Bell System Technical Journal*, 27:379-423, 623-656, July, October 1948.

[29] David Tse and Pramod Viswanath, *Fundamentals of Wireless Communication*, Cambridge University Press, New York, NY, USA, 2005.

[30] S. Sesia, M. Baker and I. Toufik, *LTE - The UMTS Long Term Evolution: From Theory to Practice*, John Wiley and Sons, 2011.

[31] Shu Lin, D. Costello and M. Miller, "Automatic-repeat-request error-control schemes", *IEEE Communications Magazine*, 22(12):5-17, December 1984.

[32] R. Dinis, P. Carvalho, L. Bernardo, R. Oliveira, M. Serrazina and P. Pinto, "Frequency-domain multipacket detection: A high throughput technique for SC-FDE systems", *2007 IEEE Global Telecommunications Conference, (GLOBECOM 2007)*, Washington DC, USA, November 2007.

[33] F. Ganhão, R. Dinis, L. Bernardo, R. Oliveira, "Analytical BER and PER Performance of Frequency-Domain Diversity Combining, Multipacket Detection and Hybrid Schemes", *IEEE Transactions in Communications*, vol. 60, n. 8, August 2012.

[34] R. Dinis, P. Silva and A. Gusmão, "IB-DFE receivers with space diversity for CP-assisted DS-CDMA and MC-CDMA systems", *European Transactions on Telecommunications*, vol. 18, pp. 791–802, June 2007.

[35] J. Medbo and P. Schramm, "Channel models for HIPERLAN/2 in different indoor scenarios", *ETSI BRAN 3ERI085B*, pp. 1-8, 1998.

[36] R. Dinis and A.Gusmão, "A Class of Nonlinear Signal Processing Schemes for Bandwidth-Efficient OFDM Transmission with Low Envelope Fluctuation", *IEEE Trans. on Communications*, November 2004.

[37] F. Ganhão, M. Pereira, L. Bernardo, R. Dinis, N. Souto, J. Silva, R. Oliveira and P. Pinto, "Energy per useful packet optimization on a TDMA HAP channel", *Proc. of 2010 IEEE Vehicular Technology Conference Fall*, September 2010.

[38] S. Cui, A. Goldsmith and A. Bahai, "Energy-constrained modulation optimization", *IEEE Transactions on Wireless Communications,* vol. 4, no. 5, pp. 2349–2360, Sept. 2005.

[39] Qin Wang, M. Hempstead and W. Yang, "A Realistic Power Consumption Model for Wireless Sensor Network Devices", *IEEE Sensor and Ad Hoc Communications and Networks, Reston, Vancouver*, volume 1, pages 286-295, September 28 2006.

[40] S. Quaglieri, M. De Sanctis, E. Cianca et al, "Performance and Energy Efficiency of Hybrid ARQ Over Ground-HAP Links", *IEEE Aerospace Conference, Big Sky, Montana, USA*, pages 1313-1321, March 2005.